

Surrogate-Based Bayesian Inference: Uncertainty Quantification and Active Learning

Andrew Gerard Roberts¹, Michael C. Dietze²,
and Jonathan H. Huggins^{1,3}

¹*Faculty of Computing and Data Sciences, Boston University, e-mail: arober@bu.edu*

²*Department of Earth and Environment, Boston University, e-mail: dietze@bu.edu*

³*Department of Mathematics and Statistics, Boston University, e-mail: huggins@bu.edu*

Abstract: Surrogate models—also called emulators—are widely used to facilitate Bayesian inference in settings where computational costs preclude the use of standard posterior inference algorithms. Their deployment is now standard practice across many scientific domains. However, integrating surrogates in statistical analyses introduces unique challenges that complicate established Bayesian workflow principles. While significant progress has been made in addressing these issues, the relevant developments are scattered across several distinct research communities, with different emphases and perspective. We present a unifying review that synthesizes the literature into a coherent framework, aiming to benefit both practitioners and methods developers. We place particular emphasis on propagating surrogate uncertainty and sequentially refining emulators via active learning, two key components of a robust surrogate-based Bayesian workflow.

MSC2020 subject classifications: Primary 62F15, 65C60; secondary 65C05.

Keywords and phrases: surrogate, emulator, metamodel, inverse problem, uncertainty quantification, uncertainty propagation, active learning, sequential design, Bayesian inference, Gaussian process, likelihood-free inference, simulation-based inference, probabilistic modeling, Markov chain Monte Carlo.

Contents

1	Introduction	2
1.1	Overview and Paper Organization	4
2	Bayesian Inference with Expensive Models	7
2.1	The Bayesian Inference Setting	8
2.2	Deterministic Bayesian Inverse Problems	8
2.3	Stochastic Bayesian Inverse Problems	10
2.3.1	Pseudo-Marginal Methods	11
2.3.2	Classical Likelihood-Free Methods	11
2.3.3	Neural Density Estimation	12
3	Emulators in Bayesian Inference	13
3.1	Regression-Based Emulators	13

3.2	Probabilistic Emulators	16
3.3	Common Model Classes	17
3.3.1	Gaussian Processes	18
3.3.2	Polynomials	18
3.3.3	Neural Networks	19
3.4	Finite vs. Infinite Dimensional Emulators	19
3.5	Practical Considerations for Different Emulator Targets	20
3.5.1	Forward Model Emulation	20
3.5.2	Log-Density Emulation	23
3.5.3	Conditional Density Emulation	25
3.6	Model Checking and Diagnostics	25
4	Surrogate-Based Posterior Approximation	26
4.1	The Plug-In Mean	27
4.2	Frameworks for Constructing Posterior Estimators	27
4.2.1	Decision Theory for Normalized Density	27
4.2.2	Decision Theory for Unnormalized Density	28
4.2.3	Uncertainty Propagation via Computation	28
4.3	Concrete Posterior Estimators	28
4.3.1	The Expected Posterior (EP)	28
4.3.2	The Expected Unnormalized Posterior (EUP)	29
4.3.3	Other Pointwise Estimators	32
4.4	Comparison and Practical Recommendations	33
5	Active Learning for Bayesian Inversion	34
5.1	Design Optimization	35
5.1.1	Problem Setup	36
5.1.2	Frameworks for Constructing Design Criteria	37
5.1.3	Concrete Acquisition Functions	38
5.1.4	Solving the Optimization Problem	42
5.2	Surrogate-Guided Sampling	43
5.3	Tempered Target Distributions	44
5.4	MCMC-Based Sequential Design	46
6	Conclusion	47
A	Gaussian Process Derivations	49
A.1	Forward Model Emulation	49
A.2	Log-Density Emulation	51
	References	52

1. Introduction

In fields ranging from climate science to astrophysics, the scientific process increasingly relies on complex, computationally expensive computer simulations (Schneider et al., 2017; Pan et al., 2025; Varma et al., 2019; Dax et al., 2021). Many such computer models contain parameters with values that cannot be specified a priori or directly estimated experimentally. Therefore, a critical task in many scientific workflows is to infer parameter values that are consistent

with observed data. Bayesian inference offers a principled framework for parameter estimation, providing mechanisms to quantify uncertainty and balance prior information with observed data (Gelman et al., 2013). However, posterior approximation algorithms such as Markov chain Monte Carlo (MCMC; Brooks et al. (2011)) and Approximate Bayesian Computation (ABC; Sunnåker et al. (2013)) require running the simulator tens or hundreds of thousands of times. When a single simulation takes minutes or hours, this cost renders these standard approaches intractable. To overcome this barrier, a rich literature has developed around *surrogate modeling* (i.e., *emulation*). The core idea is to replace the expensive simulator with a computationally-cheap statistical approximation, trained on a sparse set of simulator runs (Kennedy and O’Hagan, 2001; Gramacy, 2020). The emulator is then used in place of the expensive model, enabling the application of otherwise intractable inference algorithms.

While the premise is straightforward, deploying surrogates within a Bayesian framework presents distinct methodological and conceptual challenges. In broader statistical practice, established principles of *Bayesian workflow* help practitioners navigate the complexities of iterative model building (Gelman et al., 2020; Li et al., 2025; Gabry et al., 2019). However, the incorporation of surrogates introduces complexities that extend beyond standard considerations. To bridge this gap, we consolidate a wide body of research in order to lay out the principles underlying a robust workflow for surrogate-based Bayesian inference.

Foremost among the complexities faced in this setting is the sheer modeling challenge of fitting an accurate emulator with sparse training data. The quantities typically targeted by emulators, such as simulator outputs or the log-likelihood surface, tend to be high-dimensional or nonstationary, which poses a challenge for standard predictive models (Booth, Cooper and Gramacy, 2024). This difficulty is compounded by the fact that the posterior distribution often concentrates in a small, unknown subset of the prior support (Li and Marzouk, 2014; Papamakarios and Murray, 2016; Lu et al., 2015). The sparse set of simulator training data may completely miss this “needle in a haystack.” An emulator that is accurate in a global, prior-averaged sense may nonetheless fail to provide a reasonable approximation in the high-density region (Sinsbeck and Nowak, 2017). Even if these issues are adequately addressed, the surrogate will invariably be an imperfect representation of the true model. Posterior estimates derived using the surrogate will inherit these imperfections, potentially leading to biased and overconfident inference (Reiser et al., 2025; Roberts, Dietze and Huggins, 2026).

Despite remaining challenges, significant progress has been made in mitigating these concerns. A driving feature of these advancements is the use of emulators equipped with a notion of predictive uncertainty; i.e., models that “know what they don’t know” (Osband et al., 2023a). The use of uncertainty-aware surrogates offers several benefits and opportunities. Emulator uncertainty can be propagated through the Bayesian workflow, enabling well-calibrated posterior inference that properly accounts for the additional source of uncertainty (Bilionis and Zabaras, 2013). Acknowledging the full scope of uncertainty is often crucial for downstream decision-making and scientific inquiry (Kochenderfer

et al., 2015). Moreover, probabilistic surrogates can be used to inform the efficient allocation of computational resources. As noted above, passively sampling simulator evaluation locations often yields training data that is poorly suited to posterior estimation (Kandasamy, Schneider and Póczos, 2017). When constrained by a limited computational budget, it is therefore crucial to carefully design the simulation schedule with respect to the explicit goal of approximating the posterior (Wang and Li, 2018; Özge Sürer, Plumlee and Wild, 2024). An uncertainty-aware emulator facilitates the identification of parameter locations with the greatest potential to improve the posterior estimate. This idea forms the basis of *active learning* algorithms that sequentially allocate simulator runs optimized for posterior refinement (Kandasamy, Schneider and Póczos, 2015; Järvenpää et al., 2021; Lartaud, Humbert and Garnier, 2024).

1.1. Overview and Paper Organization

The topics highlighted above are highly interdisciplinary, spanning the statistical, applied mathematics, engineering, and machine learning literatures. In addition, the use of surrogates in practical applications has become standard across many scientific domains. By synthesizing these widespread developments, we aim to provide a unified treatment that benefits both practitioners and methods developers alike. We begin by providing a high-level overview of the paper structure.

To make the setting concrete, consider the task of inferring parameters θ using observations y_o under a Bayesian model $p(\theta, y) = \pi_0(\theta)p(y | \theta)$. We assume that characterizing the posterior density $\pi(\theta) = p(\theta | y_o)$ requires evaluations of an expensive function $f(\theta)$, which typically implies running a computer simulation. The simulator may be deterministic—in which case we directly observe the value of $f(\theta)$ when the function is queried—or stochastic, such that we only observe $\varphi(\theta)$, a noisy and potentially indirect observation of $f(\theta)$. Section 2 motivates this setup, describing the challenges imposed by expensive models in both the deterministic and noisy (i.e., simulation-based/likelihood-free) settings. Since f is assumed to be the computational bottleneck, this review focuses on methods that make efficient use of simulator runs by training a predictive model on a sparse set of evaluations $\{\theta_n, \varphi_n\}_{n=1}^N$, where $\varphi_n = \varphi(\theta_n)$. Figure 1 summarizes the high-level workflow that guides the remainder of this article, which we now outline.

Emulator Target and Initial Design. When introducing an emulator within an existing Bayesian model, one of the first decisions is choosing which quantity to emulate. Sections 3.1 and 3.5 discuss the choice of *emulator target* in depth. In general, we consider emulators that seek to learn a target map of the form $\theta \mapsto f(\theta)$. This encompasses popular strategies such as *forward model emulation* (predicting the outputs of an underlying computer model), *log-density emulation* (directly learning the log-likelihood or log-posterior surface), and *conditional likelihood estimation* (fitting a parameterized likelihood). Once the target

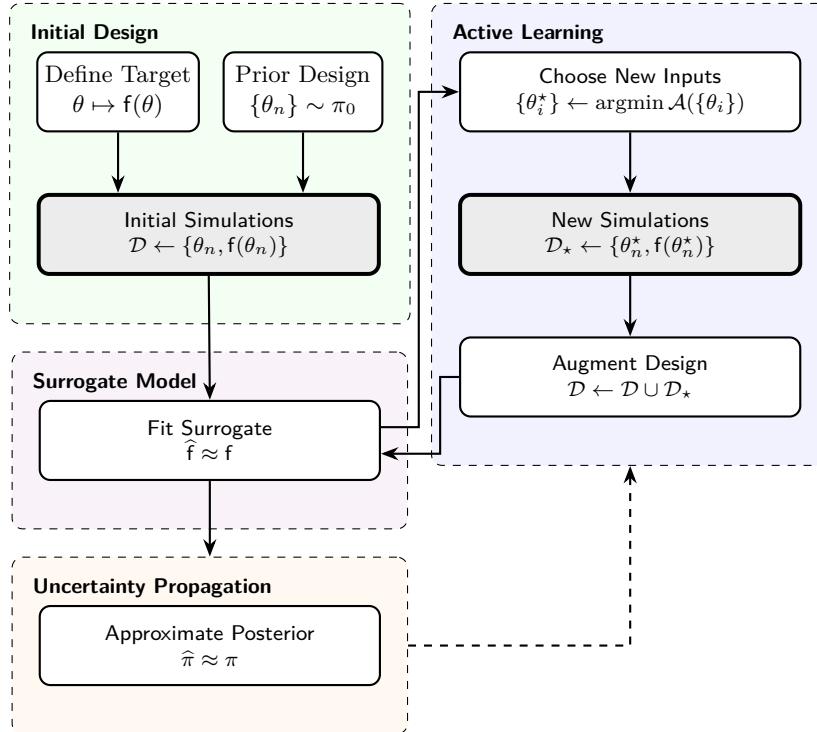


FIG 1. (Modular Surrogate-Based Bayesian Workflow) For simplicity, the diagram shows the case where noiseless target evaluations $f(\theta)$ are directly available, but the workflow also applies to the case where queries yield noisy or indirect information (see Section 3.1). The broad workflow stages consist of (1) **Initial design**: generate an initial set of training data by running the simulator and evaluating the function targeted for emulation; (2) **Surrogate training**: fit a probabilistic surrogate to the training set; (3) **Uncertainty propagation**: construct an uncertainty-aware posterior approximation using the emulator. The final component, **active learning**, describes the iterative process of augmenting the training data and updating the emulator. The current approximate posterior is sometimes used in informing the selection of new query points (dashed arrow). The gray, shaded boxes highlight the steps that require calls to the expensive simulator.

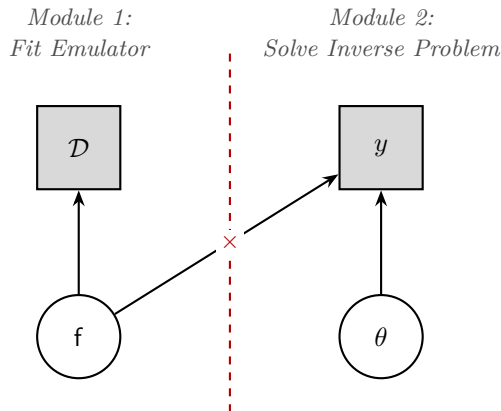


FIG 2. Graphical representation of a joint Bayesian model, with a “cut” (red dashed line) that prevents feedback from y to f . Shaded squares are observed variables (data y and simulator queries \mathcal{D}), while circles are unobserved variables (parameters θ and target map f). The joint Bayesian approach constructs a probability distribution over all quantities, then computes $p(\theta, f | y, \mathcal{D})$. The cut model severs feedback so that y does not affect inference for f .

is selected, the initial emulator training set $\mathcal{D} := \{\theta_n, \varphi_n\}_{n=1}^N$ is typically constructed by sampling input points from the prior $\{\theta_n\}_{n=1}^N \sim \pi_0$ (potentially with a space-filling adjustment to prevent clumping) and then querying the target at the sampled points. We follow the statistical design of experiments literature by referring to the input set $\{\theta_n\}_{n=1}^N$ as the *design* (Garud, Karimi and Kraft, 2017; Gramacy, 2020). The first stage (green box) in Figure 1 highlights the choice of target and the initial design construction.

Fitting the Emulator. The second stage (pink box) entails fitting a predictive model to the design data \mathcal{D} . A variety of different model classes are commonly used for this task, including Gaussian processes, polynomial chaos expansions, and neural networks (Helin et al., 2024; Bürkner et al., 2023; Li, Rudner and Wilson, 2024). To provide a unifying viewpoint, we avoid focusing on a particular model. Instead, we adopt a generic probabilistic perspective that encompasses any regression or interpolation model that, in addition to point estimates, provides some notion of predictive uncertainty. This is encoded by a probability distribution $p(f | \mathcal{D})$ that summarizes the uncertainty in the target due to limited training data \mathcal{D} . Section 3.2 provides a general perspective on probabilistic emulators, while Sections 3.3 and 3.4 highlight practical considerations for particular model classes.

Uncertainty Propagation. The trained surrogate is then deployed to estimate the posterior distribution π (yellow box). This can represent either the final output of the inference workflow or an intermediate approximation used to guide the selection of additional design points. Our framework is rooted in a *modular* workflow, in which the emulator predictive distribution $p(f | \mathcal{D})$ and

the parameter posterior $p(\theta | y_o)$ are learned in two distinct steps (Reiser et al., 2025). Modular Bayesian workflows have been shown to improve robustness to misspecification in the likelihood $p(y_o | \theta)$, in addition to offering computational advantages (Liu, Bayarri and Berger, 2009; Jacob et al., 2017). Given that the two inference stages are not coupled through an overarching probability model, uncertainty propagation is not immediately provided by standard Bayesian conditioning and marginalization. In fact, several different uncertainty-aware posterior estimates are routinely used in the literature, which approximate $p(\theta | y_o)$ while accounting for the uncertainty in $p(f | \mathcal{D})$ (Reiser et al., 2025; Roberts, Dietze and Huggins, 2026). Section 4 reviews these approaches and their trade-offs.

Remark 1. Our use of the word “modular” refers to the two-step computational workflow, similar to its use in Reiser et al. (2025); Jedhoff et al. (2026). This implies that the emulator predictive distribution $p(f | \mathcal{D})$ is obtained without referencing y_o , and then the uncertainty is propagated when performing inference for θ . This should not be confused with its usage in literature on cutting feedback in probabilistic models, in which case “modular” implies that information never flows from y_o to f during inference (Plummer, 2015). These usages are *not* equivalent. A two-step computational workflow can still introduce feedback from y_o to f during the second stage, depending on how uncertainty is propagated from the first stage. A graphical representation of cutting feedback is shown in Figure 2.

Active Learning. The final component of the workflow (purple box) consists of an iterative procedure for refining the surrogate. This represents a sequential algorithm for constructing the design, in which the current surrogate is used to identify the next batch of simulator inputs. The dashed arrow in Figure 1 emphasizes that an intermediate posterior approximation can be used to inform the design selection. In our context, we adopt a broad use of the term *active learning* to refer to algorithms that select new design points with respect to the specific goal of posterior estimation. This includes strategies that optimize goal-oriented acquisition functions (analogous to Bayesian optimization; Section 5.1), iterative sampling of approximate posteriors (Section 5.2), tempering strategies (Section 5.3), and MCMC-guided design (Section 5.4).

2. Bayesian Inference with Expensive Models

This paper concerns Bayesian inference problems in which evaluation of the likelihood (or more generally the unnormalized posterior density) incurs significant computational expense. This situation is exceedingly common in large-scale scientific and engineering applications, where the goal is to infer latent parameters related to observations through a complex computer model. When the computer model is stochastic, the challenge is compounded: computational costs remain prohibitive, and the density itself is often mathematically intractable to evaluate. While many simulation-based (or likelihood-free) methods address this

intractability by constructing an approximate likelihood, they do not avoid the computational burden. Evaluating the likelihood approximation still relies on repeated forward simulations of the underlying model, implying that the core problem of expensive density evaluations remains. This section introduces the challenges faced in both the deterministic and stochastic settings, motivating the emulator-based methods considered in the remainder of the paper.

2.1. The Bayesian Inference Setting

Consider the task of inferring unknown parameters $\theta \in \Theta \subseteq \mathbb{R}^D$ using noisy observations $y_o \in \mathbb{Y} \subseteq \mathbb{R}^P$. The Bayesian approach to this problem is to define a joint probability distribution $p(\theta, y) = \pi_0(\theta)p(y | \theta)$ over the parameters and data. The prior π_0 is a probability distribution over Θ and the conditional $p(y | \theta)$ defines the likelihood

$$\mathbf{L}(\theta) := p(y_o | \theta), \quad (1)$$

a function of θ dependent on the fixed data realization y_o . The central task of Bayesian inference is to characterize the posterior distribution

$$\pi(\theta) := p(\theta | y_o) = \frac{1}{Z} \pi_0(\theta) \mathbf{L}(\theta), \quad Z := \int_{\Theta} \pi_0(\theta) \mathbf{L}(\theta) d\theta, \quad (2)$$

which encodes the uncertainty in the parameters after observing the data. The quantities \mathbf{L} , π , and Z all depend on y_o , but we suppress this in the notation as the data realization is assumed constant throughout most of this paper. Typically, the integral defining Z is intractable, so posterior inference algorithms rely on pointwise evaluations of the *unnormalized* posterior density $\tilde{\pi}(\theta) := \pi_0(\theta) \mathbf{L}(\theta)$. A standard approach is to sample the posterior using a Markov chain Monte Carlo (MCMC) algorithm, often requiring $10^5 - 10^7$ serial evaluations of $\tilde{\pi}(\theta)$. While not a problem when $\tilde{\pi}(\theta)$ is cheap to compute, this sequential computation renders MCMC infeasible when the cost of a density evaluation is high.

2.2. Deterministic Bayesian Inverse Problems

The inference challenge posed by expensive posterior densities commonly arises in the Bayesian approach to inverse problems (Stuart, 2010). In this setting, the observation y_o typically corresponds to an observable quantity associated with a complex physical system. The goal is to recover latent parameters of interest θ that gave rise to the observed data. The bulk of the modeling effort typically consists of constructing a mechanistic model $\mathcal{G} : \Theta \rightarrow \mathbb{Y}$ encoding domain knowledge, which describes the process by which parameters produce observed quantities. We refer to \mathcal{G} as the *forward model*. The task of solving the inverse problem entails inverting the relationship to identify parameter values

consistent with a particular observation. This parameter recovery is commonly cast as a problem of Bayesian inference with a Gaussian noise model

$$y = \mathcal{G}(\theta) + \epsilon, \quad \epsilon \sim \mathcal{N}(0, \Sigma), \quad (3)$$

implying the likelihood

$$\mathsf{L}(\theta) = \det(2\pi\Sigma)^{-P/2} \exp\left\{-\frac{1}{2} \|y_o - \mathcal{G}(\theta)\|_{\Sigma}^2\right\}. \quad (4)$$

We utilize the weighted norm notation $\|x\|_A^2 := x^\top A^{-1}x$, where A is a positive definite matrix. Computing $\mathsf{L}(\theta)$ (and thus $\tilde{\pi}(\theta)$) requires the forward model evaluation $\mathcal{G}(\theta)$, which may involve running an expensive computer simulation (e.g., a numerical differential equation solver). Hence, in Bayesian inverse problems the posterior density $\tilde{\pi}(\theta)$ is often a computationally expensive, and potentially black box (i.e., difficult or impossible to differentiate), function.

Example 1 (Parameter Estimation for ODEs). In modeling the Earth system, complex dynamical models are used to simulate trajectories of various physical processes, such as temperature trends and carbon fluxes (Schneider et al., 2017; Raoult et al., 2025; Dunbar et al., 2021; Keetz et al., 2025; Huang et al., 2016; Fer et al., 2018). These models often feature empirical parameters with unknown values that must be estimated from data. As a simple illustrative example, we consider the problem of parameter estimation for an ordinary differential equation (ODE). While this example is simplified for clarity, the setup is structurally similar to many inverse problems faced in practice, such as parameter estimation for land surface models (Raoult et al., 2025). Consider a parameter-dependent initial value problem

$$\frac{d}{dt}x(t, \theta) = F(x(t, \theta), \theta), \quad x(t_0, \theta) = x_o, \quad (5)$$

describing the time evolution of S state variables $x(t, \theta) := \{x^{(s)}(t, \theta)\}_{s=1}^S$ with dynamics depending on $\theta \in \Theta$. As our focus will be on estimating these parameters from observations, we consider the parameter-to-state map

$$\theta \mapsto \{x(t, \theta) : t \in [t_0, t_1]\}. \quad (6)$$

In practice, the solution is typically approximated via a numerical discretization of the form

$$\mathcal{M} : \theta \mapsto [x_0(\theta), \dots, x_K(\theta)]^\top. \quad (7)$$

Here, $\mathcal{M} : \Theta \rightarrow \mathbb{R}^{K \times S}$ represents the map induced by a numerical solver, and $x_0(\theta), \dots, x_K(\theta)$ are approximations of the state values $x(t, \theta)$ at a finite set of time points in $[t_0, t_1]$. Going forward, we focus on the discrete-time operator \mathcal{M} , neglecting discretization error for simplicity. Finally, suppose we have observed data $y_o \in \mathbb{Y}$ that we model as a noise-corrupted function of the state trajectory.

This is formalized by the definition of an observation operator $\mathcal{H} : \mathbb{R}^{K \times S} \rightarrow \mathbb{Y}$ mapping from the state trajectory to a P -dimensional observable quantity. Assuming the data generating process

$$y = (\mathcal{H} \circ \mathcal{M})(\theta_\star) + \epsilon, \quad \epsilon \sim \mathcal{N}(0, \Sigma) \quad (8)$$

for some “true” parameter value $\theta_\star \in \Theta$, we see that this problem is of the form in Equation (3) with forward model $\mathcal{G} := \mathcal{H} \circ \mathcal{M}$. In this case, the computational cost of evaluating $\pi(\theta)$ can be high, owing to the dependence on the numerical solver $\mathcal{M}(\theta)$. \diamond

2.3. Stochastic Bayesian Inverse Problems

In many applications, the forward model may be inherently noisy (Baker et al., 2022). In this case, multiple evaluations of $\mathcal{G}(\theta)$ at the same input may yield different outputs, and the simulator can be viewed as defining a family of conditional distributions $p(\mathcal{G}(\theta) | \theta)$ indexed by θ . Let z denote the latent variables that make the simulator noisy, such that $\mathcal{G}(\theta) = \mathcal{G}(\theta; z)$ is deterministic once a value for z is fixed. The simulator thus implicitly defines the data-generating process by

$$p(y | \theta) = \int p(y | \theta, z) p_z(z | \theta) dz. \quad (9)$$

Since this integral is typically intractable, evaluations of the likelihood $L(\theta) = p(y_o | \theta)$ are unavailable. We apply the broad label *simulation-based inference (SBI)* to methods that circumvent this difficulty by relying only on samples from the simulator, rather than likelihood evaluations (Cranmer, Brehmer and Louppe, 2020; Hartig et al., 2011). The term *likelihood-free inference* is often used synonymously. In particular, we consider SBI to include purely black box methods which operate only on samples from $p(y | \theta)$, as well as those that utilize samples from $p_z(z | \theta)$ and exploit some tractable structure in $p(y | \theta, z)$. Such approaches vary widely, with their applicability depending on the simulator cost and computational budget, as well as the presence of structure in Equation (9) that can be exploited. We describe several categories of methods below, each of which can be understood as a means of constructing a tractable likelihood approximation $\widehat{L}(\theta) \approx p(y_o | \theta)$ using information from simulator runs. The resulting (approximate) unnormalized posterior density is thus subject to even more severe computational limitations as compared to $\tilde{\pi}(\theta)$ in the deterministic setting, due to the fact that computing $\widehat{L}(\theta)$ typically requires multiple replicate simulations at the same input θ . Our goal here is not to provide a comprehensive survey of SBI, but rather to highlight classes of methods that are amenable to emulation, in the sense made precise in Section 3.

2.3.1. Pseudo-Marginal Methods

In the case that $L(\theta)$ is intractable but the density $p(y | \theta, z)$ can be evaluated, then an unbiased likelihood estimate is given by

$$\bar{L}^M(\theta) := \frac{1}{M} \sum_{m=1}^M p(y_o | \theta, z_m), \quad z_m \stackrel{\text{iid}}{\sim} p_z(\cdot | \theta), \quad (10)$$

such that $\mathbb{E}_z[\bar{L}^M(\theta)] = L(\theta)$, where the expectation is respect to the simulated $\{z_m\}$. When p_z cannot be directly sampled, importance sampling and sequential Monte Carlo methods are commonly employed (Andrieu, Doucet and Holenstein, 2010). It turns out that this is sufficient to construct MCMC algorithms that exactly target the true posterior π (Andrieu and Roberts, 2009). However, the performance of these *pseudo-marginal* methods degrades when the variance of the likelihood estimate is high, which is often the case when the latent space is high-dimensional or the proposal distribution for z is poor (Deligiannidis, Doucet and Pitt, 2018). The practical application of pseudo-marginal samplers often requires many simulator calls at each value of θ in order to control the estimator variance, which is intractable for very expensive computer models. *Monte Carlo within Metropolis (MCwM)*, a closely related algorithm, can exhibit better mixing with smaller values of M , but implicitly targets an approximation to the true posterior (Alquier et al., 2016; Medina-Aguayo, Lee and Roberts, 2016).

2.3.2. Classical Likelihood-Free Methods

We next describe *Approximate Bayesian Computation* and *Synthetic Likelihood*, two classical statistical frameworks for conducting SBI. These approaches assume only the ability to generate samples $y \sim p(y | \theta)$ from the generative model defined in Equation (9).

Approximate Bayesian Computation. Approximate Bayesian Computation (ABC) refers to a broad class of methods that target approximate posteriors of the form $\hat{\pi}(\theta) \propto \pi_0(\theta)\hat{L}(\theta)$, where

$$\hat{L}(\theta) = \int \kappa_\epsilon(\mathcal{S}(y), \mathcal{S}(y_o))p(y | \theta)dy. \quad (11)$$

The likelihood is thus approximated non-parametrically by specifying some smoothing kernel κ_ϵ with bandwidth ϵ and a choice of summary statistics $\mathcal{S} : \mathbb{Y} \rightarrow \mathbb{R}^S$ (Sunnåker et al., 2013; Karabatsos and Leisen, 2018). This replaces the intractable likelihood with a smoothed version that weights simulated data y by its “closeness” to y_o . For example, if $\kappa_\epsilon(s, s') = \mathbf{1}(\|s - s'\| < \epsilon)$, then $\hat{\pi}(\theta) \propto \pi_0(\theta)p(\|\mathcal{S}(y) - \mathcal{S}(y_o)\| < \epsilon | \theta)$. Since the integral in Equation (11) is

typically intractable, the likelihood approximation is replaced with the noisy estimate

$$\bar{\mathcal{L}}^M(\theta) := \frac{1}{M} \sum_{m=1}^M \kappa_\epsilon(\mathcal{S}(y_m), \mathcal{S}(y_o)), \quad y_m \stackrel{\text{iid}}{\sim} p(y | \theta). \quad (12)$$

As in the pseudo-marginal setting, M simulator runs are required to evaluate the likelihood approximation at a point θ . Since the estimator is unbiased with respect to the likelihood in Equation (11), a pseudo-marginal algorithm can be used to target $\hat{\pi}$ (which is itself an approximation of π).

Synthetic Likelihood. As an alternative to the non-parametric ABC approximation, synthetic likelihood (SL) methods instead opt for the parametric model

$$\hat{\mathcal{L}}(\theta) = \mathcal{N}(\mathcal{S}(y_o) | m(\theta), C(\theta)), \quad (13)$$

resulting from a Gaussian assumption for the conditional $p(\mathcal{S}(y) | \theta)$ (Wood, 2010; Frazier et al., 2023; Price et al., 2018). Similar to ABC, the approximate likelihood is replaced with a noisy estimate

$$\bar{\mathcal{L}}^M(\theta) := \mathcal{N}(\mathcal{S}(y_o) | m_M(\theta), C_M(\theta)), \quad y_m \stackrel{\text{iid}}{\sim} p(y | \theta), \quad (14)$$

where $m_M(\theta)$ and $C_M(\theta)$ denote the sample mean and covariance of $\{\mathcal{S}(y_m)\}_{m=1}^M$. Pseudo-marginal and MCwM schemes can again be employed for inference. Unlike ABC, the Monte Carlo likelihood estimator is biased since $\mathbb{E}[\mathcal{N}(\mathcal{S}(y_o) | m_M(\theta), C_M(\theta))] \neq \mathcal{N}(\mathcal{S}(y_o) | m(\theta), C(\theta))$. This implies that the target distribution of a pseudo-marginal sampler is not equal to $\hat{\pi}$ and in general depends on M (Price et al., 2018).

2.3.3. Neural Density Estimation

The success of modern machine learning methods has inspired the use of more flexible conditional density estimators than those used in the classical likelihood-free approaches (Cranmer, Brehmer and Louppe, 2020). Various methods have been proposed to approximate the family of conditional densities $\{p(y | \theta)\}_{\theta \in \Theta}$ by fitting a predictive model that maps

$$\theta \mapsto q_\phi(y | \theta) \approx p(y | \theta). \quad (15)$$

The model q_ϕ is typically taken to be a neural network, with parameters ϕ estimated by minimizing the loss

$$\mathcal{L}(\phi) = - \sum_{m=1}^M \log q_\phi(y_m | \theta_m), \quad y_m \stackrel{\text{iid}}{\sim} p(y | \theta_m), \quad (16)$$

for a set of chosen points $\{\theta_m\}_{m=1}^M$. Once the model is trained, $q_\phi(y | \theta)$ can be evaluated at any pair (θ, y) without running additional simulations. Thus, unlike

the previous methods, evaluations of the approximate likelihood at new θ do not incur additional simulator cost (Zammit-Mangion, Sainsbury-Dale and Huser, 2025). Inference on the induced posterior approximation $\hat{\pi}(\theta) \propto \pi_0(\theta)q_\phi(y_o | \theta)$ is then carried out by standard methods such as MCMC. Similar workflows are used by related methods such as neural ratio estimation (Cranmer, Pavez and Louppe, 2015). We note that the MCMC step can be avoided by directly approximating the reverse conditional $y \mapsto q_\phi(\theta | y) \approx p(\theta | y)$, but such methods fall outside the scope of this paper (Papamakarios and Murray, 2016). A limitation of all neural density estimation strategies is that they typically require a large number of simulations to generate sufficient training data, limiting their applicability to expensive models (Scheurer et al., 2026).

3. Emulators in Bayesian Inference

Given the inference bottleneck imposed by computationally expensive models, many methods have been proposed to approximate the posterior using only a small set of simulator calls (Kennedy and O’Hagan, 2001; Marzouk and Najm, 2009; Higdon et al., 2015; Wang, Bui-Thanh and Ghattas, 2018). Many such approaches consist of replacing a computationally-limiting component of the model with a cheap *surrogate*, thus enabling the use of standard inference schemes on the resulting approximate model (Gramacy, 2020). In this section, we introduce the particular sub-class of surrogate models that form the focus of this article.

3.1. Regression-Based Emulators

While there is a vast literature on surrogates designed for specific model structures, we instead focus on the broadly applicable strategy of learning regression-based emulators from black-box model evaluations. Even within this class of surrogates, the regression modeling setup can vary widely, with a key decision being the choice of response variable to approximate with the regression model (Higdon et al., 2008; Özge Sürer, Plumlee and Wild, 2024; Ranjan et al., 2016).

Definition 1 (Emulator Target). We define the *emulator target* as the deterministic map $f : \Theta \rightarrow \mathbb{F}$ that the surrogate seeks to learn, where \mathbb{F} is the *target space* in which the emulated quantity lives.

When relevant, we will augment the notation from Section 2 to emphasize dependence on the target; e.g., $\pi(\theta; f)$, $L(\theta; f)$, $Z(f)$, etc. We make the assumption throughout that $\tilde{\pi}(\theta; f)$ depends on θ and f only as a function of $f(\theta)$. The target map should be chosen to alleviate the computational bottleneck; hence, the density $\tilde{\pi}(\theta; f)$ is cheap to compute once the expensive computation $f(\theta)$ is performed. We consider regression methods that approximate the target using training data $\{\theta_n, \varphi_n\}_{n=1}^N$ generated by evaluating f at a set of *design points* $\boldsymbol{\theta}_N := \{\theta_n\}_{n=1}^N$. The training responses φ_n may constitute noisy or indirect observations of $f(\theta_n)$.

Definition 2 (Simulator Observation Process). The *simulator observation process* is a stochastic process that, given an input $\theta \in \Theta$, produces an observation $\varphi(\theta) \in \Phi$ according to

$$\varphi(\theta) \sim \eta(\cdot \mid \mathbf{f}(\theta)), \quad (17)$$

where $\eta(\cdot \mid \mathbf{f}(\theta))$ is a probability measure on Φ . The simulator noise is not necessarily independent across θ , so in general $\varphi(\boldsymbol{\theta}) \sim \eta(\cdot \mid \mathbf{f}(\boldsymbol{\theta}))$ gives the joint distribution over the responses at a set of inputs $\boldsymbol{\theta} \subset \Theta$. The training responses thus take the form $\boldsymbol{\varphi}_N := \{\varphi_n\}_{n=1}^N \sim \eta(\cdot \mid \mathbf{f}(\boldsymbol{\theta}_N))$.

In many cases considered throughout this survey, the target space \mathbb{F} and simulator observation space Φ coincide; i.e., φ_n is a direct noisy observation of $\mathbf{f}(\theta_n)$. However, there are notable exceptions in which the simulator noise process is more complicated (e.g., Example 7 below). In the special case that these spaces coincide and the simulator observations are deterministic, we have $\eta(\cdot \mid \mathbf{f}(\theta)) = \delta_{\mathbf{f}(\theta)}(\cdot)$ and $\varphi_n = \mathbf{f}(\theta_n)$. The following examples identify target quantities that can be emulated to alleviate the computational burden in the problems described in Section 2.

Example 2 (Forward Model Target). Consider an inverse problem of the form $y = \mathcal{G}(\theta) + \epsilon$, as in Equation (3). In this case, we might set $\mathbf{f} := \mathcal{G}$, targeting the map implied by the forward model. If the forward model is deterministic, then $\varphi_n = \mathcal{G}(\theta_n)$, in which case the goal of the emulator is to interpolate the points $\{\theta_n, \mathcal{G}(\theta_n)\}_{n=1}^N$. Note that $\mathbb{Y} = \mathbb{F} = \Phi$; the observation space, target space, and simulator observation space coincide. \diamond

Example 3 (Log-Likelihood Target). Consider the same setup as Example 2. Instead of targeting the underlying forward model, another possibility is to target the (log) likelihood directly: $\mathbf{f}(\cdot) := \log \mathbf{L}(\cdot)$. Since the simulator is deterministic, then $\varphi_n = \log \mathbf{L}(\theta_n)$, so that the emulator seeks to interpolate the training data $\{\theta_n, \log \mathbf{L}(\theta_n)\}_{n=1}^N$. In this case, $\mathbb{F} = \Phi = \mathbb{R}$. \diamond

Example 4 (Noisy Forward Model Target). Again consider an inverse problem $y = \mathcal{G}(\theta) + \epsilon$, where now $\mathcal{G}(\theta) \sim \mathcal{N}(m(\theta), C(\theta))$. In this stochastic setting, one possible target is $\mathbf{f}(\cdot) := m(\cdot) = \mathbb{E}[\mathcal{G}(\cdot)]$. The simulator generates noisy observations via $\varphi(\theta) = m(\theta) + \epsilon(\theta)$, where $\epsilon(\theta) \sim \mathcal{N}(0, C(\theta))$ (i.e., $\eta(\cdot \mid \mathbf{f}(\theta)) = \mathcal{N}(\mathbf{f}(\theta), C(\theta))$). Therefore, the training observations are given by $\varphi_n \sim \mathcal{N}(\mathbf{f}(\theta_n), C(\theta_n))$ and the emulator seeks to smooth over the noisy training data $\{\theta_n, m(\theta_n) + \epsilon(\theta_n)\}_{n=1}^N$. As in Example 2, we have $\mathbb{Y} = \mathbb{F} = \Phi$. The computer experiments literature has explored many generalizations of this setup, including targeting other moments (e.g., $\mathbf{f}(\cdot) := [m(\cdot), C(\cdot)]$), or quantiles of the distribution of $\mathcal{G}(\theta)$ (Binois et al., 2018; Fadikar et al., 2018). \diamond

Example 5 (ABC/SL Noisy Log-Likelihood Target). Consider the SBI setting (Section 2.3.2) with an approximate likelihood $\widehat{\mathbf{L}}(\theta) \approx p(y_o \mid \theta)$ constructed using either ABC or SL. Both methods make use of noisy estimates $\bar{\mathbf{L}}^M(\theta) \approx \widehat{\mathbf{L}}(\theta)$ constructed from samples $\{y_m\}_{m=1}^M \sim p(y \mid \theta)$. To eliminate the requirement

for simulator runs at every evaluation point θ , one can instead fit an emulator targeting $f(\cdot) := \log \widehat{L}(\cdot)$ to sparse training data $\{\theta_n, \varphi_n\}_{n=1}^N$. The training response φ_n is generated by sampling $\{y_n^{(m)}\}_{m=1}^M \stackrel{\text{iid}}{\sim} p(y | \theta_n)$ and then computing the log-likelihood estimate $\varphi_n := \log \bar{L}^M(\theta_n)$ using $\{y_n^{(m)}\}_{m=1}^M$ (Wilkinson, 2014; Järvenpää et al., 2021). Here we have $\mathbb{F} = \Phi = \mathbb{R}$. Note that we maintain the convention that N is the number of design inputs θ_n . The number of simulator runs is NM due to replicate runs at the same inputs. One can also consider varying the number of replicate simulations based on the particular input (Binois et al., 2018). \diamond

Example 6 (Pseudo-Marginal Noisy Log-Likelihood Target). Consider the pseudo-marginal setting from Section 2.3.1, in which a noisy, unbiased likelihood estimator is given by $\bar{L}^M(\theta) = M^{-1} \sum_{m=1}^M p(y_o | z_m, \theta)$, where $z_m \stackrel{\text{iid}}{\sim} p_z(\cdot | \theta)$. As in Example 5, the need to run the simulator at each new θ can be addressed by fitting an emulator targeting $f(\cdot) := \log L(\theta)$ (Drovandi, Moores and Boys, 2018). However, in this case the target is the *exact* log-likelihood, since unbiased likelihood estimates are available in the pseudo-marginal setting. A training observation at input θ_n is constructed by sampling $\{z_n^{(m)}\}_{m=1}^M \stackrel{\text{iid}}{\sim} p_z(\cdot | \theta_n)$ and computing the log-likelihood estimate $\varphi_n := \log \bar{L}^M(\theta_n)$ using $\{z_n^{(m)}\}_{m=1}^M$. Again we have $\mathbb{F} = \Phi = \mathbb{R}$. \diamond

Example 7 (Conditional Density Target). Consider the approach to conditional density estimation described in Section 2.3.3, in which training pairs $\{\theta_n, y_n\}_{n=1}^N$ generated via $y_n \stackrel{\text{iid}}{\sim} p(y | \theta_n)$ are used to optimize the parameters ϕ of a flexible conditional density estimator $q_\phi(y | \theta) \approx p(y | \theta)$. In this case, the emulator directly targets the conditional density $f(\theta) := p(\cdot | \theta)$, implying that \mathbb{F} is a space of probability densities over \mathbb{Y} . In practice, y is often replaced by hand-crafted or learned summary statistics $\mathcal{S}(y)$, but we suppress this in the notation for brevity (Radev et al., 2020). The simulator observation process is given by $\varphi(\theta) = y \sim \eta(\cdot | f(\theta))$, where $\eta(\cdot | p(\cdot | \theta)) = p(\cdot | \theta)$. That is, the target $f(\theta)$ is a probability distribution, and the simulator observation $\varphi(\theta)$ is a sample from that distribution. Here, $\Phi = \mathbb{Y}$, while \mathbb{F} is a space of densities over \mathbb{Y} . This problem is thus structurally distinct from the previous examples, in that the training observations $\varphi_n = y_n$ provide only indirect information about the target f . \diamond

The preceding examples describe several modeling setups that yield training data $\mathcal{D}_N := \{\theta_n, \varphi_n\}_{n=1}^N$. We define a *regression-based emulator* as a predictive model f_N (e.g., a regressor or interpolator) fit to training data of this form. If f_N is deterministic (i.e., $f_N(\theta)$ is a point prediction of $f(\theta)$), then the induced density approximation $\tilde{\pi}(\theta; f_N)$ can be fed to standard inference algorithms such as MCMC, provided that emulator predictions can be computed relatively cheaply (here let $\tilde{\pi}$ be the exact density or a target approximation as in the ABC/SL case). However, as noted in the introduction, this raises the concern

that the posterior estimate can be simultaneously biased and overconfident. Two complementary strategies to mitigate this concern are to (1) reduce the error by generating more training data and (2) propagate the surrogate uncertainty. As both are facilitated by emulators equipped with a notion of predictive uncertainty, we henceforth focus on *probabilistic emulators*—models that provide predictions in the form of probability distributions.

Remark 2. The terms “emulator” and “surrogate” are widely used in the literature in varying contexts, often synonymously. In this review, we reserve the term *emulator* for the predictive model f_N that directly approximates the target f . We use *surrogate* more broadly for any downstream quantity that depends on f_N . For example, $\pi(\theta; f_N)$ is the surrogate density for $\pi(\theta; f)$ that is induced by the underlying emulator f_N .

3.2. Probabilistic Emulators

In general, we allow f_N to be any model that provides a predictive distribution, such that $f_N(\theta)$ is a random quantity summarizing uncertainty in the true target value $f(\theta)$. To encompass both parametric and nonparametric models (e.g., Gaussian processes), we adopt the general perspective of f_N as a random function. Conceptually, we think of the randomness in f_N as quantifying *epistemic uncertainty*, which in principle could be reduced, were it computationally feasible to evaluate f at any given input (Hüllermeier and Waegeman, 2021).

Definition 3 (Probabilistic Emulator). Given training data \mathcal{D}_N generated as described in Definition 2, a *probabilistic emulator* is a random function $f_N : \Theta \rightarrow \mathbb{F}$ whose distribution ν_N depends on \mathcal{D}_N . For any finite collection $\boldsymbol{\theta} = \{\theta_b\}_{b=1}^B \subset \Theta$, we write $\nu_N(\boldsymbol{\theta})$ for the marginal distribution of $f_N(\boldsymbol{\theta}) = [f_N(\theta_1), \dots, f_N(\theta_B)]$ and $\nu_N(\theta)$ for the marginal at a single point.

The predictive distribution ν_N represents the uncertainty about the deterministic target f , not the variability in the simulator observation process φ . Any emulator satisfying our definition must therefore separate epistemic uncertainty from observation noise. This poses no limitation for standard surrogate constructions (e.g., a regression model with additive noise). In addition to ν_N , we will find it useful to consider the predictive distribution $p(\varphi(\theta) \mid \mathcal{D}_N)$ over the simulator observation process.

Definition 4 (Predictive Simulator Observation Process). Given the prior simulator observation process $\varphi(\theta) \sim \eta(\cdot \mid f(\theta))$ and emulator $f_N \sim \nu_N$, let $\varphi_N(\theta)$ denote the predictive process over simulator observations, with distribution

$$\eta_N(\cdot \mid \theta) := \int \eta(\cdot \mid f(\theta)) \nu_N(df). \quad (18)$$

The quantity η_N represents a convolution of the epistemic uncertainty ν_N with the simulator noise η .

While in general f_N and φ_N may not even be defined over the same space, the following example demonstrates a special case where $\mathbb{F} = \Phi$ and the two processes are closely related.

Example 8. Suppose the simulator generates observations via the process

$$\varphi(\theta) = f(\theta) + \epsilon(\theta), \quad \epsilon(\theta) \sim \mathcal{N}(0, C(\theta)). \quad (19)$$

If the emulator produces Gaussian predictions $f_N(\theta) \sim \mathcal{N}(\mu_N(\theta), s_N^2(\theta))$ (independent of $\epsilon(\theta)$), then the predictive simulator observation process is given by

$$\varphi_N(\theta) \sim \mathcal{N}(\mu_N(\theta), s_N^2(\theta) + C(\theta)). \quad (20)$$

In this case, f_N and φ_N have the same expectation, and differ only in that the covariance of the latter accounts for the sampling variability $\epsilon(\theta)$ of the observation process. This special case arises in standard Gaussian process modeling setups (see Section 3.3.1). \diamond

The following notation is used throughout the remainder of the paper. Let \mathbb{E}_{ν_N} denote expectation with respect to ν_N . Supposing for the moment that $\mathbb{F} = \mathbb{R}$, define the pointwise predictive mean $\mu_N(\theta) := \mathbb{E}_{\nu_N}[f_N(\theta)]$ and variance $s_N^2(\theta) := \text{Var}_{\nu_N}[f_N(\theta)]$. While some emulators provide only pointwise predictions, many also encode correlational structure across input values. We thus denote the covariance $k_N(\theta, \theta') := \text{Cov}_{\nu_N}[f_N(\theta), f_N(\theta')]$, noting that $k_N(\theta, \theta) = s_N^2(\theta)$. For a batch $\boldsymbol{\theta}$ of B inputs, $\mu_N(\boldsymbol{\theta})$ and $s_N^2(\boldsymbol{\theta})$ are the mean vector and covariance matrix of $f_N(\boldsymbol{\theta})$, respectively. Similarly, given another set $\boldsymbol{\theta}'$ of B' inputs, we write $k_N(\boldsymbol{\theta}, \boldsymbol{\theta}')$ to denote the $B \times B'$ cross covariance. In the case that $\mathbb{F} = \mathbb{R}^S$ for some finite integer S , we interpret $\mu_N(\boldsymbol{\theta})$ and $s_N^2(\boldsymbol{\theta})$ as the predictive mean vector and covariance matrix over the different output dimensions. To avoid complicating notation, we do not extend the vectorized input notation $\mu_N(\boldsymbol{\theta})$ to the multi-output setting. We make clarifying remarks when necessary to avoid ambiguity. We use analogous notation for expectations with respect to η_N .

The randomness in the emulator induces randomness in downstream quantities such as $Z(f_N)$, $\tilde{\pi}(\cdot; f_N)$, and $\pi(\cdot; f_N)$. When discussing such induced random variables we make use of the shorthands Z_N , $\tilde{\pi}_N$, and π_N when explicit reference to the underlying emulator is not necessary. For a deterministic surrogate, the induced approximation to the posterior distribution is immediate. In the probabilistic setting, it is not immediately clear how to perform approximate inference using the random posterior π_N , a topic discussed in depth in Section 4.

3.3. Common Model Classes

In this section, we highlight several popular models that fall under our definition of *probabilistic surrogate*.

3.3.1. Gaussian Processes

Gaussian processes (GPs) are widely used as surrogate models, with extensive applications in response surface modeling for computer experiments (Sacks et al., 1989; Satner, Williams and Notz, 2018), black-box optimization (Shahriari et al., 2016), reliability analysis (Pritam Ranjan and Michailidis, 2008; Cole et al., 2023), and parameter calibration (Kennedy and O’Hagan, 2001; Sung and Tuo, 2024). For in-depth treatments, we refer to Gramacy (2020); Rasmussen (2004); Helin et al. (2024).

A typical GP-based workflow consists of specifying a prior $f_0 \sim \mathcal{GP}(\mu_0, k_0)$ over the target function f , defined by a prior mean function $\mu_0(\cdot)$ and covariance function (i.e., kernel) $k_0(\cdot, \cdot)$. The defining property of a GP is its Gaussian finite-dimensional marginal distributions $f_0(\boldsymbol{\theta}) \sim \mathcal{N}(\mu_0(\boldsymbol{\theta}), k_0(\boldsymbol{\theta}, \boldsymbol{\theta}))$. Commonly, the hyperparameters defining the mean and kernel are optimized, though Bayesian treatments are also possible (Riis et al., 2022). With fixed hyperparameters and Gaussian observation noise $\varphi(\boldsymbol{\theta}) \mid f \sim \mathcal{N}(f(\boldsymbol{\theta}), \sigma^2 I)$, the emulator is constructed by closed-form conditioning $f_N := f_0 \mid [\varphi(\boldsymbol{\theta}_N) = \boldsymbol{\varphi}_N] \sim \mathcal{GP}(\mu_N, k_N)$, with the conditional mean and kernel given by

$$\begin{aligned} \mu_N(\boldsymbol{\theta}) &= \mu_0(\boldsymbol{\theta}) + k_0(\boldsymbol{\theta}, \boldsymbol{\theta}_N)K^{-1}[\boldsymbol{\varphi}_N - \mu_0(\boldsymbol{\theta}_N)] \\ k_N(\boldsymbol{\theta}, \boldsymbol{\theta}) &= k_0(\boldsymbol{\theta}, \boldsymbol{\theta}) - k_0(\boldsymbol{\theta}, \boldsymbol{\theta}_N)K^{-1}k_0(\boldsymbol{\theta}_N, \boldsymbol{\theta}), \end{aligned} \quad (21)$$

where $K := k_0(\boldsymbol{\theta}_N, \boldsymbol{\theta}_N) + \sigma^2 I$. The predictive observation process is likewise given by the conditional $\varphi_N := \varphi \mid [\varphi(\boldsymbol{\theta}_N) = \boldsymbol{\varphi}_N]$. The result is again a GP of the form in Equation (21), with the one modification that the predictive covariance $k_N(\boldsymbol{\theta}, \boldsymbol{\theta}) + \sigma^2 I$ accounts for the observation noise. The relationship between f_N and φ_N follows that given in Example 8.

Thus, in their most basic form GP surrogates are Gaussian predictors $f_N(\boldsymbol{\theta}) \sim \mathcal{N}(\mu_N(\boldsymbol{\theta}), s_N^2(\boldsymbol{\theta}))$, where $s_N^2(\boldsymbol{\theta}) = k_N(\boldsymbol{\theta}, \boldsymbol{\theta})$. Extensions of the GP methodology can produce more flexible emulators with non-Gaussian predictive distributions. A non-Gaussian noise model breaks the closed-form conditional and requires numerical methods for inference (e.g., MCMC). Other extensions include fully Bayesian GPs (Riis et al., 2022) and deep GPs (Sauer, Cooper and Gramacy, 2023; Sauer, Gramacy and Higdon, 2023), which typically yield predictions in the form of (infinite) mixtures of Gaussians.

3.3.2. Polynomials

Surrogates that consist of linear combinations of polynomial basis functions are commonly used in the engineering and applied mathematics literatures. Polynomial chaos expansions (PCEs; McClarren (2018, Chapter 9)) are a particular example whereby a polynomial basis is used to approximate a random variable $f(\boldsymbol{\theta})$ as a function of a random input $\boldsymbol{\theta} \sim \pi_0$. In particular, the expansion is of the form

$$f_R(\boldsymbol{\theta}) = \sum_{r=1}^R c_r \psi_r(\boldsymbol{\theta}), \quad (22)$$

where ψ_1, \dots, ψ_R are orthogonal polynomials with respect to π_0 . Once constructed, a PCE is often used to approximate moments of $f(\theta)$. More relevant to our context, the map $f_R(\theta)$ can also be used as a surrogate for $f(\theta)$. With fixed coefficients c_r , this map is deterministic and thus PCEs do not fall within our definition of probabilistic surrogates. We nonetheless highlight them here due to their popularity, the fact that they can be converted into random surrogates by considering Bayesian treatments of the coefficients (Bhattacharyya, 2020; Bürkner et al., 2023; Reiser et al., 2025), and their use in conjunction with probabilistic surrogates (e.g., as the mean function of a GP; Marinescu et al. (2023); Bradford and Imsland (2021); Sinsbeck and Nowak (2017)). PCE surrogates have been employed to accelerate Bayesian inversion in various applications (Marzouk and Najm, 2009; Reiser et al., 2025; Lu et al., 2015).

3.3.3. Neural Networks

In regimes where the input dimension D and computational budget N are large, neural networks are well-suited to serve as surrogate models. Bayesian treatment of neural network parameters provides probabilistic predictions, but in practice significant approximations are required for inference (Mena, Pujol and Vitrià, 2021; Li, Rudner and Wilson, 2024). Practical strategies include Laplace approximations (MacKay, 1992), variational inference (Graves, 2011), Monte Carlo dropout (Gal and Ghahramani, 2016), and partially Bayesian networks (Sharma et al., 2023; Tran et al., 2019). Another popular method is *deep ensembles*, which summarize uncertainty via an ensemble of neural networks with randomized initializations (Lakshminarayanan, Pritzel and Blundell, 2017; Lueckmann et al., 2019). Alternative approaches, such as *epinets*, produce predictive distributions without ensembling by modifying the architecture of a single neural network (Osband et al., 2023a,b). We refer to Abdar et al. (2021); He et al. (2025); Mena, Pujol and Vitrià (2021) for thorough surveys of uncertainty quantification in deep learning.

3.4. Finite vs. Infinite Dimensional Emulators

Since ν_N is a probability distribution over *functions*, $f \sim \nu_N$ is a trajectory (i.e., sample path) of f_N . While we adopt this functional perspective for generality, the randomness in f_N may stem from a finite set of parameters. To clarify this distinction, we call f_N *finite-dimensional* if it can be written as $f_N(\cdot) = g(\cdot; \phi_N)$ for some finite-dimensional random vector ϕ_N and non-random function g . When this is not possible, then f_N is *infinite-dimensional*. Standard parametric models (linear regression, neural networks) are finite-dimensional, while GPs (with standard choices of the kernel) are infinite-dimensional. A relevant consequence of this difference is that trajectories of finite-dimensional emulators can be sampled via

$$f(\cdot) := g(\cdot; \phi), \quad \phi \sim \text{law}(\phi_N), \quad (23)$$

where $\text{law}(\cdot)$ denotes the probability distribution of its argument. The sampled trajectory $f(\cdot)$ can now be evaluated at any input value. For infinite-dimensional models, it is computationally infeasible to sample trajectories, as this would require storing an infinite-dimensional function in computer memory. Instead, the surrogate can typically be characterized by the set of distributions $\nu_N(\boldsymbol{\theta})$ over finite-dimensional subsets $\boldsymbol{\theta}$. Infinite-dimensional GPs can be approximated by finite-dimensional models in various ways, often relying on a finite set of basis functions (Wilson et al., 2021, 2020).

3.5. Practical Considerations for Different Emulator Targets

While the choice of emulator target is inherently problem-dependent, one is often faced with multiple competing options for a particular problem. Section 3.1 presented several examples with varying targets; we now provide a more detailed discussion of their practical tradeoffs. To this end, we group different approaches into three broad classifications: *forward model emulation* (targeting the underlying forward map), *log-density emulation* (directly emulating the log of the likelihood or posterior surface), and *conditional density estimation* (learning a flexible parametric density estimator). The former two categories are also compared in Stuart and Teckentrup (2018); Bai, Teckentrup and Zygalakis (2024); Lie, Sullivan and Teckentrup (2018); Roberts, Dietze and Huggins (2026).

3.5.1. Forward Model Emulation

The high computational cost in Bayesian inverse problems stems primarily from the underlying forward model. A natural strategy to alleviate this bottleneck is to fit an emulator directly targeting \mathcal{G} , as in Examples 2 and 4. The following example analyzes the density surrogate $\tilde{\pi}(\boldsymbol{\theta}; f_N)$ induced by an underlying forward model emulator f_N , under Gaussian assumptions.

Example 9 (Forward Model Emulation, Gaussian Setting). Consider the setting of a Bayesian inverse problem with an additive Gaussian noise model (Equation (3)). Assume an emulator f_N has been fit to approximate the true forward model \mathcal{G} . This induces an approximation of the unnormalized posterior density

$$\tilde{\pi}(\boldsymbol{\theta}; f_N) = \pi_0(\boldsymbol{\theta})\mathcal{N}(y_o | f_N(\boldsymbol{\theta}), \Sigma), \quad (24)$$

for each $\boldsymbol{\theta} \in \Theta$. In general, the distribution of $\tilde{\pi}(\boldsymbol{\theta}; f_N)$ depends on the predictive distribution of f_N . The additional assumption $f_N(\boldsymbol{\theta}) \sim \mathcal{N}(\mu_N(\boldsymbol{\theta}), s_N^2(\boldsymbol{\theta}))$ facilitates closed-form computation of the first two moments,

$$\begin{aligned} \mathbb{E}_{\nu_N} [\tilde{\pi}(\boldsymbol{\theta}; f_N)] &= \pi_0(\boldsymbol{\theta})\mathcal{N}(y_o | \mu_N(\boldsymbol{\theta}), \Sigma + s_N^2(\boldsymbol{\theta})) \\ \text{Var}_{\nu_N} [\tilde{\pi}(\boldsymbol{\theta}; f_N)] &= \pi_0^2(\boldsymbol{\theta}) \left[\frac{\mathcal{N}(y_o | \mu_N(\boldsymbol{\theta}), \frac{1}{2}\Sigma + s_N^2(\boldsymbol{\theta}))}{\det(2\pi\Sigma)^{1/2}} - \frac{\mathcal{N}(y_o | \mu_N(\boldsymbol{\theta}), \frac{1}{2}[\Sigma + s_N^2(\boldsymbol{\theta})])}{\det(2\pi[\Sigma + s_N^2(\boldsymbol{\theta})])^{1/2}} \right], \end{aligned}$$

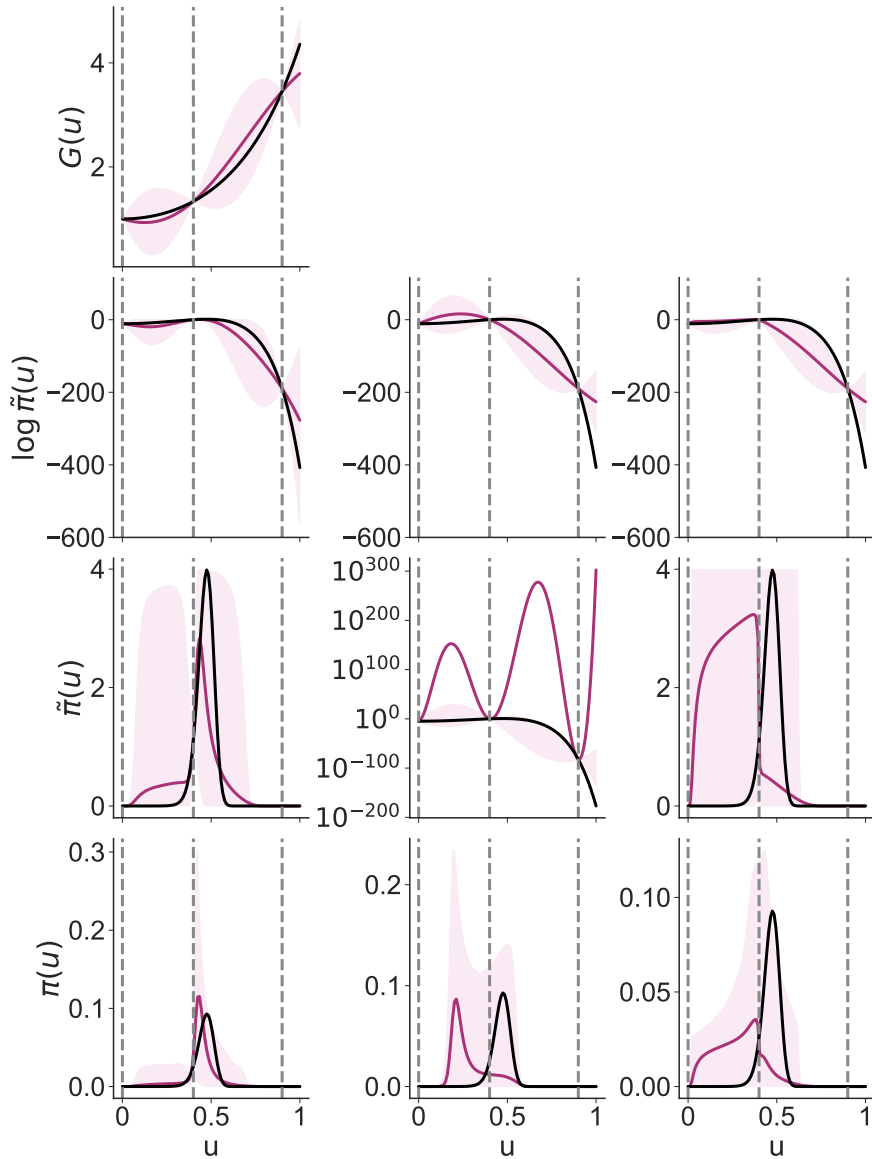


FIG 3. Pushforward distributions induced by GP forward model emulator (left column), GP log-posterior emulator (middle column), and a clipped (upper bounded) GP log-posterior emulator (right column). The plots summarize the pointwise marginal distributions of each quantity; in particular, the means (magenta lines) and 95% credible intervals (shaded regions). The black lines are ground truth (no emulation) and the gray dashed lines indicate the locations of the design inputs used to train the surrogates. The respective rows represent the surrogate-induced distributions over the (1) forward model, (2) unnormalized log-posterior density, (3) unnormalized posterior density, and (4) normalized posterior density. The top middle and top right entries are blank because the log-density surrogates do not produce an approximation of the forward model. The magenta lines in the third and fourth rows represent $\hat{\pi}_N^{\text{sup}}$ and $\hat{\pi}_N^{\text{op}}$, respectively (see Section 4).

a fact that has been leveraged frequently in the literature (Stuart and Teckentrup, 2018; Bai, Teckentrup and Zygalakis, 2024; Zhang et al., 2020, 2016; Özge Sürer, Plumlee and Wild, 2024; Villani, Unger and Weiser, 2024; Lartaud, Humbert and Garnier, 2024; Dunbar et al., 2021; Cleary et al., 2021). The left column of Figure 3 visualizes how the uncertainty in a GP forward model emulator propagates to downstream quantities within this setting. \diamond

In general, the architecture of a forward model emulator is dictated by the properties of the forward model itself. A common challenge in this context is the high dimensionality of the observation space, particularly for models with complex spatial or temporal structure; examples include epidemic modeling (Fadikar et al., 2018), engineering design (Yeh et al., 2017), ecological forecasting (Dietzel and Reichert, 2014; Dagon et al., 2020), and climate modeling (Schneider et al., 2017; Dunbar et al., 2021). Emulators for such complex model outputs typically rely on some form of dimensionality reduction. Common approaches include:

1. *Basis Expansion*: Representing the model output with respect to a small number of basis vectors, and emulating the scalar basis coefficients (e.g., via principal components analysis or proper orthogonal decomposition; Higdon et al. (2008); Fadikar et al. (2018); Yeh et al. (2017)).
2. *Feature Extraction*: Targeting low-dimensional summary statistics of the model outputs (Schneider et al., 2017; Dunbar et al., 2021; Huang et al., 2016; Ray et al., 2015). In ABC/SL, this implies emulating the same summary statistics used to form the approximate likelihoods (Meeds and Welling, 2014).
3. *Specialized Architectures*: Exploiting the recursive structure of model outputs for forward models with dynamical structure (Conti et al., 2009; Conti and O’Hagan, 2010; Liu and West, 2009; Mohammadi, Challenor and Goodfellow, 2019; Aakula, Fer and Vira, 2025).

Other options include emulating each output independently (Eriksson and Poloczek, 2021; Huang et al., 2020; Özge Sürer, Plumlee and Wild, 2024; Meeds and Welling, 2014) or adopting a tractable model for cross-output correlations (Bonilla, Chai and Williams, 2007; Maddox et al., 2021).

Despite these challenges, there are many practical benefits to the forward model emulation strategy. Practitioners often wish to perform various tasks using the forward model, aside from parameter estimation (e.g., sensitivity analysis). A forward model surrogate may be re-used across different tasks. Moreover, in principle f_N does not depend on either the observed data or the particular statistical model (the prior and likelihood). Therefore, the cost of emulator training is *amortized* over multiple data realizations y_o or changes to the statistical model. However, in practice the design of the forward model may be inherently intertwined with the data, limiting the potential for amortization.

Example 10 (Limitations of Amortization). Consider the setting from Example 1, which considers dynamical models of the form $\frac{dx}{dt}x(t, \theta) = F(x(t, \theta), \theta)$. Suppose the observed data y_o consists of noisy monthly averages of one of the

state variables. A natural emulation strategy is to target the corresponding monthly averages of the model outputs. However, this construction ties the emulator to the structure of the data. If statistical considerations lead one to change the temporal resolution of y_o to weekly averages, the emulator will need to be re-structured and trained again. Even if the data structure is constant, in order to be re-used for new data realizations y_o the emulator must also account for the fact that underlying forcing data and initial conditions will also change. Specialty emulators for dynamic models seek to address this challenge (Conti et al., 2009). \diamond

3.5.2. Log-Density Emulation

Given that most posterior inference algorithms require only an unnormalized density as input, an alternative to forward model emulation is to directly target the log-likelihood or the unnormalized log-posterior, approaches we collectively refer to as *log-density emulation*. While one could also consider modeling the likelihood or posterior surface directly, emulating on the log scale is generally preferred to improve numerical stability, enforce non-negativity of the resulting density approximation, and yield a smoother target surface (Wang and Li, 2018; Wilkinson, 2014). The following example analyzes the density surrogate $\tilde{\pi}(\theta; f_N)$ induced by a log-likelihood emulator f_N , under Gaussian assumptions.

Example 11 (Log-Likelihood Emulation, Gaussian Setting). In the case that the emulator is fit to the log-likelihood, the induced unnormalized posterior approximation is of the form

$$\tilde{\pi}(\theta; f_N) = \pi_0(\theta) \exp\{f_N(\theta)\}. \quad (25)$$

Under the assumption $f_N(\theta) \sim \mathcal{N}(\mu_N(\theta), s_N^2(\theta))$, this quantity is log-normally distributed, with moments

$$\begin{aligned} \mathbb{E}_{\nu_N} [\tilde{\pi}(\theta; f_N)] &= \pi_0(\theta) \exp\left\{\mu_N(\theta) + \frac{1}{2}s_N^2(\theta)\right\} \\ \text{Var}_{\nu_N} [\tilde{\pi}(\theta; f_N)] &= \pi_0^2(\theta) [\exp\{s_N^2(\theta)\} - 1] \exp\{2\mu_N(\theta) + s_N^2(\theta)\}, \end{aligned} \quad (26)$$

a fact noted in Drovandi, Moores and Boys (2018); Järvenpää et al. (2021); Helin et al. (2024); Bai, Teckentrup and Zygalakis (2024). Gaussian process log-density emulators have been used both for deterministic inverse problems (Helin et al., 2024; Bai, Teckentrup and Zygalakis, 2024; Dinkel et al., 2024; Riccius et al., 2026; Joseph et al., 2015; Kim and Sanz-Alonso, 2024; Riccius et al., 2026; Fer et al., 2018; Keetz et al., 2025), as well as in the SBI setting (Wilkinson, 2014; Drovandi, Moores and Boys, 2018; Lebel et al., 2019; Oakley and Youngman, 2017; Järvenpää et al., 2021; Järvenpää and Corander, 2024).

The predictive distribution of a GP log-density emulator is plotted in Figure 3 (second row, second column). Inspecting the induced distribution $\tilde{\pi}_N$ (third row, second column), we see that the predictive mean $\mathbb{E}_{\nu_N} [\tilde{\pi}_N(\theta)]$ is highly sensitive

to the GP variance, providing a poor summary of $\tilde{\pi}_N$. The third column shows how this sensitivity is reduced when an upper bound is enforced on the emulator predictive distribution. \diamond

The primary appeal of log-density emulation is that it collapses a potentially high-dimensional observation space into a single scalar output (Ranjan et al., 2016; Lebel et al., 2019; Astudillo and Frazier, 2019). However, this simplification introduces several challenges. Log-densities often exhibit a large dynamic range and nonstationary behavior, which can be difficult for standard surrogates to capture (Wang and Li, 2018; Özge Sürer, Plumlee and Wild, 2024; Wilkinson, 2014). Furthermore, because additive errors in the log-domain become multiplicative errors when exponentiated, the resulting posterior approximations are highly sensitive to emulator misspecification (Roberts, Dietze and Huggins, 2026). A further complication arises when likelihood parameters (e.g., the noise covariance Σ in Equation (3)) are unknown. While one can expand the emulator’s input space to include these parameters (Bliznyuk et al., 2008; Dietzel and Reichert, 2014), this increases the input dimensionality and can further complicate the target surface. Alternatively, some likelihoods admit a sufficient statistic that can be emulated independently of the likelihood parameters (Fer et al., 2018). This is similar in spirit to emulating a measure of discrepancy between the observed and simulated data in ABC applications (Gutmann and Corander, 2016; Järvenpää et al., 2019). Finally, we note that log-density emulators are fit with respect to a particular data realization y_o and statistical modeling setup. While forward model emulators offer some potential for amortizing the training cost over changes in y_o or the model (subject to caveats; see Example 10), log-density emulators are by design dependent on fixed values of these quantities.

Log-Likelihood vs. Log-Posterior Emulation. Since the prior density is typically cheap to evaluate, it appears natural to approximate only the log-likelihood. However, several studies opt to emulate the unnormalized log-posterior directly (Dietzel and Reichert, 2014; Kandasamy, Schneider and Póczos, 2017; Kim and Sanz-Alonso, 2024). While the choice may seem numerically inconsequential (one can be converted to the other via a deterministic shift by the log-prior), there are tradeoffs to consider. Emulating the log-posterior allows one to incorporate within the surrogate the known constraint that the posterior must decay in the tails. In contrast, the log-likelihood’s tail behavior may be difficult to characterize a priori, presenting an additional challenge for surrogate model specification. Conversely, constraining tail behavior in certain surrogate models (e.g., GPs) can be difficult, and the failure to do so in log-posterior emulation can lead to pathological results (Järvenpää and Corander, 2024). Another downside of log-posterior emulation is that the surrogate depends on the prior; any update to the prior model may necessitate re-training (depending on the probabilistic structure of the emulator). A final consideration is whether the log-posterior or log-likelihood surface is easier to emulate. In general, this will depend on the relative strength of the prior and the likelihood, as well as

their particular functional forms. In settings where the likelihood dominates the prior, the practical difference between these two target surfaces diminishes.

3.5.3. Conditional Density Emulation

We return to the setting of Section 2.3 and Example 7, in which a neural network $q_\phi(y | \theta)$ is trained to learn the mapping from θ to the corresponding conditional density $p(\cdot | \theta)$. The emulator targets the probability density itself, not its value at a particular point. The training responses are sampled from the conditionals $\varphi_n = y_n \sim p(y | \theta_n)$ at a set of design points $\{\theta_n\}$. As opposed to the preceding emulator classes, the responses are not simply noisy observations of the target. Nonetheless, this approach fits naturally within our framework for uncertainty propagation and active learning. Once an estimate ϕ_N for the neural network parameters is produced, the challenge shifts to performing inference using the surrogate $\tilde{\pi}_N(\theta) = \pi_0(\theta)q_{\phi_N}(y_o | \theta)$. In practice, ϕ_N is usually a point estimate and thus emulator uncertainty is not quantified. However, various techniques can be utilized to obtain a predictive distribution (see Section 3.3.3), and thus propagate emulator uncertainty during inference (Lueckmann et al., 2019).

As with the other emulator classes, the selection of the input training points θ_n is a design decision that will control the approximation accuracy in different regions of Θ (Papamakarios, Sterratt and Murray, 2019; Durkan, Papamakarios and Murray, 2018; Lueckmann et al., 2019). Design considerations are also influenced by whether the emulator is going to be applied to many different data realizations y_o or a single fixed observation. The former setting typically requires much larger upfront simulation cost, but this cost is amortized over subsequent datasets (Radev et al., 2020).

We note that the flexibility in the input design is not shared by the closely related approach of *neural posterior estimation*, which directly learns the posterior from samples (Papamakarios and Murray, 2016; Radev et al., 2020). This approach does not fall within our framework as it emulates a target as a function of y (rather than θ) and does not offer as much flexibility in the input design (samples θ_n must come from the prior, or otherwise be appropriately re-weighted).

Neural estimation methods often require generating a large amount of training data, making them inapplicable in the case of expensive simulators. Addressing this challenge is an active area of research (Bharti et al., 2025; Krouglova et al., 2025). One approach to enable neural estimation with limited simulator budgets is to incorporate a second layer of emulation, for example by using an underlying forward model emulator to generate training data for a conditional density estimator (Scheurer et al., 2026).

3.6. Model Checking and Diagnostics

Proper model checking and validation is an integral step in any statistical analysis. In addition to standard Bayesian model checking for the underlying statistical model (Gelman et al., 2013; Gabry et al., 2019), the emulator adds another

component which should be validated. The modular framework provides the opportunity to evaluate the emulator predictive performance (with respect to f) in isolation, as is standard for any predictive model. The particular evaluation metrics will depend on the model class, but standard techniques like cross-validation can be applied in conjunction with scoring rules for evaluating probabilistic predictions (Gneiting and Raftery, 2007). Diagnostics for GP emulators are discussed in Bastos and O’Hagan (2009).

In addition to evaluating f_N in isolation, the emulator fit should be validated with respect to its use in downstream posterior estimation; e.g., the quality of the induced approximations L_N , $\tilde{\pi}_N$, and π_N can be assessed. Reiser et al. (2025) adapt Bayesian simulation-based calibration checks to jointly validate the underlying statistical model, the emulator, and the posterior inference algorithm. One consideration that should be kept in mind is that $\pi_N(\cdot) = \pi(\cdot; f_N)$ is only well-defined if each trajectory $\tilde{\pi}(\cdot; f)$ is integrable, so that $Z(f)$ exists. This may not hold, for example, for a stationary GP over an unbounded domain Θ . Ideally, the emulator would encode the inductive bias that the posterior tails must decay. However, this is challenging in general and common practical solutions simply truncate the prior to avoid difficulties associated with tail behavior (Kim and Sanz-Alonso, 2024; Fer et al., 2018; Roberts, Dietze and Huggins, 2026). More careful theoretical treatment related to the existence of $Z(f)$ for GP emulators is detailed in Stuart and Teckentrup (2018); Lie, Sullivan and Teckentrup (2018).

4. Surrogate-Based Posterior Approximation

The ultimate objective of Bayesian inference is to characterize the posterior distribution π , which is then used for downstream decision-making. Consequently, the central challenge in surrogate-based Bayesian inference is not merely fitting the emulator, but effectively utilizing it to approximate π (Stuart and Teckentrup, 2018; Sinsbeck and Nowak, 2017). Any discrepancy between the emulator and the target map introduces bias into the posterior estimate. While iterative refinement can asymptotically eliminate this bias (Section 5), computational budgets often preclude this luxury. To mitigate bias and properly calibrate uncertainty, the surrogate’s predictive uncertainty must be acknowledged within the posterior approximation (Bilionis and Zabaras, 2013; Roberts, Dietze and Huggins, 2026). However, as noted by Reiser et al. (2025), there is no single “correct” mechanism for propagating surrogate uncertainty. In this section, we survey the conceptual frameworks for deriving these approximations and detail specific estimators proposed in the literature.

Remark 3. Throughout the remainder of the paper, we let π denote the target distribution for Bayesian inference. This is typically the exact posterior, but could also be the approximate targets $\hat{\pi}$ utilized in the ABC and SL settings (Section 2.3.2). Our aim is to focus on the uncertainty in the surrogate $\pi(\theta; f_N)$ induced by the emulator, not to analyze additional layers of approximation considered in methods like ABC/SL.

4.1. The Plug-In Mean

We begin by establishing a baseline: ignoring surrogate uncertainty entirely. The *plug-in mean* approximation replaces the random surrogate with its deterministic predictive mean μ_N , yielding:

$$\pi_N^{\text{mean}}(\theta) := \frac{\tilde{\pi}(\theta; \mu_N)}{Z(\mu_N)}. \quad (27)$$

While computationally straightforward and widely applied (Järvenpää et al., 2021; Lebel et al., 2019; Dietzel and Reichert, 2014; Reiser et al., 2025; Huang et al., 2016; Lueckmann et al., 2019; Bilonis and Zabarar, 2013), this approach is only justified if the emulator is highly accurate, an assumption rarely satisfied in complex problems. In general, disregarding the surrogate uncertainty leads to biased posterior approximations with miscalibrated uncertainties (Reiser et al., 2025; Bilonis and Zabarar, 2013; Stuart and Teckentrup, 2018; Roberts, Dietze and Huggins, 2026).

4.2. Frameworks for Constructing Posterior Estimators

To move beyond the plug-in baseline, we outline three conceptual frameworks that provide a rigorous foundation for the propagation of surrogate uncertainty.

4.2.1. Decision Theory for Normalized Density

Given that the emulator f_N is a random function, the induced posterior π_N is a random probability measure, provided that f_N is constructed such that this measure is well-defined. We generally treat π_N as a random density to avoid measure-theoretic technicalities. One principled approach is to construct a deterministic approximation that best summarizes the uncertainty encoded in π_N . Roberts, Dietze and Huggins (2026) formalize this via the variational objective

$$q_\star := \operatorname{argmin}_{q \in \mathcal{Q}} \mathbb{E}_{\nu_N}[\mathcal{L}(q, \pi_N)], \quad (28)$$

for a loss function \mathcal{L} and space of densities \mathcal{Q} . Estimators derived from this perspective naturally account for the coupling between the unnormalized density and the normalizing constant. However, the global dependence on Z_N (a function of the entire random function f_N) often renders inference challenging for approximations of this form. The random measure perspective is introduced in Stuart and Teckentrup (2018) and adopted in Roberts, Dietze and Huggins (2026); Helin et al. (2024); Lie, Sullivan and Teckentrup (2018); Teckentrup (2020).

4.2.2. Decision Theory for Unnormalized Density

To circumvent the difficulties stemming from the random normalizing constant, an alternative approach is to estimate the *unnormalized* density $\tilde{\pi}_N$ directly. When only the likelihood depends on the surrogate, this is often equivalent to producing an approximate likelihood. Working with the unnormalized density is computationally attractive as $\tilde{\pi}_N(\theta)$ depends only on the marginal distribution of $f_N(\theta)$. Adopting a decision-theoretic viewpoint (Sinsbeck and Nowak, 2017), we seek the estimator \tilde{q}_\star that minimizes the expected loss

$$\tilde{q}_\star := \operatorname{argmin}_{\tilde{q} \in \tilde{\mathcal{Q}}} \mathbb{E}_{\nu_N} [\mathcal{L}(\tilde{q}, \tilde{\pi}_N)], \quad (29)$$

over a set of candidate functions $\tilde{\mathcal{Q}}$. The final approximate posterior is obtained by normalizing \tilde{q}_\star post-hoc. While computationally convenient, these *pointwise estimators* ignore the correlation structure of the surrogate (Roberts, Dietze and Huggins, 2026), as well as the probabilistic coupling between Z_N and $\tilde{\pi}_N(\theta)$. This decision theoretic approach was originally proposed in Sinsbeck and Nowak (2017) and subsequently utilized in Järvenpää et al. (2019); Järvenpää et al. (2021); Järvenpää and Corander (2024); Helin et al. (2024).

4.2.3. Uncertainty Propagation via Computation

Finally, rather than defining an explicit target density, the posterior approximation can be defined *implicitly* as the output of a randomized algorithm. Järvenpää and Corander (2024) adopt this perspective, seeking to characterize how emulator uncertainty propagates through an MCMC algorithm. In this case, posterior inference is viewed as a direct forward propagation of surrogate uncertainty through the sampling machinery.

This viewpoint naturally leads to the modification of standard inference algorithms via the injection of additional noise; e.g., sampling emulator realizations at each iteration of an MCMC or importance sampling scheme. A comprehensive survey of such algorithms is presented in Llorente et al. (2025). Noisy MCMC schemes are studied in Alquier et al. (2016); Medina-Aguayo, Lee and Roberts (2016); Andrieu and Roberts (2009).

4.3. Concrete Posterior Estimators

We now examine specific estimators derived from these frameworks.

4.3.1. The Expected Posterior (EP)

Under the random measure framework (Section 4.2.1), minimizing the expected Kullback-Leibler (KL) divergence yields the mean of the random density, or the

expected posterior (EP; Reiser et al. (2025)):

$$\pi_N^{\text{ep}}(\theta) := \mathbb{E}_{\nu_N}[\pi_N(\theta)] = \int \pi(\theta; f) \nu_N(\text{d}f). \quad (30)$$

Roberts, Dietze and Huggins (2026) derive the EP from this viewpoint and argue for its use as a principled default posterior approximation in many applications. From the perspective of modular Bayesian inference, the EP can also be viewed as a *cut distribution*, provided that f_N is fit using Bayesian methods (Plummer, 2015; Reiser et al., 2025). In particular, supposing the emulator predictive distribution takes the form of a Bayesian posterior $\nu_N(f) \propto \nu_0(f)p(\mathcal{D}_N | f)$, then the EP arises as a KL-optimal approximation to the joint model

$$p(\theta, f, y, \mathcal{D}_N) = \pi_0(\theta)\nu_0(f)p(y | \theta, f)p(\mathcal{D}_N | f), \quad (31)$$

subject to the constraint that the f -marginal equals ν_N (and is thus not informed by y ; Roberts, Dietze and Huggins (2026)).

Functionally, the EP is a mixture distribution averaging the posteriors induced by all possible surrogate trajectories. This interpretation suggests a nested sampling scheme (Algorithm 1) to marginalize over the trajectories $f \sim \nu_N$.

Algorithm 1 Direct sampling from π_N^{ep}

```

1: function SAMPLEEP( $\pi_N, K, M$ )
2:   for  $k \leftarrow 1, \dots, K$  do ▷ Parallelizable
3:      $f^{(k)} \sim \nu_N$  ▷ Sample emulator trajectory
4:      $\theta^{(k,1)}, \dots, \theta^{(k,M)} \sim \pi(\cdot; f^{(k)})$  ▷ Sample posterior given trajectory
5:   end for
6:   return  $\{\theta^{(k,m)}\}_{1 \leq k \leq K, 1 \leq m \leq M}$ 
7: end function

```

A practical implementation of this algorithm typically employs Metropolis-within-Monte-Carlo (MwMC), in which a separate MCMC scheme is run for each iteration of the loop (line 2) in order to produce approximate samples $\theta^{(k,m)}$ from each posterior trajectory $\pi(\cdot; f^{(k)})$ (Garegnani, 2021; Reiser et al., 2025). However, sampling full trajectories (line 3) is non-trivial for infinite-dimensional models like GPs, a limitation that likely hindered early adoption of the EP (Stuart and Teckentrup, 2018; Sinsbeck and Nowak, 2017; Järvenpää et al., 2021). Recent advances utilize approximate inference schemes tailored to GP emulators to overcome this challenge (Roberts, Dietze and Huggins, 2026; Lebel et al., 2019).

4.3.2. The Expected Unnormalized Posterior (EUP)

To avoid integrating over the normalizing constant, as required by the EP, one can average the numerator and denominator independently. This yields the *ex-*

	Plug-In Mean	EUP	EP
Ratio Estimator	$\frac{\tilde{\pi}(\theta; \mathbb{E}_{\nu_N}[f_N])}{Z(\mathbb{E}_{\nu_N}[f_N])}$	$\frac{\mathbb{E}_{\nu_N}[\tilde{\pi}(\theta; f_N)]}{\mathbb{E}_{\nu_N}[Z(f_N)]}$	$\mathbb{E}_{\nu_N} \left[\frac{\tilde{\pi}(\theta; f_N)}{Z(f_N)} \right]$
Mixing Dist.	$\delta_{\mu_N}(df)$	$\nu_N(df y_o)$	$\nu_N(df)$

TABLE 1

Different perspectives on normalized density approximations defined by various forms of averaging. (Top) Interpretations as ratio estimators. The EUP is a ratio of expectations, while the EP is an expectation of a ratio. Only the EP considers the coupling between the numerator and denominator. (Bottom) Interpretations as mixture distributions of the form $\int \pi(\theta; f)\omega(df)$; i.e., a weighted mixture over surrogate-induced posterior trajectories. The bottom row gives the form of the mixing distribution $\omega(df)$ for each approximation. We write $\nu_N(df | y_o)$ to denote the distribution proportional to $Z(f)\nu_N(df)$, and δ_{μ_N} for the Dirac measure centered at μ_N .

pected unnormalized posterior (EUP) ¹

$$\pi_N^{\text{eup}}(\theta) := \frac{\mathbb{E}_{\nu_N}[\tilde{\pi}_N(\theta)]}{\mathbb{E}_{\nu_N}[Z_N]} = \int \pi(\theta; f)\nu_N(df | y_o), \quad (32)$$

where we have defined $\nu_N(df | y_o) \propto Z(f)\nu_N(df)$. Analogous to the EP, the EUP is also a mixture of posterior trajectories, but the mixing distribution re-weights ν_N by $Z(f)$ (which depends on y_o). Thus, the EUP up-weights trajectories $\pi(\theta; f)$ with high “evidence” $Z(f)$ (Roberts, Dietze and Huggins, 2026). The EUP also corresponds to the L^2 -optimal estimator under the unnormalized decision-theoretic framework from Section 4.2.2 (Sinsbeck and Nowak, 2017). Because the expectation $\mathbb{E}_{\nu_N}[\tilde{\pi}_N(\theta)]$ can often be computed in closed form (see examples below) or unbiasedly estimated, the EUP enables the use of standard MCMC or pseudo-marginal algorithms (Andrieu and Roberts, 2009; Garegnani, 2021; Drovandi, Moores and Boys, 2018).

The EUP was originally proposed in Bilonis and Zabarar (2013), in which it is derived as the marginal $p(\theta | y_o, \mathcal{D}_N)$ under the joint model in Equation (31). This implies that the EUP is not “modular” in the cut Bayesian inference sense—the feedback from y_o to f is introduced via the uncertainty propagation mechanism. The hierarchical perspective extends to the case where ν_N is not given by a Bayesian posterior; in particular, the EUP is the marginal $p(\theta | y_o)$ under the model

$$f \sim \nu_N, \quad \theta \sim \pi_0, \quad y | f, \theta \sim p(y | \theta, f). \quad (33)$$

Similar hierarchical modeling perspectives are considered in Sinsbeck and Nowak (2017); Stuart and Teckentrup (2018); Helin et al. (2024); Roberts, Dietze and Huggins (2026).

¹Stuart and Teckentrup (2018); Helin et al. (2024); Bai, Teckentrup and Zygalakis (2024) refer to this as the *marginal approximation*, while Reiser et al. (2025) instead use the term *expected likelihood*. We prefer *expected unnormalized posterior*, as used in Roberts, Dietze and Huggins (2026), since it also encompasses log-posterior emulators.

Bounds on the Hellinger distance between the EUP and ground truth posterior under GP emulators are proved in [Stuart and Teckentrup \(2018\)](#); [Helin et al. \(2024\)](#); [Lie, Sullivan and Teckentrup \(2018\)](#). [Roberts, Dietze and Huggins \(2026\)](#) study the EUP as an approximation to the EP, demonstrating that the two distributions can deviate when $\pi_N(\theta)$ and $Z(\theta)$ are highly correlated at particular “influential” values of θ , which is more likely to occur when the pointwise marginals $\tilde{\pi}_N(\theta)$ are heavy-tailed. [Table 1](#) compares the plug-in mean, EUP, and EP estimators as (i) ratio estimators, and (ii) mixture distributions aggregating surrogate-induced posterior trajectories.

Example 12 (EUP, Gaussian Forward Model Emulator). Consider the setting from [Example 9](#), where $\tilde{\pi}_N(\theta) = \pi_0(\theta)\mathcal{N}(y_o | f_N(\theta), \Sigma)$ and $f_N(\theta) \sim \mathcal{N}(\mu_N(\theta), s_N^2(\theta))$. Under these assumptions, the EUP is given by

$$\begin{aligned} \pi_N^{\text{EUP}}(\theta) &\propto \mathbb{E}_{\nu_N} [\pi_0(\theta)\mathcal{N}(y_o | f_N(\theta), \Sigma)] \\ &= \pi_0(\theta)\mathcal{N}(y_o | \mu_N(\theta), \Sigma + s_N^2(\theta)). \end{aligned} \quad (34)$$

Thus, in this setting the EUP admits a natural data space interpretation. The original inverse problem $y = \mathcal{G}(\theta) + \epsilon$ is replaced by $y = \mu_N(\theta) + \zeta_N(\theta) + \epsilon$, with the parameter-dependent noise term $\zeta_N(\theta) \sim \mathcal{N}(0, s_N^2(\theta))$ accounting for the uncertainty in the forward model ([Cleary et al., 2021](#); [Stuart and Teckentrup, 2018](#)). Observe that $\tilde{\pi}_N^{\text{EUP}}(\theta) \rightarrow \pi_0(\theta)$ as $s_N^2(\theta) \rightarrow \infty$, implying that ignorance about the true forward model results in prior reversion ([Roberts, Dietze and Huggins, 2026](#)). The particular EUP estimator in [Equation \(34\)](#) is utilized in [Özge Sürer, Plumlee and Wild \(2024\)](#); [Lartaud, Humbert and Garnier \(2024\)](#); [Helin et al. \(2024\)](#); [Bai, Teckentrup and Zygalakis \(2024\)](#); [Cleary et al. \(2021\)](#); [Dunbar et al. \(2021\)](#); [Villani, Unger and Weiser \(2024\)](#); [Zhang et al. \(2020, 2016\)](#). \diamond

Example 13 (EUP, Gaussian Log-Likelihood Emulator). Recall the setup from [Example 11](#), where $\tilde{\pi}_N(\theta) = \pi_0(\theta) \exp\{f_N(\theta)\}$ and $f_N(\theta) \sim \mathcal{N}(\mu_N(\theta), s_N^2(\theta))$. Under these assumptions, the EUP is given by

$$\begin{aligned} \pi_N^{\text{EUP}}(\theta) &\propto \mathbb{E}_{\nu_N} [\pi_0(\theta) \exp\{f_N(\theta)\}] \\ &= \pi_0(\theta) \exp\left\{\mu_N(\theta) + \frac{1}{2}s_N^2(\theta)\right\} \\ &= \tilde{\pi}_N^{\text{mean}}(\theta) \exp\left\{\frac{1}{2}s_N^2(\theta)\right\}. \end{aligned} \quad (35)$$

The final expression demonstrates that, in this setting, the EUP inflates the plug-in mean estimator where uncertainty is large ([Stuart and Teckentrup, 2018](#); [Helin et al., 2024](#); [Järvenpää et al., 2021](#)). The estimator scales very quickly as surrogate uncertainty increases, with $\tilde{\pi}_N^{\text{EUP}}(\theta) \rightarrow \infty$ as $s_N^2(\theta) \rightarrow \infty$. Thus, unlike the forward model analog in [Example 12](#), the EUP does not exhibit prior reversion under surrogate ignorance ([Roberts, Dietze and Huggins, 2026](#)). Due to the exponential dependence in [Equation \(35\)](#), this distribution can be

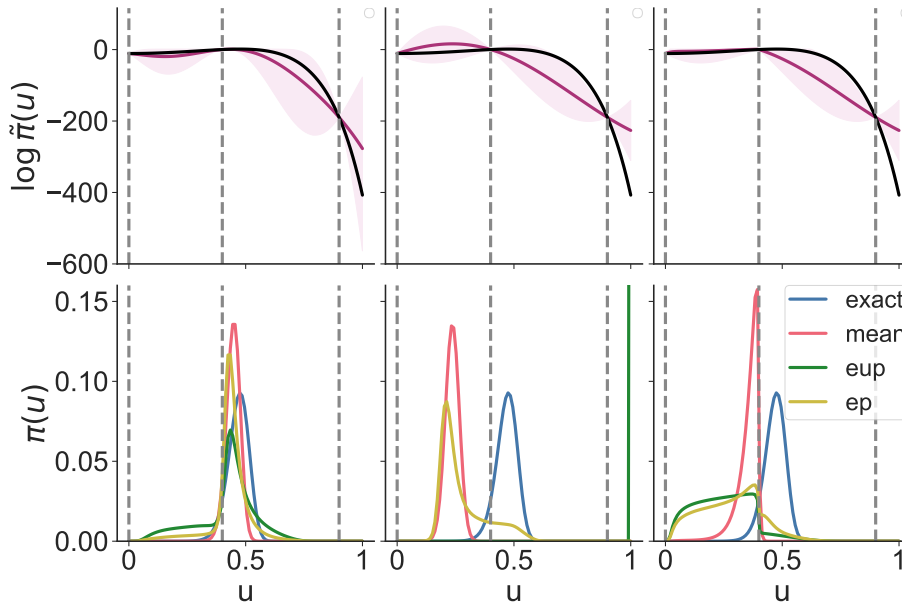


FIG 4. A continuation of the example in Figure 3. From left to right, the columns correspond to the GP forward model emulator, GP log-posterior emulator, and clipped (upper bounded) GP log-posterior emulator. The top row summarizes the pointwise marginal distributions of $\log \tilde{\pi}_N(\theta)$, showing the mean (magenta line) and 90% intervals against the true log-posterior (black). The bottom row presents different normalized posterior approximations relative to the true posterior (blue line). The vertical dashed lines indicate the locations of the design points.

highly sensitive to small changes in $\mu_N(\theta)$ and $s_N^2(\theta)$, making it particularly susceptible to extreme concentration in small regions with large uncertainty (Roberts, Dietze and Huggins, 2026; Järvenpää et al., 2021; Drovandi, Moores and Boys, 2018). This is illustrated in the second column of Figure 4; while the GP fit (first row) appears reasonable, the induced EUP is effectively a point mass centered at the most uncertain location, a pathology that the EP avoids. The third column illustrates that the EUP is stabilized by enforcing an upper bound on the GP predictive distribution. \diamond

4.3.3. Other Pointwise Estimators

The instability of the EUP in log-density emulation (Example 13) has motivated alternative pointwise estimators.

Marginal Quantiles. To improve robustness, Järvenpää et al. (2021) propose using pointwise quantiles of $\tilde{\pi}_N(\theta)$ rather than the mean. As detailed in

Example 14, setting the quantile probability $\alpha > 0.5$ inflates the posterior in regions with higher uncertainty, but scales more moderately relative to the EUP.

Marginal Modes. Järvenpää and Corander (2024) utilize the pointwise mode of $\tilde{\pi}_N(\theta)$. This effectively penalizes regions with high surrogate variance, encouraging the posterior to decay in these regions. While this can have the desirable effect of promoting tail decay in the posterior estimate, it neglects uncertain regions that may in reality contain posterior mass.

Expected Log-Likelihood. In the forward model emulation setting, Reiser et al. (2025) consider a posterior estimate proportional to $\pi_0(\theta) \exp\{\mathbb{E}_{\nu_N}[\log L(\theta; f_N)]\}$ and draw a connection with power-scaled likelihoods. However, the authors ultimately recommend the EP and EUP as preferred alternatives to this method.

Example 14 (Quantile Estimator, Gaussian Log-Likelihood Emulator). We return to the setting from Example 11 with a Gaussian log-likelihood emulator. Let $\mathbb{Q}^\alpha(\cdot)$ denote the $\alpha \in (0, 1)$ quantile of its argument with respect to ν_N . A quantile-based estimate in this setting takes the form

$$\begin{aligned} \pi_N^\alpha(\theta) &\propto \pi_0(\theta) \mathbb{Q}^\alpha(\exp\{f_N(\theta)\}) = \pi_0(\theta) \exp\{\mu_N(\theta) + q(\alpha)s_N(\theta)\} \\ &= \tilde{\pi}_N^{\text{mean}}(\theta) \exp\{q(\alpha)s_N(\theta)\}, \end{aligned}$$

where $q(\alpha)$ is the α -quantile of $\mathcal{N}(0, 1)$. This expression is of the same form as the EUP in Example 13, but the uncertainty inflation term scales more slowly as a function of $s_N(\theta)$. The special case $\alpha = 1/2$ (i.e., the median) reduces to the plug-mean approximation, while values $\alpha > 1/2$ imply the density will be inflated in regions of higher surrogate uncertainty. The quantile approximation arises from the unnormalized decision theoretic viewpoint by considering losses of the L^1 variety (Järvenpää et al., 2021; Järvenpää and Corander, 2024). Quantile-based estimators are also utilized in Dinkel et al. (2024); Keetz et al. (2025). \diamond

4.4. Comparison and Practical Recommendations

In general, there is no one-size-fits-all uncertainty propagation method; the best choice in a particular instance depends on the goals of the practitioner and the particular problem at hand. Following Roberts, Dietze and Huggins (2026), we recommend the EP as a reasonable default for problems where uncertainty calibration is of central importance or where the likelihood surrogate $L(\cdot; f_N)$ is misspecified with respect to $L(\cdot)$. The EP enforces a clear separation between learning \mathbf{f} and learning θ , which aligns with the view that the emulator is a computational artifact, rather than a true latent parameter in y_o 's data generating process. This separation is especially desirable when $L(\cdot; f_N)$ is misspecified, following from the fact that the EP can be interpreted as a cut posterior, which is specifically designed to mitigate problems of misspecification (Plummer, 2015;

Liu, Bayarri and Berger, 2009). The EP simply mixes together each component distribution $\pi(\cdot; f)$ with mixing weights $\nu_N(f)$. These weights encode the quality of the surrogate fit to the target, without considering the downstream fit to the data y_o . Generally speaking, the EP tends to be more diffuse (i.e., conservative) relative to the EUP, and more likely to preserve qualitative features such as multimodality in π_N (Roberts, Dietze and Huggins, 2026).

By contrast, the EUP weights each component distribution by $Z(f)\nu_N(f)$, where $Z(f)$ depends on y_o . Thus, the weight given to a posterior trajectory $\pi(\cdot; f)$ takes into account both the quality of the surrogate fit to the target, in addition to the marginal likelihood of y_o given f . This follows from a hierarchical Bayesian perspective where the emulator is treated as a latent variable governing the data generating process for y_o . The EUP yields a good approximation to the true posterior when $L(\cdot; f_N)$ is well-specified (the approximation is exact when $L(\cdot; f_N)$ is unbiased). However, under misspecification the EUP can produce undesirable and counterintuitive results. For example, a trajectory f may be a poor approximation to f , but the EUP may up-weight $\pi(\cdot; f)$ if the bad emulator prediction happens to fit the data y_o well. In general, weighting trajectories by $Z(f)$ is reasonable when a high value of $Z(f)$ provides a reliable signal of approximation quality. This happens when the true simulator is well-specified, and emulator approximation errors with respect to f degrade the overall model fit to y_o in a way that is reflected in $Z(f)$. In general, these conditions are difficult to satisfy. One clear example is the log-density emulation setting in Example 13. In this case, $Z(f)$ is artificially inflated by the emulator uncertainty, in which case the weights are a poor reflection of “evidence” for y_o . For a more thorough comparison of the EUP and EP, we refer to Roberts, Dietze and Huggins (2026); Reiser et al. (2025).

Loosely speaking, when the shape of $\pi(\cdot; f)$ does not vary significantly with f then the difference between the EUP and EP diminishes (Roberts, Dietze and Huggins, 2026). Certain emulators such as GPs naturally lead to greater shape variability relative to more constrained parametric approximations. If computational resources allow, both the EP and EUP can be computed to test the sensitivity to a particular method. In some cases, neither distribution may provide an adequate summary of π_N ; the final row of Figure 3 illustrates that the full distribution of this random posterior contains more information than any of the deterministic approximations alone provide. Further work is needed to develop computationally efficient means of summarizing this uncertainty. Moreover, in certain settings deterministic approximations other than the EP or EUP may be more adequate, such as those designed for robustness in specific cases (Frazier and Nott, 2025).

5. Active Learning for Bayesian Inversion

Up until this point, we have considered a fixed surrogate model fit to training data obtained from simulator runs at a set of design points $\theta_N := \{\theta_1, \dots, \theta_N\}$. The simplest approach to select these points is to sample from some distribution

over Θ (e.g., the prior π_0). Popular variants employ space-filling adjustments to encourage the design points to be spread out (Garud, Karimi and Kraft, 2017). Such a “one-shot” design is appealing in that it allows for maximal parallelism in simulator runs. However, the posterior distribution commonly concentrates on a small subset of the prior support, implying that a prior-based design will likely allocate the majority of points in regions with negligible posterior mass. In many such cases, one cannot hope to achieve an acceptable posterior approximation with a static design based solely on prior information.

To address this issue, the design can instead be constructed sequentially, with information from the current simulations used to inform the selection of new design points. We refer to this broad class of algorithms as *active learning* for Bayesian inverse problems. At the extreme end of this spectrum is a *pure sequential* strategy, where simulations are performed serially, one at a time. This allows for the most informed design point selection, but fails to exploit parallel computing resources and is thus impractical in many large-scale applications. To balance these extremes, practical approaches typically adopt a batch-sequential workflow: simulator runs are spread across multiple rounds, with a batch of model runs executed in parallel each round. For simplicity, we focus on this “synchronous parallel” setting, though asynchronous parallelism is also possible (Kandasamy et al., 2018).

The central challenge faced in active learning is navigating the “exploration vs. exploitation” trade-off (Shahriari et al., 2016; Badia et al., 2020). Algorithms must exploit current information to refine the surrogate in known high-probability regions, while simultaneously exploring high-uncertainty areas to avoid missing other important regions.

Active learning algorithms have been explored extensively in the context of Bayesian inference. Our focus here is on the sub-class of methods where design points are selected sequentially to refine a surrogate model with the goal of improving a posterior approximation. We identify three (non-mutually exclusive) strategies that are commonly used for this purpose:

1. *Design Optimization*: Explicitly optimizing an objective function to select the next batch of points.
2. *Tempering*: Constructing a sequence of intermediate target distributions to guide the surrogate toward the posterior.
3. *MCMC-based Exploration*: Embedding the design construction directly within a posterior sampling algorithm.

5.1. Design Optimization

Many active learning algorithms explicitly define a design criterion, or *acquisition function*, that quantifies the utility of running the simulator at a set of candidate locations. This objective function is then optimized at each round of the active learning procedure to select the next batch of design points. Similar approaches are also widely applied in other applications involving surrogate

models. For example, the field of Bayesian optimization focuses on defining acquisition functions tailored to the optimization of black-box functions (Shahriari et al., 2016). Acquisition functions for Bayesian inversion are analogous, but should instead encode the explicit goal of estimating the posterior distribution.

To better appreciate the considerations involved in defining an acquisition function, it is useful to consider how the criterion should behave in the absence of uncertainty. In Bayesian optimization, clearly the ideal behavior is to return the optimum of the function being optimized. In the present context, it is less clear which arrangement of points is optimal in representing a probability distribution with a surrogate model. Results suggest that the points should be sampled from an over-dispersed variant of the distribution, thereby ensuring adequate coverage of the tails (Helin et al., 2024; Briol et al., 2017). These results are consistent with the intuitive notion that design points should be placed in high-probability regions, while also ensuring adequate coverage to constrain the global surrogate behavior. With imperfect information, acquisition functions must balance this ideal with the need to reduce uncertainty in poorly explored regions.

The following sections explore design criteria that seek to navigate this particular flavor of an exploration-exploitation tradeoff. We begin by formalizing the problem, discuss theoretical frameworks used for deriving design criteria, and then offer a survey of concrete acquisitions used in the literature. We close the section with a brief discussion of practical methods for carrying out the optimization of acquisition functions.

5.1.1. Problem Setup

Throughout this section, we consider an emulator f_N that has been trained on an existing design $\mathcal{D}_N = \{\boldsymbol{\theta}_N, \boldsymbol{\varphi}_N\}$, with the goal being to select a new batch $\boldsymbol{\theta} \subset \Theta$ of B design points. For an acquisition function $\mathcal{A} : \Theta^B \rightarrow \mathbb{R}$, the batch is selected by solving the optimization problem

$$\boldsymbol{\theta}_* := \underset{\boldsymbol{\theta} \in \Theta^B}{\operatorname{argmin}} \mathcal{A}(\boldsymbol{\theta}). \quad (36)$$

By focusing on only one step of a potentially multi-stage sequential design algorithm, we implicitly restrict our focus to *myopic* (i.e., one-step look-ahead) strategies, which do not factor in the effect of future design acquisitions when selecting the current batch. Non-myopic strategies have been considered (e.g., via dynamic programming), though they typically come at the cost of significant computational expense (Gonzalez, Osborne and Lawrence, 2016; Chevalier, 2013).

For a candidate batch $\boldsymbol{\theta}$, let $\boldsymbol{\theta}_{N+B} := \{\boldsymbol{\theta}_N, \boldsymbol{\theta}\}$ denote the extended set of design points, f_{N+B} the updated emulator, and $\tilde{\pi}_{N+B}$ the resulting unnormalized posterior surrogate. When necessary, we make explicit the dependence on the new training data by writing $f_{N+B}^{\boldsymbol{\theta}, \boldsymbol{\varphi}}$ and $\tilde{\pi}_{N+B}^{\boldsymbol{\theta}, \boldsymbol{\varphi}}$, where $\boldsymbol{\varphi} \sim \eta(\cdot \mid \mathbf{f}(\boldsymbol{\theta}))$. We similarly write $\mathcal{A}(\boldsymbol{\theta}) = \mathcal{A}(\boldsymbol{\theta}; \boldsymbol{\theta}_N, \boldsymbol{\varphi}_N)$ when it is helpful to emphasize the dependence of the acquisition function on the current training data.

Remark 4. The process of updating the surrogate from f_N to f_{N+B} will depend on the particular model in use. For GP surrogates, this entails conditioning $f_{N+B} := f_N \mid [\varphi_N(\boldsymbol{\theta}) = \boldsymbol{\varphi}]$, typically requiring $\mathcal{O}(N^2B + B^3)$ operations. The GP hyperparameters may also be updated, at the cost of $\mathcal{O}([N + B]^3)$ scaling. For parametric models, the surrogate update will entail re-estimation of the model parameters using the augmented dataset.

5.1.2. Frameworks for Constructing Design Criteria

Similar to the posterior estimators in Section 4, design criteria are commonly derived from first-principles frameworks.

Decision Theoretic Framework. Recall the unnormalized density decision theoretic framework formalized in Equation (29), whereby an unnormalized posterior estimate is chosen as the optimizer of an expected loss:

$$\tilde{q}_N := \operatorname{argmin}_{\tilde{q} \in \tilde{\mathcal{Q}}} \mathbb{E}_{\nu_N}[\mathcal{L}(\tilde{q}, \tilde{\pi}_N)]. \quad (37)$$

The minimal value of the objective function is known as the *Bayes' risk*:

$$\mathcal{R}_N := \mathbb{E}_{\nu_N}[\mathcal{L}(\tilde{q}_N, \tilde{\pi}_N)]. \quad (38)$$

If the surrogate is updated using $\{\boldsymbol{\theta}, \boldsymbol{\varphi}\}$, it will yield a corresponding Bayes' risk $\mathcal{R}_{N+B}^{\boldsymbol{\theta}, \boldsymbol{\varphi}}$. A natural design strategy is to choose $\boldsymbol{\theta}$ so that this risk is as small as possible. The problem, of course, is that we cannot observe $\boldsymbol{\varphi}$ without evaluating $f(\boldsymbol{\theta})$. Thus, we marginalize these values under the assumption $\boldsymbol{\varphi} \sim \eta_N(\boldsymbol{\theta})$, which models the unobserved responses according to the current predictive distribution over simulator observations (recall Definition 4). This yields an acquisition function of the form

$$\mathcal{A}(\boldsymbol{\theta}) := \mathbb{E}_{\boldsymbol{\varphi} \sim \eta_N(\boldsymbol{\theta})} [\mathcal{R}_{N+B}^{\boldsymbol{\theta}, \boldsymbol{\varphi}}]. \quad (39)$$

In principle, this framework could be modified to consider a loss $\mathcal{L}(q, \pi_N)$ between *normalized* densities (as in Equation (28)). To our knowledge this has not been considered in practice due to the practical difficulties caused by the normalizing constant.

Stepwise Uncertainty Reduction (SUR). *Stepwise Uncertainty Reduction (SUR)* is another theoretical framework that has been used to develop and analyze sequential design algorithms for applications such as optimization and reliability analysis (Bect, Bachoc and Ginsbourger, 2019; Bect et al., 2011). The framework has also recently been used in solving Bayesian inverse problems (Lartaud, Humbert and Garnier, 2024). Let $\mathcal{H}(f_N)$ denote a scalar-valued uncertainty measure we would like to minimize. SUR acquisition functions are defined as the expected one-step-ahead uncertainty

$$\mathcal{A}(\boldsymbol{\theta}) := \mathbb{E}_{\boldsymbol{\varphi} \sim \eta_N(\boldsymbol{\theta})} [\mathcal{H}(f_{N+B}^{\boldsymbol{\theta}, \boldsymbol{\varphi}})]. \quad (40)$$

This framework is quite general, and particular choices of \mathcal{H} coincide with criteria derived using the Bayesian decision theoretic approach. The primary benefit of SUR is theoretical, as it provides general conditions to ensure that the uncertainty will converge to zero if the algorithm is repeated indefinitely.

5.1.3. Concrete Acquisition Functions

We now provide a survey of design criteria used in the literature.

Local Single-Point Criteria. Before describing acquisition functions derived from the above frameworks, we introduce some common heuristic strategies. When optimizing for a single design point ($B = 1$), an intuitive approach is to simply select the input where the uncertainty in $\pi_N(\theta)$ is largest. Owing to the challenge of dealing with the random normalizing constant Z_N , previous work has opted to instead target the uncertainty in the unnormalized density surrogate $\tilde{\pi}_N(\theta)$. If predictive variance is used as the measure of uncertainty, this yields the *maximum variance* criterion

$$\mathcal{A}(\theta) := -\text{Var}_{\nu_N}[\tilde{\pi}_N(\theta)], \quad (41)$$

which is negated to align with our convention of minimizing acquisition functions. Alternative “maximum uncertainty” criteria can be defined by changing the measure of uncertainty (e.g., variance, entropy, interquartile range) and the target quantity for which uncertainty is assessed (e.g., $\tilde{\pi}_N$, f_N). Figure 5 plots $\mathcal{A}(\theta)$ under varying combinations of these choices for different underlying emulators. The particular criterion in Equation (41) is used in Lueckmann et al. (2019) for sequential neural likelihood estimation, with the variance approximated using a deep ensemble. The below example notes other cases in which it is used in conjunction with GP emulators.

Example 15 (Maximum Variance, Log-Density Emulator). Consider the Gaussian log-likelihood emulation setting from Example 13 where

$$\tilde{\pi}_N(\theta) = \pi_0(\theta) \exp\{f_N(\theta)\}, \quad f_N(\theta) \sim \mathcal{N}(\mu_N(\theta), s_N^2(\theta)). \quad (42)$$

In this case, the maximum variance acquisition is

$$\mathcal{A}(\theta) = -\pi_0^2(\theta) [\exp\{s_N^2(\theta)\} - 1] \exp\{2\mu_N(\theta) + s_N^2(\theta)\}, \quad (43)$$

which favors the selection of points both where the current log-likelihood estimate $\mu_N(\theta)$ and the emulator uncertainty $s_N^2(\theta)$ are large. This criterion is used in Kandasamy, Schneider and Póczos (2017); Alawieh, Goodman and Bell (2020), though Järvenpää et al. (2021); Wang and Li (2018) argue that it provides a misleading measure of uncertainty due to the heavy tails of $\tilde{\pi}_N(\theta)$. They propose using the interquartile range or entropy as more robust uncertainty metrics in this setting. The acquisition in Equation (43) is plotted in Figure 5 (second row, second column), compared to the interquartile range and entropy alternatives. \diamond

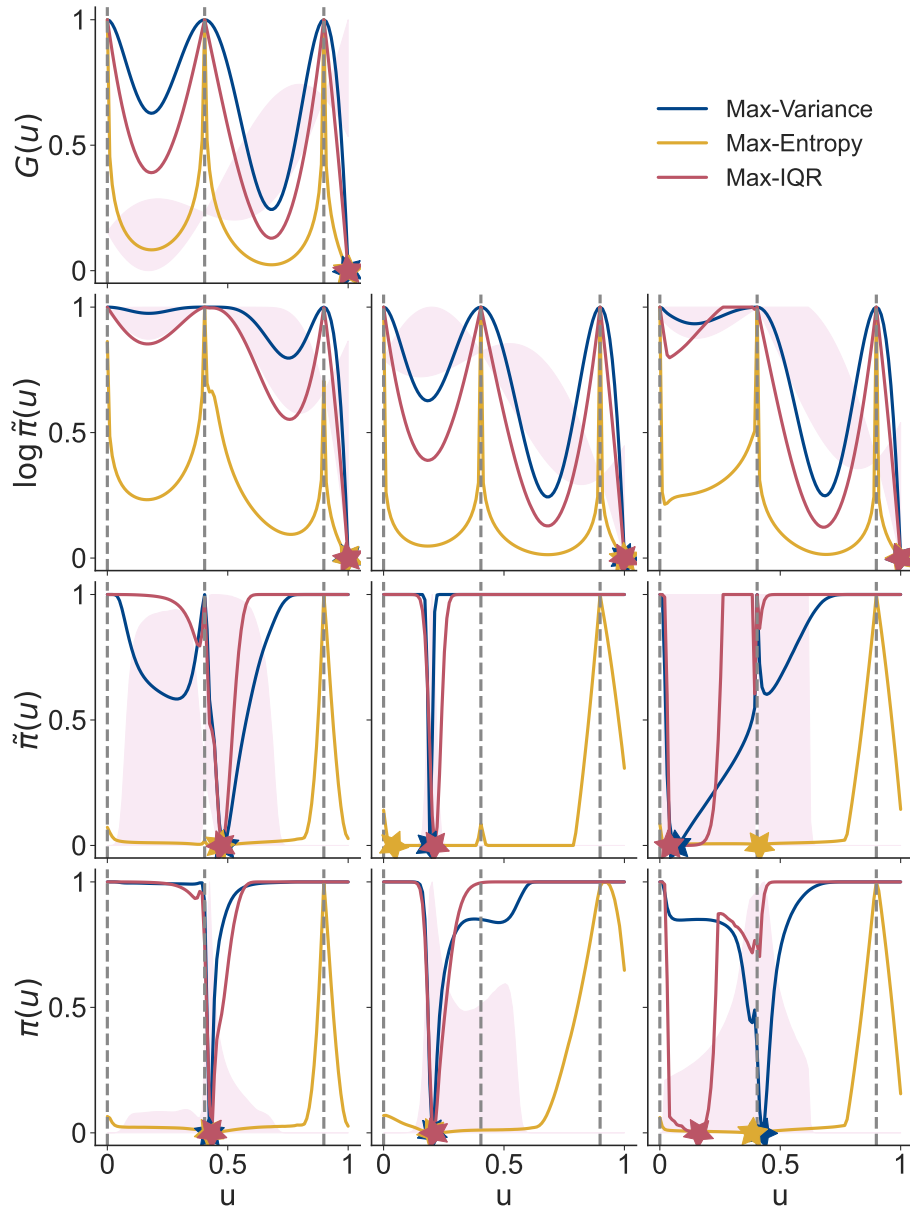


FIG 5. A continuation of Figures 3 and 4. The shaded regions summarize the surrogate push-forward distributions as before. The lines correspond to different “maximum uncertainty” criteria $\mathcal{A}(\theta)$ targeting uncertainty in the respective distributions. For example, the blue lines in the left column (from top to bottom) show $-\text{Var}(f_N(\theta))$, $-\text{Var}(\log \tilde{\pi}_N(\theta))$, $-\text{Var}(\tilde{\pi}_N(\theta))$, and $-\text{Var}(\pi_N(\theta))$, where f_N is a forward model emulator. The two other lines similarly show the (negated) pointwise entropy and interquartile range, and the columns vary the underlying emulator. The star markers indicate the optimal value for each acquisition function.

A variety of other single-point acquisition strategies have been explored in the literature. Several authors have borrowed criteria from Bayesian optimization to target the placement of new design points in high-posterior regions (Takhtaganov and Müller, 2018; Gutmann and Corander, 2016; Kim and Sanz-Alonso, 2024). The strategy proposed by Kim and Sanz-Alonso (2024) explicitly decouples exploration and exploitation via a two-point acquisition; the first point is chosen as the maximizer of the current log-posterior estimate (exploitation) and the second is sampled from π_0 (exploration).

While nominally designed for the pure sequential $B = 1$ setting, single-point criteria can be adapted for batch acquisition. The simple approach of selecting the B points with the smallest acquisition values can result in a batch of very similar points. Greedy heuristics, discussed in Section 5.1.4, can prevent this undesirable “clumping” behavior. Alternatively, “stochastic” variants of maximum uncertainty criteria can be defined by sampling from a density proportional to $-\mathcal{A}(\theta)$, rather than optimizing the criterion (Gutmann and Corander, 2016; Järvenpää et al., 2019). This encourages exploration, and provides a mechanism for batch selection.

Global Multipoint Criteria. While computationally convenient, single-point criteria suffer from two primary drawbacks: (1) they are not naturally defined in the batch sequential setting; and (2) they are purely local, neglecting the global impact a new design point has across Θ . The latter property commonly results in maximum uncertainty criteria targeting points in the edges or tails of the parameter space (e.g., Gramacy, 2020, Section 6.2.1). We now introduce a class of acquisition functions, referred to as *Expected Conditional Uncertainty (ECU)* criteria, that address both of these limitations.

Intuitively, ECU acquisitions arise from the following logic: we would like to select an input batch θ that results in an updated (unnormalized) posterior estimate $\tilde{\pi}_{N+B}$ with the lowest possible uncertainty on average over Θ .² Given that we cannot typically compute this uncertainty without observing φ , we utilize the same approach described for the Bayes’ risk (Equation (39)) and marginalize over this quantity with respect to η_N . As a concrete example, if we again choose variance as our measure of uncertainty, we obtain the expected conditional variance

$$\mathcal{A}(\theta) := \int_{\Theta} \mathbb{E}_{\varphi \sim \eta_N(\theta)} \left\{ \text{Var}_{\nu_{N+B}} [\tilde{\pi}(\theta; f_{N+B}^{\theta, \varphi}) \mid \theta, \varphi] \right\} \rho(d\theta), \quad (44)$$

where ρ is a measure over Θ . Variations of ECU criteria can be created by changing the measure of uncertainty (e.g., variance, entropy, interquartile range), the target quantity (e.g., $\tilde{\pi}_N$, f_N), and the weighting measure ρ . For example, targeting the variance of f_N with uniform ρ yields the classical integrated mean squared prediction error (Gorodetsky and Marzouk, 2016). Järvenpää and Corander (2024) target uncertainty in the acceptance probability of a

²As before, this could be extended to operate directly on the normalized densities. While arguably more principled, this also leads to more challenging calculations.

Metropolis-Hastings algorithm, deriving ECU-style acquisitions under a Bayesian decision theoretic framework. Similarly, [Järvenpää et al. \(2019\)](#) derive an integrated variance criterion targeting uncertainty in the ABC approximation to the (unnormalized) posterior.

The expected variance term in Equation (44) admits a closed form in the settings of Examples 12 and 13, as shown below. These examples also demonstrate how ECU criteria can be interpreted within the decision theoretic and SUR frameworks.

Example 16 (Expected Conditional Variance, Log-Density Emulator). We continue Example 15, extending the maximum variance criterion into the expected conditional variance. With this setup, the ECU-variance criterion in Equation (44) reduces to

$$\mathcal{A}(\boldsymbol{\theta}) = \int_{\Theta} \text{Var}_{\nu_N} [\tilde{\pi}_N(\theta) \mid \varphi_N(\boldsymbol{\theta}) = \mu_N(\boldsymbol{\theta})] \tau_N(\theta; \boldsymbol{\theta}) \rho(d\theta) \quad (45)$$

where

$$\text{Var}_{\nu_N} [\tilde{\pi}_N(\theta) \mid \varphi_N(\boldsymbol{\theta}) = \mu_N(\boldsymbol{\theta})] = \pi_0^2(\theta) \exp\{2\mu_N(\theta) + s_{N+B}^2(\theta; \boldsymbol{\theta})\} \cdot [\exp\{s_{N+B}^2(\theta; \boldsymbol{\theta})\} - 1]$$

and

$$\tau_N(\theta; \boldsymbol{\theta}) = \exp\{2(s_N^2(\theta) - s_{N+B}^2(\theta; \boldsymbol{\theta}))\}.$$

We write $s_{N+B}^2(\theta; \boldsymbol{\theta})$ for the predictive variance of the updated GP, which does not depend on the unobserved response φ . The first term in Equation (45) is the variance of the unnormalized posterior surrogate that results from updating f_N with $\{\boldsymbol{\theta}, \mu_N(\boldsymbol{\theta})\}$; i.e., the current GP prediction is treated as if it were the true response. The second term accounts for the uncertainty in the true response: the penalty $s_N^2(\theta) - s_{N+B}^2(\theta; \boldsymbol{\theta})$ is large when the input batch $\boldsymbol{\theta}$ is highly “influential.”

The expected conditional variance acquisition corresponds to the Bayes’ risk under an L^2 loss ([Järvenpää et al., 2021](#)). It can also be viewed as an SUR acquisition with uncertainty measure $\mathcal{H}(f_N) := \int \text{Var}_{\nu_N} [\tilde{\pi}_N(\theta)] \rho(d\theta)$. This acquisition is considered in [Järvenpää et al. \(2021\)](#), but the authors ultimately recommend alternative robust criteria defined using the interquartile range in place of the variance. \diamond

Example 17 (Expected Conditional Variance, Forward Model Emulator). Consider the Gaussian forward model setting with $\tilde{\pi}_N(\theta) = \pi_0(\theta) \mathcal{N}(y_o \mid f_N(\theta), \Sigma)$, $f_N(\theta) \sim \mathcal{N}(\mu_N(\theta), s_N^2(\theta))$. Letting $C_N(\theta) := \Sigma + s_N^2(\theta)$ and $C_{N+B}(\theta) := \Sigma + s_{N+B}^2(\theta; \boldsymbol{\theta})$, the expected conditional variance criterion simplifies to

$$\mathcal{A}(\boldsymbol{\theta}) = \int_{\Theta} \pi_0^2(\theta) \left[\frac{\mathcal{N}(y_o \mid \mu_N(\theta), C_N(\theta) - \frac{1}{2}\Sigma)}{2^{P/2} \det(2\pi\Sigma)^{1/2}} - \frac{\mathcal{N}(y_o \mid \mu_N(\theta), C_N(\theta) - \frac{1}{2}C_{N+B}(\theta; \boldsymbol{\theta}))}{2^{P/2} \det(2\pi C_{N+B}(\theta; \boldsymbol{\theta}))^{1/2}} \right] \rho(d\theta). \quad (46)$$

Sinsbeck and Nowak (2017) are the first to propose an ECU-variance criterion in the forward model emulation setting, and Özge Sürer, Plumlee and Wild (2024); Özge Sürer (2026) utilize similar acquisitions. Lartaud, Humbert and Garnier (2024) alternatively consider a criterion of the form

$$\mathcal{A}(\boldsymbol{\theta}) = \int_{\Theta} s_{N+B}^2(\boldsymbol{\theta}; \boldsymbol{\theta}) \pi_N^{\text{eup}}(d\boldsymbol{\theta}), \quad (47)$$

corresponding to the SUR uncertainty metric $\mathcal{H}(f_N) := \int \text{Var}_{\nu_N}[f_N(\boldsymbol{\theta})] \pi_N^{\text{eup}}(d\boldsymbol{\theta})$. The integrand considers uncertainty in the forward model emulator (exploration), while the measure $\rho = \pi_N^{\text{eup}}$ weights by the current posterior approximation (exploitation). \diamond

Outside of special cases (Binois et al., 2018; Miller and Mak, 2025; Koermer et al., 2024) the outer integral (over Θ) in ECU criteria is not tractable. Monte Carlo approximations are possible but would yield a stochastic optimization problem. A simpler and more common solution is to utilize a sample average approximation

$$\mathcal{A}(\boldsymbol{\theta}) := \frac{1}{J} \sum_{j=1}^J \mathbb{E}_{\boldsymbol{\varphi} \sim \eta_N(\boldsymbol{\theta})} \left\{ \text{Var}_{\nu_{N+B}}[\pi(\boldsymbol{\theta}_j; f_{N+B}^{\boldsymbol{\theta}; \boldsymbol{\varphi}}) \mid \boldsymbol{\theta}, \boldsymbol{\varphi}] \right\}, \quad \boldsymbol{\theta}_j \stackrel{\text{iid}}{\sim} \rho, \quad (48)$$

in which the $\boldsymbol{\theta}_j$ are sampled once and then fixed, maintaining a deterministic objective function (Gorodetsky and Marzouk, 2016; Balandat et al., 2020).

5.1.4. Solving the Optimization Problem

We comment briefly on algorithms to actually carry out the optimization of the acquisition function in Equation (36). Detailed treatments of this topic are available across the Bayesian optimization and computer experiments literatures (Wilson, Hutter and Deisenroth, 2018; Balandat et al., 2020; Gramacy, 2020; Wynn, 1970). In general, the task of minimizing $\mathcal{A}(\boldsymbol{\theta})$ involves a challenging non-convex optimization problem over DB variables. Gradient-based optimization of acquisitions defined by sample-average approximations (Equation (48)) has been shown to perform favorably in moderate dimensions (Gorodetsky and Marzouk, 2016). This approach is implemented in the BoTorch Python package (Balandat et al., 2020). Alternatively, a large portion of the literature eschews continuous optimization in favor of discrete methods. These algorithms take the form of a subset selection problem, with the optimal batch selected from a finite set of candidate points. This presents a challenging combinatorial optimization problem, commonly solved by employing stochastic exchange algorithms (e.g., Federov exchange) to find a local minimum (Fedorov, 1972; Wynn, 1970; Loepky, Moore and Williams, 2010).³

³Exchange algorithms can also be employed to optimize over continuous space and leverage gradient information.

To avoid the joint optimization over Θ^B altogether, greedy approximations are also common in practice (Järvenpää et al., 2021; Özge Sürer, Plumlee and Wild, 2024). These methods seek to approximate the joint optimum using a sequence of B simpler optimization problems over Θ . Since this procedure proceeds one point at a time, it provides the opportunity to use single-point criteria (Section 5.1.3) in batch optimization. Under this approach, the first point θ_1 is selected by optimizing $\mathcal{A}(\theta)$ as in the pure sequential setting. The remaining $b = 2, \dots, B - 1$ points are added sequentially by minimizing $\mathcal{A}(\theta; \boldsymbol{\theta}_{N+b-1}, \boldsymbol{\varphi}_{N+b-1})$. In pure sequential design, the response $\varphi(\theta_b)$ is observed every iteration. Greedy batch design differs in that $\varphi(\theta_b)$ is not observed until the entire batch has been selected. This implies that the objective function must be approximated in solving this sequence of optimization problems, typically by imputing the unknown responses $\varphi(\theta_b)$ with pseudo-observations. *Kriging Believer* and *Constant Liar* are two such heuristics (Ginsbourger, Le Riche and Carraro, 2010). After selecting θ_b , the Kriging Believer strategy updates the surrogate with the pseudo-observation $\{\theta_b, \mu_N(\theta_b)\}$, while Constant Liar instead uses $\{\theta_b, c\}$ for some pre-determined constant c . An extension of this approach consists of generating multiple candidate batches using varying heuristics, and then leveraging a batch acquisition function to select among the candidates (Chevalier and Ginsbourger, 2013).

5.2. Surrogate-Guided Sampling

Instead of optimizing an explicit acquisition function, the particular goal of posterior approximation suggests a simple alternative: sample the batch $\boldsymbol{\theta}$ from the current posterior estimate (e.g., π_N^{ep}). This yields an active learning procedure with the form of a fixed-point iteration; the current posterior estimate is used to select the next batch, which is then used to update the posterior estimate, and so on (Papamakarios and Murray, 2016; Papamakarios, Sterratt and Murray, 2019; Zhang et al., 2020; Dinkel et al., 2024; Zhang et al., 2016). Fer et al. (2018) adopt a variant of this strategy, sampling from a mixture of the current approximate posterior and the prior, with the mixture weights representing a user-defined tuning parameter. Zeng et al. (2022) consider a similar prior-posterior mixture, with a Latin hypercube adjustment to encourage the new design points to be spread out. Xu et al. (2024) draw samples from the current approximate posterior, and then update these samples with an iteration of an ensemble Kalman algorithm, a method with close connections to the *calibrate*, *emulate*, *sample* workflow (Cleary et al. (2021); see Section 5.3). Surrogate-based sampling is also commonly used in sequential algorithms for constructing neural density estimators (Papamakarios and Murray, 2016; Papamakarios, Sterratt and Murray, 2019; Durkan, Papamakarios and Murray, 2018). This approach is especially convenient in this setting given that (unlike acquisition-based approaches) it does not require a probabilistic emulator, which can be difficult to train for neural networks.

These sampling-based approaches enjoy the practical benefits of being inherently parallel and avoiding a difficult optimization problem. In this sense,

they are similar in spirit to Thompson sampling for batch Bayesian optimization (Kandasamy et al., 2018). Sampling from a mixture of the prior and current posterior estimate can be viewed as an explicit decoupling of exploration and exploitation, similar to the methods proposed in Kim and Sanz-Alonso (2024). One could try to combine the strengths of sampling-based and optimization-based approaches by first sampling candidates from the current posterior estimate and then running an optimization algorithm to select the final subset; the ECU acquisition in Equation (47) might be viewed as an instance of this approach.

Overall, sampling-based approaches offer a promising avenue in large-scale applications where parallelization is crucial, and the simulator cost only allows for a few rounds of sequential design with large batch sizes.

5.3. Tempered Target Distributions

The sequential design strategies of the previous section are motivated by the observation that a static, prior-based design will often fail to allocate points in high-density regions when the posterior is concentrated. They address this problem by building up the design sequentially, targeting the placement of points where the surrogate-estimated posterior is large, balanced with exploration of regions with high surrogate uncertainty. A concern with such algorithms is that they may require many iterations to identify the high-density regions, exhausting the budget exploring unimportant areas. This problem arises when the surrogate approximation of the posterior is quite poor in the early stages of the algorithm, causing acquisition functions based on the surrogate to inefficiently explore the parameter space (Wilkinson, 2014).

One approach to mitigate this issue builds on the recognition that it may be unrealistic and counterproductive to directly target the posterior in the initial stages of the algorithm. Instead, the surrogate target can be allowed to vary over the rounds in the active learning procedure, tracking a sequence of intermediate distributions that bridge between the prior and posterior. Since the earlier distributions are less concentrated, the surrogate approximation will tend to be more reasonable and thus more useful in guiding the placement of the next round of design points. *Tempering* strategies of this form are widely utilized in computational statistics; we focus on their use in conjunction with surrogate models.

Tempering algorithms traverse from prior to posterior through a sequence of interpolating distributions $\pi_0, \pi_1, \dots, \pi_T$, where π_0 is the prior and $\pi_T = \pi$ the posterior. Common choices are based on geometric bridges of the form $\pi_t(\theta) \propto \pi_0(\theta)L(\theta)^{\beta_t}$ with $0 = \beta_0 < \dots < \beta_T = 1$. This approach forms the basis of sequential Monte Carlo (SMC) algorithms, used both for statistical estimation in time-varying systems (i.e., particle filters) as well as posterior estimation for static inverse problems (Doucet, de Freitas and Gordon, 2001; Naesseth, Lindsten and Schön, 2019). Unlike MCMC, these methods are naturally parallelizable, but can still require many likelihood evaluations. Surrogate models offer one avenue to lower this cost, and may be integrated into a tempering framework in a variety of different ways.

The role of the intermediate distributions π_t may differ depending on the emulator target. In forward model emulation, the target \mathcal{G} is constant. However, the design strategy may vary over t to produce an approximation of \mathcal{G} optimized for π_t . The sequence of surrogates may thus be *local*, in the sense that certain design points are discarded or downweighted to target predictions in the high-density region with respect to π_t (Wilkinson, 2014; Li and Marzouk, 2014). In other cases, the surrogate target itself may evolve. For example, at iteration t a log-posterior surrogate is fit to training data of the form $\{\theta_n, \log \pi_t(\theta_n)\}$, which again may constitute a sub-sampled or weighted modification of the total training set. Note that design points from previous rounds can still be re-used without additional model simulations. For example, in the case of geometric bridging distributions, $\log \pi_t(\theta) = \log \pi_0(\theta) + \beta_t \log L(\theta)$, implying that previous likelihood evaluations simply need to be rescaled for use in future steps.

While tempering methods are diverse, we restrict our focus to three broad categories: (1) algorithms relying on sequential importance sampling; (2) algorithms that utilize approximate Kalman-style updates to traverse between the bridging distributions; and (3) other related methods.

Importance Sampling. In principle, importance sampling provides the means to transform samples from a prior proposal distribution into posterior samples using evaluations of the likelihood function (Owen, 2013, Chapter 9). When utilizing tempering, these updates are applied sequentially such that π_t acts as the proposal distribution for π_{t+1} . To reduce the computational cost of the likelihood evaluations, surrogates can be leveraged in various ways to approximate these updates. One natural strategy is to replace π_t with a surrogate-based estimate $\hat{\pi}_t$, then apply the importance sampling machinery to sample $\hat{\pi}_{t+1}$. Samples from $\hat{\pi}_{t+1}$ can then be chosen as the new batch of design points. Dinkel et al. (2024) adopt this approach with a GP log-posterior surrogate, never discarding design points and thus maintaining a global surrogate approximation throughout the algorithm. By contrast, Li and Marzouk (2014) focus on the construction of local polynomial chaos surrogates. The $\hat{\pi}_t$ are estimated using a variational approximation, with the variational objective approximated using importance sampling and the current surrogate model. Cérou, Héas and Rousset (2025) propose an adaptive SMC scheme that actively samples new design points to reduce surrogate error. Both Li and Marzouk (2014); Cérou, Héas and Rousset (2025) automatically adapt the temperature schedule $\{\beta_t\}$, negating the need for a priori specification.

Ensemble Kalman Updates. While importance sampling techniques are widely applicable, they can suffer from known pathologies in moderate to high dimensions. Ensemble Kalman methods, rooted in linear Gaussian methodology, sacrifice exact updates $\pi_t \mapsto \pi_{t+1}$ for robustness and are widely used in high-dimensional settings (Iglesias, Law and Stuart, 2013). These approximate methods can be used as a drop-in replacement for the importance sampling updates discussed in the previous section. Xu et al. (2024) proceed in this spirit, first sampling from an intermediate posterior approximation using MCMC and

then feeding the resulting samples through an ensemble Kalman update to produce the next batch of design points. [Picchini, Simola and Corander \(2023\)](#) utilize ensemble Kalman updates to build a sequence of proposal distributions for an MCMC sampler.

Instead of interleaving Kalman steps with surrogate updates, another popular strategy consists of first running several iterations of a Kalman algorithm and then utilizing the resulting approximate posterior samples as an initial design for an emulator. This methodology, known as the *Calibrate, Emulate, Sample (CES)* approach ([Cleary et al., 2021](#)), is an instance of the general idea of using an approximate sampling or optimization algorithm to cheaply generate design points in the high-density regions. Surrogate-based posterior approximations may then be constructed to refine the initial coarse approximation. A variety of ensemble Kalman methods, falling under the umbrella label *Ensemble Kalman Inversion (EKI)*, may be utilized in the first stage of CES algorithms ([Gjini et al., 2025](#); [Dunbar et al., 2024, 2021](#); [Keetz et al., 2025](#)).

Other Approaches. A variety of other methods utilize tempering-like strategies outside of the traditional SMC framework. For example, [Joseph et al. \(2015, 2019\)](#) solve a sequence of optimization problems to deterministically sample from a probability distribution using a minimum energy criterion. These algorithms utilize both tempering and local GP surrogates to improve efficiency.

The framework of [Wang and Li \(2018\)](#) does not explicitly use tempering, but similarly leverages a sequence of intermediate distributions. They factor the unnormalized posterior density as $\tilde{\pi}(\theta) = \pi_0(\theta)L(\theta) = \exp\{g_t(\theta)\}\pi_t(\theta)$, where a GP emulator targets $g_t(\theta) := \log\{\tilde{\pi}(\theta)/\pi_t(\theta)\}$ and the density π_t is a free parameter. The emulator target varies as π_t changes, but the quantity $\exp\{g_t(\theta)\}\pi_t(\theta)$ always provides an approximation of $\tilde{\pi}$. For $\pi_t = \pi_0$, $g_t(\theta)$ is the log-likelihood, but if $\pi_t = \pi$ then $g_t(\theta)$ reduces to a constant. Thus, the idea is that the emulation target becomes simpler to approximate over the course of the algorithm. [Xu et al. \(2024\)](#) adapt this idea in developing an algorithm tailored to multi-modal posteriors.

[Wilkinson \(2014\)](#) suggests an alternative method that iteratively eliminates “implausible” regions of the parameter space. A sequence of local GP surrogates are trained only on points in the current plausible region, and are used for determining the plausible region for the next iteration.

5.4. MCMC-Based Sequential Design

Finally, we highlight a class of active learning strategies that interleave surrogate refinement and posterior sampling within a unified algorithm. The goals of such approaches vary, spanning purely approximate schemes as well as so-called “exact-approximate” algorithms that strive for asymptotic convergence to the exact posterior π . We provide a high-level overview of these methods here, referring to [Llorente et al. \(2025\)](#) for a more detailed survey.

The idea of accelerating MCMC using a surrogate dates back to the delayed acceptance mechanism of [Christen and Fox \(2005\)](#). Delayed acceptance

schemes are exact-approximate algorithms that improve efficiency by filtering our poor proposals using the surrogate, but ultimately require exact simulations when a proposal is accepted (Paun and Husmeier, 2021; Rasmussen, 2003). To further reduce computational costs, many methods also use the surrogate in making acceptance decisions, which generally results in inexact samplers (i.e., the target distribution is no longer π). Others seek a middle ground by using the surrogate in acceptance decisions only when the model is confident in its predictions; when uncertainty exceeds some threshold, an exact simulation is triggered. These additional simulator runs are used to update the surrogate, thus refining the emulator design over the course of the algorithm. This updating is often halted after the simulation budget is exceeded, at which point the sampler proceeds with a fixed surrogate targeting an approximate posterior (Järvenpää and Corander, 2024; Bliznyuk, Ruppert and Shoemaker, 2012). At this stage, any of the posterior estimates from Section 4 may be employed.

In defining a criterion for triggering additional simulations, a principled choice is to consider uncertainty in the Metropolis-Hastings acceptance probability $\alpha(\theta, \tilde{\theta})$ (Meeds and Welling, 2014; Conrad et al., 2016; Järvenpää and Corander, 2024). When the surrogate-induced uncertainty in this quantity is large, the Markov chain is unsure whether or not to accept the proposed value $\tilde{\theta}$. Meeds and Welling (2014) characterize the probability of making an incorrect decision under the distribution induced by a GP surrogate in a simulation-based inference setting. Järvenpää and Corander (2024) refine these results under a GP log-likelihood surrogate, providing an analytical characterization of the uncertainty in $\alpha(\theta, \tilde{\theta})$. Riccius et al. (2026); Drovandi, Moores and Boys (2018) adopt a more heuristic approach, triggering design augmentation when the variance in $f_N(\tilde{\theta})$ exceeds a predefined threshold. Conrad et al. (2016) also consider uncertainty in the acceptance probability, but in contrast to the above approaches, they (1) allow surrogate refinement to continue indefinitely, theoretically establishing asymptotic exactness under certain conditions; and (2) utilize local surrogate models, such that only a local subset of the design is used when predicting at a particular location.

Due to the serial nature of MCMC algorithms, these methods are limited in their ability to leverage parallel computing resources. They are thus typically most appropriate for simulators of modest computational expense, when it is still feasible to perform many runs sequentially. This is especially true for exact-approximate schemes; the price to be paid for asymptotic exactness is a larger number of simulator runs (Conrad et al., 2016).

6. Conclusion

In this paper, we presented a comprehensive synthesis of surrogate-based methodology for Bayesian inference. Our review emphasized uncertainty propagation and active learning, two key elements of a robust surrogate-based Bayesian workflow. While research in these areas has enabled more efficient and reliable use of surrogates, there remains significant opportunity for further progress.

Training emulators to approximate very expensive simulators continues to present a significant hurdle. Gaussian processes are often the tool of choice in this setting. However, constructing GP models for high-dimensional input spaces or nonstationary target surfaces is highly non-trivial (Doumont et al., 2025; Booth, Cooper and Gramacy, 2024). Neural networks offer scalability, but typically require large training sets that are unattainable for expensive computer models. Moreover, while many approaches have been proposed to produce predictive distributions for neural networks, uncertainty quantification in deep learning generally remains an open problem (Abdar et al., 2021). The development of emulators combining the strengths of GPs and neural networks is a promising research direction. Emulators geared towards posterior approximation may achieve this balance by exploiting structure in the Bayesian inverse problem (e.g., Cui et al. (2014)).

These challenges are further exacerbated when the simulator is noisy, which typically necessitates larger simulator budgets. Neural density estimation is a powerful SBI paradigm for constructing flexible and amortized emulators (Cranmer, Brehmer and Louppe, 2020). However, it often requires large training sets that are not feasible for very expensive computer models. By contrast, methods from the computer experiments community target the small training set regime, but are typically not explicitly aligned with the goal of posterior approximation (Baker et al., 2022). Combining ideas from these two communities may prove a fruitful avenue for research; for example, using emulators to generate training data for a neural estimator (Scheurer et al., 2026), or designing more query-efficient conditional density estimators (Fadikar et al., 2018).

In discussing emulator uncertainty propagation in Section 4, we emphasized the EP and EUP, while highlighting a number of alternative posterior approximations. Given that there is no one-size-fits-all approach, further work is needed to provide guidance in specific applications. In addition, considerations such as robustness to misspecification may lead to alternative uncertainty propagation methods with superior performance in particular settings (e.g., improving the robustness of posteriors derived using log-density emulators). Connections to areas such as semi-modular and generalized Bayesian inference may prove helpful in this regard (Carmona, 2023; Frazier and Nott, 2025).

As illustrated in Section 5, many strategies have been proposed for sequentially refining a surrogate for posterior approximation. In general, more work is required to better understand their tradeoffs and inform the choice of a particular algorithm in practice. Both experimental and theoretical results are likely needed to close this gap, building upon early work in this area (Helin et al., 2024; Kim and Sanz-Alonso, 2024; Järvenpää et al., 2021; Lartaud, Humbert and Garnier, 2024). While many previous studies have focused on active learning with single-point or small batch acquisitions, there is relatively little research in the challenging setting of sequential design algorithms with few iterations and large batch sizes (Järvenpää et al., 2021; Özge Sürer, Plumlee and Wild, 2024; Durkan, Papamakarios and Murray, 2018). This situation arises when the simulator is expensive but parallel computing resources are available. Surrogate-guided sampling (Section 5.2) appears to be a natural and practical approach

in this context, but to our knowledge has not been rigorously investigated.

We hope this review serves as a first step towards categorizing the many choices that users face when incorporating an emulator within a Bayesian analysis. Further work is needed to better understand the tradeoffs between these choices, provide general guidance for practitioners, and develop standardized diagnostics for surrogate-based Bayesian workflow.

Appendix A: Gaussian Process Derivations

We now derive the expressions presented in the examples considering GP emulators throughout the paper. Let $f_N \sim \mathcal{GP}(\mu_N, k_N)$, with $s_N^2(\theta) = k_N(\theta, \theta)$. We focus on two settings amenable to analytical calculations: (1) forward model emulation with a Gaussian likelihood; and (2) log-likelihood emulation. All expectations are assumed to be with respect to f_N unless otherwise noted.

Before proceeding with the specific cases, we prove a general result that characterizes the uncertainty in the GP predictive mean due to an unobserved target response. This result will be used in deriving the expected conditional uncertainty acquisition functions. A similar result is presented in [Järvenpää et al. \(2021\)](#).

Lemma A.1. *Let $f_{N+B}^{\theta, \varphi} \sim \mathcal{GP}(\mu_{N+B}^{\theta, \varphi}, k_{N+B}^{\theta, \varphi})$ denote the GP f_N conditioned on the additional training points $\{\theta, \varphi\}$. Assume $\varphi \sim \mathcal{N}(\mu_N(\theta), s_N^2(\theta))$. Then, for any $\theta \in \Theta$, the randomness in $\mu_{N+B}^{\theta, \varphi}(\theta)$ as a function of φ is characterized by*

$$\mu_{N+B}^{\theta, \varphi}(\theta) \sim \mathcal{N}(\mu_N(\theta), k_N(\theta) - k_{N+B}^{\theta}(\theta)). \quad (49)$$

Proof. Note that the GP predictive kernel depends only on the input locations, not the responses. First recall the form of the GP predictive mean

$$\mu_{N+B}^{\theta, \varphi}(\theta) = \mu_N(\theta) + k_N(\theta, \theta) K_N^{-1}[\varphi - \mu_N(\theta)] k_N(\theta, \theta), \quad (50)$$

where $K_N := s_N^2(\theta) + \sigma^2 I$ as in Equation (50) (in this case f_N acts as the GP prior). This quantity is an affine function of the Gaussian random vector φ and is thus Gaussian distributed. Computing its mean and variance yields the desired result. \square

A.1. Forward Model Emulation

The forward model emulation setting yields the unnormalized posterior surrogate $\tilde{\pi}_N(\theta) = \pi_0(\theta) \mathcal{N}(y_o | f_N(\theta), \Sigma)$. We begin by computing the mean and variance of this quantity. The variance derivation uses the following lemma.

Lemma A.2. *Let $\mathcal{N}(m, C)$ be a Gaussian distribution on \mathbb{R}^P with C a symmetric, positive-definite matrix. Then, for $y \in \mathbb{R}^P$,*

$$\mathcal{N}(y | m, C)^2 = 2^{-P/2} \det(2\pi C)^{-1/2} \mathcal{N}(y | m, C/2).$$

Proof.

$$\begin{aligned}
\mathcal{N}(y \mid m, C)^2 &= \det(2\pi C)^{-1} \exp\left\{-\frac{1}{2}(y-m)^\top \left[\frac{1}{2}C\right]^{-1} (y-m)\right\} \\
&= \det(2\pi C)^{-1} \det(2\pi(1/2)C)^{1/2} \mathcal{N}(y \mid m, C/2) \\
&= 2^{-P/2} \det(2\pi C)^{-1/2} \mathcal{N}(y \mid m, C/2)
\end{aligned}$$

□

The expressions for the first two moments of $\tilde{\pi}_N(\theta)$ in Example 9 follow directly from the following result with A set to the identity.

Proposition A.3. *Let $\mu \sim \mathcal{N}(m, C)$ be a D -dimensional Gaussian vector and $A \in \mathbb{R}^{P \times D}$ a fixed matrix. Assuming Σ and C are symmetric, positive definite matrices, then*

$$\begin{aligned}
\mathbb{E}[\mathcal{N}(y \mid A\mu, \Sigma)] &= \mathcal{N}(y \mid Am, \Sigma + ACA^\top) \\
\text{Var}[\mathcal{N}(y \mid A\mu, \Sigma)] &= \frac{\mathcal{N}(y \mid Am, \frac{1}{2}\Sigma + ACA^\top)}{2^{P/2} \det(2\pi\Sigma)^{1/2}} - \frac{\mathcal{N}(y \mid Am, \frac{1}{2}[\Sigma + ACA^\top])}{2^{P/2} \det(2\pi[\Sigma + ACA^\top])^{1/2}}
\end{aligned}$$

Proof. The expectation follows immediately from the expression for the convolution of two Gaussians. For the variance, we have

$$\begin{aligned}
\text{Var}[\mathcal{N}(y \mid A\mu, \Sigma)] &= \mathbb{E}[\mathcal{N}(y \mid A\mu, \Sigma)^2] - \mathbb{E}[\mathcal{N}(y \mid A\mu, \Sigma)]^2 \\
&= \mathbb{E}[\mathcal{N}(y \mid A\mu, \Sigma)^2] - \mathcal{N}(y \mid Am, \Sigma + ACA^\top)^2. \quad (51)
\end{aligned}$$

Starting with the first term, we apply Lemma A.2 and the convolution formula, respectively, to obtain

$$\begin{aligned}
\mathbb{E}[\mathcal{N}(y \mid A\mu, \Sigma)^2] &= 2^{-P/2} \det(2\pi\Sigma)^{-1/2} \mathbb{E}[\mathcal{N}(y \mid A\mu, \Sigma/2)] \\
&= 2^{-P/2} \det(2\pi\Sigma)^{-1/2} \mathcal{N}(y \mid Am, \Sigma/2 + ACA^\top).
\end{aligned}$$

For the second term in Equation (51), another application of Lemma A.2 gives

$$\begin{aligned}
&\mathcal{N}(y \mid Am, \Sigma + ACA^\top)^2 \\
&= 2^{-P/2} \det(2\pi[\Sigma + ACA^\top])^{-1/2} \mathcal{N}(y \mid Am, [\Sigma + ACA^\top]/2).
\end{aligned}$$

Plugging these expressions back into Equation (51) completes the proof. □

The EUP $\tilde{\pi}_N^{\text{EUP}}(\theta) = \pi_0(\theta) \mathcal{N}(y_o \mid \mu_N(\theta), \Sigma + s_N^2(\theta))$ follows immediately from this result. We next derive the expected variance term that appears in the acquisition function from Example 17.

Proposition A.4. *Let $\tilde{\pi}(\theta; f_{N+B}^{\theta, \varphi}) = \pi_0(\theta) \mathcal{N}(y_o \mid f_{N+B}^{\theta, \varphi}(\theta), \Sigma)$ denote the unnormalized posterior surrogate induced by updating the emulator f_N with new*

training data $\{\boldsymbol{\theta}, \boldsymbol{\varphi}\}$. Under the assumption $\boldsymbol{\varphi} \sim \mathcal{N}(\mu_N(\boldsymbol{\theta}), s_N^2(\boldsymbol{\theta}))$, the expected conditional variance is given by

$$\mathbb{E}_{\boldsymbol{\varphi}} \left\{ \text{Var}[\tilde{\pi}(\boldsymbol{\theta}; f_{N+B}^{\boldsymbol{\theta}, \boldsymbol{\varphi}}) \mid \boldsymbol{\theta}, \boldsymbol{\varphi}] \right\} = \pi_0^2(\boldsymbol{\theta}) \left[\frac{\mathcal{N}(y_o \mid \mu_N(\boldsymbol{\theta}), C_N(\boldsymbol{\theta}) - \frac{1}{2}\Sigma)}{2^{P/2} \det(2\pi\Sigma)^{1/2}} - \right. \quad (52)$$

$$\left. \frac{\mathcal{N}(y_o \mid \mu_N(\boldsymbol{\theta}), C_N(\boldsymbol{\theta}) - \frac{1}{2}C_{N+B}(\boldsymbol{\theta}; \boldsymbol{\theta}))}{2^{P/2} \det(2\pi C_{N+B}(\boldsymbol{\theta}; \boldsymbol{\theta}))^{1/2}} \right], \quad (53)$$

where $C_N(\boldsymbol{\theta}; \boldsymbol{\theta}) := \Sigma + s_N^2(\boldsymbol{\theta})$, $C_{N+B}(\boldsymbol{\theta}; \boldsymbol{\theta}) := \Sigma + s_{N+B}^2(\boldsymbol{\theta}; \boldsymbol{\theta})$, and $s_{N+B}^2(\boldsymbol{\theta}; \boldsymbol{\theta}) := k_{N+B}^{\boldsymbol{\theta}}(\boldsymbol{\theta}, \boldsymbol{\theta})$.

Proof. The prior density is a constant, and thus is pulled out of the variance and squared. Applying Proposition A.3, the conditional variance term thus becomes

$$\begin{aligned} \text{Var}[\mathcal{N}(y_o \mid f_{N+B}^{\boldsymbol{\theta}, \boldsymbol{\varphi}}(\boldsymbol{\theta}), \Sigma) \mid \boldsymbol{\theta}, \boldsymbol{\varphi}] &= \quad (54) \\ \frac{\mathcal{N}(y_o \mid \mu_{N+B}^{\boldsymbol{\theta}, \boldsymbol{\varphi}}(\boldsymbol{\theta}), \frac{1}{2}\Sigma + s_{N+B}^2(\boldsymbol{\theta}; \boldsymbol{\theta}))}{\det(2\pi\Sigma)^{1/2}} &- \frac{\mathcal{N}(y_o \mid \mu_{N+B}^{\boldsymbol{\theta}, \boldsymbol{\varphi}}(\boldsymbol{\theta}), \frac{1}{2}[\Sigma + s_{N+B}^2(\boldsymbol{\theta}; \boldsymbol{\theta})])}{\det(2\pi[\Sigma + s_{N+B}^2(\boldsymbol{\theta}; \boldsymbol{\theta})])^{1/2}}. \end{aligned}$$

The denominators in the above expression can be pulled out of the outer expectation and are seen to equal the denominators in the desired expression. We thus complete the proof by computing the expectation of the numerators with respect to $\boldsymbol{\varphi}$. Applying Lemma A.1 and Proposition A.3 yields

$$\begin{aligned} &\mathbb{E}_{\boldsymbol{\varphi}}[\mathcal{N}(y_o \mid \mu_{N+B}^{\boldsymbol{\theta}, \boldsymbol{\varphi}}(\boldsymbol{\theta}), \Sigma/2 + s_{N+B}^2(\boldsymbol{\theta}; \boldsymbol{\theta}))] \\ &= \mathcal{N}(y_o \mid \mu_N(\boldsymbol{\theta}), [\Sigma/2 + s_{N+B}^2(\boldsymbol{\theta}; \boldsymbol{\theta})] + [s_N^2(\boldsymbol{\theta}) - s_{N+B}^2(\boldsymbol{\theta}; \boldsymbol{\theta})]) \\ &= \mathcal{N}(y_o \mid \mu_N(\boldsymbol{\theta}), \Sigma/2 + s_N^2(\boldsymbol{\theta})) \end{aligned}$$

and

$$\begin{aligned} &\mathbb{E}_{\boldsymbol{\varphi}}[\mathcal{N}(y_o \mid \mu_{N+B}^{\boldsymbol{\theta}, \boldsymbol{\varphi}}(\boldsymbol{\theta}), [\Sigma + s_{N+B}^2(\boldsymbol{\theta}; \boldsymbol{\theta})]/2)] \\ &= \mathcal{N}(y_o \mid \mu_N(\boldsymbol{\theta}), [\Sigma + s_{N+B}^2(\boldsymbol{\theta}; \boldsymbol{\theta})]/2 + [s_N^2(\boldsymbol{\theta}) - s_{N+B}^2(\boldsymbol{\theta}; \boldsymbol{\theta})]) \\ &= \mathcal{N}(y_o \mid \mu_N(\boldsymbol{\theta}), [\Sigma/2 + s_N^2(\boldsymbol{\theta})] - s_{N+B}^2(\boldsymbol{\theta}; \boldsymbol{\theta})/2). \end{aligned}$$

We now rearrange the covariances of the above expressions to obtain

$$\begin{aligned} \Sigma/2 + s_N^2(\boldsymbol{\theta}) &= C_N(\boldsymbol{\theta}) - \Sigma/2 \\ [\Sigma/2 + s_N^2(\boldsymbol{\theta})] - s_{N+B}^2(\boldsymbol{\theta}; \boldsymbol{\theta})/2 &= C_N(\boldsymbol{\theta}) - C_{N+B}(\boldsymbol{\theta})/2. \end{aligned}$$

□

A.2. Log-Density Emulation

The log-likelihood emulation setting yields the unnormalized posterior surrogate $\tilde{\pi}_N(\boldsymbol{\theta}) = \pi_0(\boldsymbol{\theta}) \exp\{f_N(\boldsymbol{\theta})\}$. This is a log-normal process and thus the mean and variance in Example 11 follow immediately from the known forms of log-normal moments. We now derive the form of the expected conditional variance criterion in Example 16.

Proposition A.5. Let $\tilde{\pi}(\theta; f_{N+B}^{\theta, \varphi}) = \pi_0(\theta) \exp\{f_{N+B}^{\theta, \varphi}(\theta)\}$ denote the unnormalized posterior surrogate induced by updating the emulator f_N with new training data $\{\theta, \varphi\}$. Under the assumption $\varphi \sim \mathcal{N}(\mu_N(\theta), s_N^2(\theta))$, the expected conditional variance is given by

$$\mathbb{E}_{\varphi} \left\{ \text{Var}[\tilde{\pi}(\theta; f_{N+B}^{\theta, \varphi}) \mid \theta, \varphi] \right\} = \text{Var}_{\nu_N} [\tilde{\pi}_N(\theta) \mid \varphi_N(\theta) = \mu_N(\theta)] \tau_N(\theta; \theta), \quad (55)$$

where

$$\tau_N(\theta; \theta) = \exp\{2(s_N^2(\theta) - s_{N+B}^2(\theta; \theta))\}. \quad (56)$$

The first term in Equation (55) is computed by conditioning the GP on $\{\theta, \mu_N(\theta)\}$ and then evaluating the log-normal variance of the resulting unnormalized posterior surrogate. See Example 16 for the explicit expression.

Proof. After pulling out the constant $\pi_0(\theta)$, note that

$$\exp\{f_N(\theta)\} \mid [\varphi_N(\theta) = \varphi] \sim \text{Lognormal}(\mu_{N+B}^{\theta, \varphi}(\theta), s_{N+B}^2(\theta; \theta)). \quad (57)$$

Applying the formula for a log-normal variance yields

$$\text{Var}[\exp\{f_N(\theta)\} \mid \varphi_N(\theta) = \varphi] = \varsigma \cdot \exp\{2\mu_{N+B}^{\theta, \varphi}(\theta)\}, \quad (58)$$

where

$$\varsigma := [\exp\{s_{N+B}^2(\theta; \theta)\} - 1] \exp\{s_{N+B}^2(\theta; \theta)\}$$

is not a function of the random variable φ . Applying Lemma A.1 gives

$$\exp\{2\mu_{N+B}^{\theta, \varphi}(\theta)\} \sim \text{Lognormal}(2\mu_N(\theta), 4[s_N^2(\theta) - s_{N+B}^2(\theta; \theta)]),$$

which has the log-normal mean

$$\begin{aligned} \mathbb{E}_{\varphi}[\exp\{2\mu_{N+B}^{\theta, \varphi}(\theta)\}] &= \exp\{2\mu_N(\theta)\} \exp\{2[s_N^2(\theta) - s_{N+B}^2(\theta; \theta)]\} \\ &= \exp\{2\mu_N(\theta)\} \tau(\theta; \theta). \end{aligned}$$

Plugging this expression back into Equation (58) gives

$$\begin{aligned} \mathbb{E}_{\varphi} \text{Var}[\exp\{f_N(\theta)\} \mid \varphi_N(\theta) = \varphi] &= \varsigma \cdot \exp\{2\mu_N(\theta)\} \tau(\theta; \theta) \\ &= \text{Var}_{\nu_N} [\tilde{\pi}_N(\theta) \mid \varphi(\theta) = \mu_N(\theta)] \tau_N(\theta; \theta). \end{aligned}$$

□

References

- AAKULA, V., FER, I. and VIRA, J. (2025). Emulator-based calibration of a dynamic grassland model using recurrent neural networks and Hamiltonian Monte Carlo. *European Journal of Agronomy* **170** 127769. <https://doi.org/10.1016/j.eja.2025.127769>

- ABDAR, M., POURPANAH, F., HUSSAIN, S., REZAZADEGAN, D., LIU, L., GHAVAMZADEH, M., FIEGUTH, P., CAO, X., KHOSRAVI, A., ACHARYA, U. R., MAKARENKOV, V. and NAHAVANDI, S. (2021). A review of uncertainty quantification in deep learning: Techniques, applications and challenges. *Inf. Fusion* **76** 243–297. <https://doi.org/10.1016/j.inffus.2021.05.008>
- ALAWIEH, L., GOODMAN, J. and BELL, J. B. (2020). Iterative construction of Gaussian process surrogate models for Bayesian inference. *Journal of Statistical Planning and Inference* **207** 55–72. <https://doi.org/10.1016/j.jspi.2019.11.002>
- ALQUIER, P., FRIEL, N., EVERITT, R. and BOLAND, A. (2016). Noisy Monte Carlo: convergence of Markov chains with approximate transition kernels. *Statistics and Computing* **26** 29–47. <https://doi.org/10.1007/s11222-014-9521-x>
- ANDRIEU, C., DOUCET, A. and HOLENSTEIN, R. (2010). Particle Markov chain Monte Carlo methods. *Journal of the Royal Statistical Society Series B: Statistical Methodology* **72** 269–342. <https://doi.org/10.1111/j.1467-9868.2009.00736.x>
- ANDRIEU, C. and ROBERTS, G. O. (2009). The pseudo-marginal approach for efficient Monte Carlo computations. *The Annals of Statistics* **37** 697 – 725. <https://doi.org/10.1214/07-AOS574>
- ASTUDILLO, R. and FRAZIER, P. (2019). Bayesian Optimization of Composite Functions. In *Proceedings of the 36th International Conference on Machine Learning* (K. CHAUDHURI and R. SALAKHUTDINOV, eds.). *Proceedings of Machine Learning Research* **97** 354–363. PMLR.
- BADIA, A. P., SPRECHMANN, P., VITVITSKYI, A., GUO, D., PIOT, B., KAPTUROWSKI, S., TIELEMAN, O., ARJOVSKY, M., PRITZEL, A., BOLT, A. and BLUNDELL, C. (2020). Never Give Up: Learning Directed Exploration Strategies.
- BAI, T., TECKENTRUP, A. L. and ZYGALAKIS, K. C. (2024). Gaussian processes for Bayesian inverse problems associated with linear partial differential equations. *Statistics and Computing* **34**. <https://doi.org/10.1007/s11222-024-10452-2>
- BAKER, E., BARBILLON, P., FADIKAR, A., GRAMACY, R. B., HERBEI, R., HIGDON, D., HUANG, J., JOHNSON, L. R., MA, P., MONDAL, A., PIRES, B., SACKS, J. and SOKOLOV, V. (2022). Analyzing Stochastic Computer Models: A Review with Opportunities. *Statistical Science* **37** 64–89. <https://doi.org/10.1214/21-STS822>
- BALANDAT, M., KARRER, B., JIANG, D. R., DAULTON, S., LETHAM, B., WILSON, A. G. and BAKSHY, E. (2020). BoTorch: A Framework for Efficient Monte-Carlo Bayesian Optimization. In *Advances in Neural Information Processing Systems* **33**.
- BASTOS, L. S. and O’HAGAN, A. (2009). Diagnostics for Gaussian Process Emulators. *Technometrics* **51** 425–438. <https://doi.org/10.1198/TECH.2009.08019>
- BECT, J., BACHOC, F. and GINSBOURGER, D. (2019). A supermartingale ap-

- proach to Gaussian process based sequential design of experiments. *Bernoulli* **25** 2883 – 2919. <https://doi.org/10.3150/18-BEJ1074>
- BECT, J., GINSBOURGER, D., LI, L., PICHENY, V. and VAZQUEZ, E. (2011). Sequential design of computer experiments for the estimation of a probability of failure. *Statistics and Computing* **22** 773-793. <https://doi.org/10.1007/s11222-011-9241-4>
- BHARTI, A., HUANG, D., KASKI, S. and BRIOL, F.-X. (2025). Cost-aware simulation-based inference. In *Proceedings of The 28th International Conference on Artificial Intelligence and Statistics* (Y. LI, S. MANDT, S. AGRAWAL and E. KHAN, eds.). *Proceedings of Machine Learning Research* **258** 28–36. PMLR.
- BHATTACHARYYA, B. (2020). Global sensitivity analysis: A Bayesian learning based polynomial chaos approach. *Journal of Computational Physics* **415** 109539. <https://doi.org/10.1016/j.jcp.2020.109539>
- BILIONIS, I. and ZABARAS, N. (2013). Solution of inverse problems with limited forward solver evaluations: a Bayesian perspective. *Inverse Problems* **30** 015004. <https://doi.org/10.1088/0266-5611/30/1/015004>
- BINOIS, M., HUANG, J., GRAMACY, R. B. and LUDKOVSKI, M. (2018). Replication or Exploration? Sequential Design for Stochastic Simulation Experiments. *Technometrics* **61** 7–23. <https://doi.org/10.1080/00401706.2018.1469433>
- BLIZNYUK, N., RUPPERT, D. and SHOEMAKER, C. A. (2012). Local Derivative-Free Approximation of Computationally Expensive Posterior Densities. *Journal of Computational and Graphical Statistics* **21** 676–695. PMID: 29861616; PMCID: PMC5978778. <https://doi.org/10.1080/10618600.2012.681255>
- BLIZNYUK, N., RUPPERT, D., SHOEMAKER, C., REGIS, R., WILD, S. and MUGUNTHAN, P. (2008). Bayesian Calibration and Uncertainty Analysis for Computationally Expensive Models Using Optimization and Radial Basis Function Approximation. *Journal of Computational and Graphical Statistics* **17** 270-294. <https://doi.org/10.1198/106186008X320681>
- BONILLA, E. V., CHAI, K. and WILLIAMS, C. (2007). Multi-task Gaussian Process Prediction. In *Advances in Neural Information Processing Systems* (J. PLATT, D. KOLLER, Y. SINGER and S. ROWEIS, eds.) **20**. Curran Associates, Inc.
- BOOTH, A. S., COOPER, A. and GRAMACY, R. B. (2024). Nonstationary Gaussian Process Surrogates. <https://doi.org/10.48550/arXiv.2305.19242>
- BRADFORD, E. and IMSLAND, L. (2021). Combining Gaussian processes and polynomial chaos expansions for stochastic nonlinear model predictive control. <https://doi.org/10.48550/arXiv.2103.05441>
- BRIOL, F.-X., OATES, C. J., COCKAYNE, J., CHEN, W. Y. and GIROLAMI, M. (2017). On the Sampling Problem for Kernel Quadrature. In *Proceedings of the 34th International Conference on Machine Learning* (D. PRECUP and Y. W. TEH, eds.). *Proceedings of Machine Learning Research* **70** 586–595. PMLR.
- BROOKS, S., GELMAN, A., JONES, G. and MENG, X.-L., eds. (2011). *Handbook*

- of *Markov Chain Monte Carlo*, 1st ed. Chapman and Hall/CRC. <https://doi.org/10.1201/b10905>
- BÜRKNER, P.-C., KRÖKER, I., OLADYSHKIN, S. and NOWAK, W. (2023). A fully Bayesian sparse polynomial chaos expansion approach with joint priors on the coefficients and global selection of terms. *Journal of Computational Physics* **488** 112210. <https://doi.org/10.1016/j.jcp.2023.112210>
- CARMONA, C. U. (2023). Bayesian Semi-Modular Inference: theory and methods for inference in multi-modular settings under model misspecification, PhD thesis, University of Oxford.
- CÉROU, F., HÉAS, P. and ROUSSET, M. (2025). Adaptive Reduced Tempering for Bayesian Inverse Problems and Rare Event Simulation. *SIAM/ASA Journal on Uncertainty Quantification* **13** 2022-2053. <https://doi.org/10.1137/24M170510X>
- CHEVALIER, C. (2013). Fast uncertainty reduction strategies relying on Gaussian process models, PhD thesis.
- CHEVALIER, C. and GINSBOURGER, D. (2013). Fast Computation of the Multi-Points Expected Improvement with Applications in Batch Selection. In *Learning and Intelligent Optimization* (G. NICOSIA and P. PARDALOS, eds.) 59–69. Springer Berlin Heidelberg, Berlin, Heidelberg.
- CHRISTEN, J. A. and FOX, C. (2005). Markov chain Monte Carlo Using an Approximation. *Journal of Computational and Graphical Statistics* **14** 795–810. <https://doi.org/10.1198/106186005X76983>
- CLEARY, E., GARBUNO-INIGO, A., LAN, S., SCHNEIDER, T. and STUART, A. M. (2021). Calibrate, emulate, sample. *Journal of Computational Physics* **424** 109716. <https://doi.org/10.1016/j.jcp.2020.109716>
- COLE, D. A., GRAMACY, R. B., WARNER, J. E., BOMARITO, G. F., LESER, P. E. and LESER, W. P. (2023). Entropy-based adaptive design for contour finding and estimating reliability. *Journal of Quality Technology* **55** 43–60. <https://doi.org/10.1080/00224065.2022.2053795>
- CONRAD, P. R., MARZOUK, Y. M., PILLAI, N. S. and AND, A. S. (2016). Accelerating Asymptotically Exact MCMC for Computationally Intensive Models via Local Approximations. *Journal of the American Statistical Association* **111** 1591–1607. <https://doi.org/10.1080/01621459.2015.1096787>
- CONTI, S. and O’HAGAN, A. (2010). Bayesian emulation of complex multi-output and dynamic computer models. *Journal of Statistical Planning and Inference* **140** 640-651. <https://doi.org/10.1016/j.jspi.2009.08.006>
- CONTI, S., GOSLING, J. P., OAKLEY, J. E. and O’HAGAN, A. (2009). Gaussian process emulation of dynamic computer codes. *Biometrika* **96** 663-676. <https://doi.org/10.1093/biomet/asp028>
- CRANMER, K., BREHMER, J. and LOUPPE, G. (2020). The frontier of simulation-based inference. *Proceedings of the National Academy of Sciences* **117** 30055–30062. <https://doi.org/10.1073/pnas.1912789117>
- CRANMER, K., PAVEZ, J. and LOUPPE, G. (2015). Approximating Likelihood Ratios with Calibrated Discriminative Classifiers.
- CUI, T., MARTIN, J., MARZOUK, Y. M., SOLONEN, A. and SPANTINI, A. (2014). Likelihood-informed dimension reduction for nonlinear inverse prob-

- lems. *Inverse Problems* **30** 114015. <https://doi.org/10.1088/0266-5611/30/11/114015>
- DAGON, K., SANDERSON, B. M., FISHER, R. A. and LAWRENCE, D. M. (2020). A machine learning approach to emulation and biophysical parameter estimation with the Community Land Model, version 5. *Advances in Statistical Climatology, Meteorology and Oceanography* **6** 223–244. <https://doi.org/10.5194/ascmo-6-223-2020>
- DAX, M., GREEN, S. R., GAIR, J., MACKE, J. H., BUONANNO, A. and SCHÖLKOPF, B. (2021). Real-Time Gravitational Wave Science with Neural Posterior Estimation. *Phys. Rev. Lett.* **127** 241103. <https://doi.org/10.1103/PhysRevLett.127.241103>
- DELIGIANNIDIS, G., DOUCET, A. and PITT, M. K. (2018). The correlated pseudo-marginal method. *Journal of the Royal Statistical Society Series B: Statistical Methodology* **80** 839–870. <https://doi.org/10.1111/rssb.12280>
- DIETZEL, A. and REICHERT, P. (2014). Bayesian inference of a lake water quality model by emulating its posterior density. *Water Resources Research* **50** 7626–7647. <https://doi.org/10.1002/2012WR013086>
- DINKEL, M., GEITNER, C. M., ROBALO REI, G., NITZLER, J. and WALL, W. A. (2024). Solving Bayesian inverse problems with expensive likelihoods using constrained Gaussian processes and active learning. *Inverse Problems* **40** 095008. <https://doi.org/10.1088/1361-6420/ad5eb4>
- DOUCET, A., DE FREITAS, N. and GORDON, N. (2001). *An Introduction to Sequential Monte Carlo Methods In Sequential Monte Carlo Methods in Practice* 3–14. Springer New York, New York, NY. https://doi.org/10.1007/978-1-4757-3437-9_1
- DOUMONT, C., FAN, D., MAUS, N., GARDNER, J. R., MOSS, H. and PLEISS, G. (2025). We Still Don’t Understand High-Dimensional Bayesian Optimization.
- DROVANDI, C. C., MOORES, M. T. and BOYS, R. J. (2018). Accelerating pseudo-marginal MCMC using Gaussian processes. *Computational Statistics & Data Analysis* **118** 1–17. <https://doi.org/10.1016/j.csda.2017.09.002>
- DUNBAR, O. R. A., GARBUNO-INIGO, A., SCHNEIDER, T. and STUART, A. M. (2021). Calibration and Uncertainty Quantification of Convective Parameters in an Idealized GCM. *Journal of Advances in Modeling Earth Systems* **13** e2020MS002454. e2020MS002454 2020MS002454. <https://doi.org/10.1029/2020MS002454>
- DUNBAR, O. R. A., BIELI, M., GARBUNO-ÍÑIGO, A., HOWLAND, M., DE SOUZA, A. N., MANSFIELD, L. A., WAGNER, G. L. and EFRAT-HENRICI, N. (2024). CalibrateEmulateSample.jl: Accelerated Parametric Uncertainty Quantification. *Journal of Open Source Software* **9** 6372. <https://doi.org/10.21105/joss.06372>
- DURKAN, C., PAPAMAKARIOS, G. and MURRAY, I. (2018). Sequential Neural Methods for Likelihood-free Inference.
- ERIKSSON, D. and POLOCZEK, M. (2021). Scalable Constrained Bayesian Op-

- timization. In *Proceedings of The 24th International Conference on Artificial Intelligence and Statistics* (A. BANERJEE and K. FUKUMIZU, eds.). *Proceedings of Machine Learning Research* **130** 730–738. PMLR.
- FADIKAR, A., HIGDON, D., CHEN, J., LEWIS, B., VENKATRAMANAN, S. and MARATHE, M. (2018). Calibrating a Stochastic, Agent-Based Model Using Quantile-Based Emulation. *SIAM/ASA Journal on Uncertainty Quantification* **6** 1685–1706. <https://doi.org/10.1137/17M1161233>
- FEDOROV, V. (1972). *Theory of Optimal Experiments Designs*.
- FER, I., KELLY, R., MOORCROFT, P. R., RICHARDSON, A. D., COWDERY, E. M. and DIETZE, M. C. (2018). Linking big models to big data: efficient ecosystem model calibration through Bayesian model emulation. *Bio-geosciences* **15** 5801–5830. <https://doi.org/10.5194/bg-15-5801-2018>
- FRAZIER, D. T. and NOTT, D. J. (2025). Cutting Feedback and Modularized Analyses in Generalized Bayesian Inference. *Bayesian Analysis* **20** 1647–1675.
- FRAZIER, D. T., NOTT, D. J., DROVANDI, C. and KOHN, R. (2023). Bayesian Inference Using Synthetic Likelihood: Asymptotics and Adjustments. *Journal of the American Statistical Association* **118** 2821–2832. <https://doi.org/10.1080/01621459.2022.2086132>
- GABRY, J., SIMPSON, D., VEHTARI, A., BETANCOURT, M. and GELMAN, A. (2019). Visualization in Bayesian workflow. *Journal of the Royal Statistical Society Series A: Statistics in Society* **182** 389–402. <https://doi.org/10.1111/rssa.12378>
- GAL, Y. and GHAHRAMANI, Z. (2016). Dropout as a Bayesian Approximation: Representing Model Uncertainty in Deep Learning. In *Proceedings of The 33rd International Conference on Machine Learning* (M. F. BALCAN and K. Q. WEINBERGER, eds.). *Proceedings of Machine Learning Research* **48** 1050–1059. PMLR, New York, New York, USA.
- GAREGNANI, G. (2021). Sampling Methods for Bayesian Inference Involving Convergent Noisy Approximations of Forward Maps. <https://doi.org/10.48550/arXiv.2111.03491>
- GARUD, S. S., KARIMI, I. A. and KRAFT, M. (2017). Design of computer experiments: A review. *Computers & Chemical Engineering* **106** 71–95. ESCAPE-26. <https://doi.org/10.1016/j.compchemeng.2017.05.010>
- GELMAN, A., CARLIN, J. B., STERN, H. S., DUNSON, D. B., VEHTARI, A. and RUBIN, D. B. (2013). *Bayesian Data Analysis*, 3rd ed. CRC Press, Boca Raton, FL.
- GELMAN, A., VEHTARI, A., SIMPSON, D., MARGOSSIAN, C. C., CARPENTER, B., YAO, Y., KENNEDY, L., GABRY, J., BÜRKNER, P.-C. and MODRÁK, M. (2020). Bayesian Workflow. <https://doi.org/10.48550/arXiv.2011.01808>
- GINSBOURGER, D., LE RICHE, R. and CARRARO, L. (2010). *Kriging Is Well-Suited to Parallelize Optimization In Computational Intelligence in Expensive Optimization Problems* 131–162. Springer Berlin Heidelberg, Berlin, Heidelberg. https://doi.org/10.1007/978-3-642-10701-6_6
- GJINI, R., MORZFELD, M., DUNBAR, O. R. A. and SCHNEIDER, T. (2025). The Ensemble Kalman Inversion Race.

- GNEITING, T. and RAFTERY, A. E. (2007). Strictly Proper Scoring Rules, Prediction, and Estimation. *Journal of the American Statistical Association* **102** 359–378. <https://doi.org/10.1198/016214506000001437>
- GONZALEZ, J., OSBORNE, M. and LAWRENCE, N. (2016). GLASSES: Relieving The Myopia Of Bayesian Optimisation. In *Proceedings of the 19th International Conference on Artificial Intelligence and Statistics* (A. GRETTON and C. C. ROBERT, eds.). *Proceedings of Machine Learning Research* **51** 790–799. PMLR, Cadiz, Spain.
- GORODETSKY, A. and MARZOUK, Y. (2016). Mercer Kernels and Integrated Variance Experimental Design: Connections Between Gaussian Process Regression and Polynomial Approximation. *SIAM/ASA Journal on Uncertainty Quantification* **4** 796–828. <https://doi.org/10.1137/15M1017119>
- GRAMACY, R. B. (2020). *Surrogates: Gaussian Process Modeling, Design and Optimization for the Applied Sciences*. Chapman Hall/CRC, Boca Raton, Florida. <http://bobby.gramacy.com/surrogates/>.
- GRAVES, A. (2011). Practical Variational Inference for Neural Networks. In *Advances in Neural Information Processing Systems* (J. SHAWE-TAYLOR, R. ZEMEL, P. BARTLETT, F. PEREIRA and K. Q. WEINBERGER, eds.) **24**. Curran Associates, Inc.
- GUTMANN, M. U. and CORANDER, J. (2016). Bayesian Optimization for Likelihood-Free Inference of Simulator-Based Statistical Models. *Journal of Machine Learning Research* **17** 1–47.
- HARTIG, F., CALABRESE, J. M., REINEKING, B., WIEGAND, T. and HUTH, A. (2011). Statistical inference for stochastic simulation models – theory and application. *Ecology Letters* **14** 816–827. <https://doi.org/10.1111/j.1461-0248.2011.01640.x>
- HE, W., JIANG, Z., XIAO, T., XU, Z. and LI, Y. (2025). A Survey on Uncertainty Quantification Methods for Deep Learning. <https://doi.org/10.48550/arXiv.2302.13425>
- HELIN, T., STUART, A. M., TECKENTRUP, A. L. and ZYGALAKIS, K. C. (2024). Introduction to Gaussian Process Regression in Bayesian Inverse Problems, with New Results on Experimental Design for Weighted Error Measures. In *Monte Carlo and Quasi-Monte Carlo Methods* (A. HINRICHS, P. KRITZER and F. PILLICHSHAMMER, eds.) 49–79. Springer International Publishing, Cham. https://doi.org/10.1007/978-3-031-59762-6_3
- HIGDON, D., GATTIKER, J., WILLIAMS, B. and RIGHTLEY, M. (2008). Computer Model Calibration Using High-Dimensional Output. *Journal of the American Statistical Association* **103** 570–583. <https://doi.org/10.1198/016214507000000888>
- HIGDON, D., MCDONNELL, J. D., SCHUNCK, N., SARICH, J. and WILD, S. M. (2015). A Bayesian approach for parameter estimation and prediction using a computationally intensive model. *Journal of Physics G: Nuclear and Particle Physics* **42** 034009. <https://doi.org/10.1088/0954-3899/42/3/034009>
- HUANG, M., RAY, J., HOU, Z., REN, H., LIU, Y. and SWILER, L. (2016). On the applicability of surrogate-based Markov chain Monte Carlo-Bayesian inversion to the Community Land Model: Case studies at flux tower sites.

- Journal of Geophysical Research: Atmospheres* **121** 7548–7563. <https://doi.org/10.1002/2015JD024339>
- HUANG, J., GRAMACY, R. B., BINOIS, M. and LIBRASCHI, M. (2020). On-site surrogates for large-scale calibration. *Applied Stochastic Models in Business and Industry* **36** 283–304. <https://doi.org/10.1002/asmb.2523>
- HÜLLERMEIER, E. and WAEGEMAN, W. (2021). Aleatoric and epistemic uncertainty in machine learning: an introduction to concepts and methods. *Mach Learn* **110** 457–506. <https://doi.org/10.1007/s10994-021-05946-3>
- IGLESIAS, M. A., LAW, K. J. H. and STUART, A. M. (2013). Ensemble Kalman methods for inverse problems. *Inverse Problems* **29** 045001. <https://doi.org/10.1088/0266-5611/29/4/045001>
- JACOB, P. E., MURRAY, L. M., HOLMES, C. C. and ROBERT, C. P. (2017). Better together? Statistical learning in models made of modules. <https://doi.org/10.48550/arXiv.1708.08719>
- JÄRVENPÄÄ, M. and CORANDER, J. (2024). Approximate Bayesian inference from noisy likelihoods with Gaussian process emulated MCMC. *Journal of Machine Learning Research* **25** 1–55. <https://doi.org/10.48550/arXiv.2104.03942>
- JÄRVENPÄÄ, M., GUTMANN, M. U., VEHTARI, A. and MARTTINEN, P. (2021). Parallel Gaussian Process Surrogate Bayesian Inference with Noisy Likelihood Evaluations. *Bayesian Analysis* **16** 147 – 178. <https://doi.org/10.1214/20-BA1200>
- JEDHOFF, S., KUTABI, H., MEYER, A. and BÜRKNER, P.-C. (2026). Efficient Uncertainty Propagation in Bayesian Two-Step Procedures.
- JOSEPH, V. R., DASGUPTA, T., TUO, R. and AND, C. F. J. W. (2015). Sequential Exploration of Complex Surfaces Using Minimum Energy Designs. *Technometrics* **57** 64–74. <https://doi.org/10.1080/00401706.2014.881749>
- JOSEPH, V. R., WANG, D., GU, L., LYU, S. and AND, R. T. (2019). Deterministic Sampling of Expensive Posteriors Using Minimum Energy Designs. *Technometrics* **61** 297–308. <https://doi.org/10.1080/00401706.2018.1552203>
- JÄRVENPÄÄ, M., GUTMANN, M., PLESKA, A., VEHTARI, A. and MARTTINEN, P. (2019). Efficient Acquisition Rules for Model-Based Approximate Bayesian Computation. *Bayesian Analysis* **14**. <https://doi.org/10.1214/18-BA1121>
- KANDASAMY, K., SCHNEIDER, J. and PÓCZOS, B. (2015). Bayesian Active Learning for Posterior Estimation. In *Proceedings of the 24th International Conference on Artificial Intelligence. IJCAI'15* 3605–3611. AAAI Press.
- KANDASAMY, K., SCHNEIDER, J. and PÓCZOS, B. (2017). Query efficient posterior estimation in scientific experiments via Bayesian active learning. *Artificial Intelligence* **243** 45–56. <https://doi.org/10.1016/j.artint.2016.11.002>
- KANDASAMY, K., KRISHNAMURTHY, A., SCHNEIDER, J. and POCZOS, B. (2018). Parallelised Bayesian Optimisation via Thompson Sampling. In *Proceedings of the Twenty-First International Conference on Artificial Intelligence and Statistics* (A. STORKEY and F. PEREZ-CRUZ, eds.). *Proceedings of Machine Learning Research* **84** 133–142. PMLR.

- KARABATSOS, G. and LEISEN, F. (2018). An approximate likelihood perspective on ABC methods. *Statistics Surveys* **12** 66 – 104. <https://doi.org/10.1214/18-SS120>
- KEETZ, L. T., AALSTAD, K., FISHER, R. A., POPPE TERÁN, C., NAZ, B., PIRK, N., YILMAZ, Y. A. and SKARPAAS, O. (2025). Inferring Parameters in a Complex Land Surface Model by Combining Data Assimilation and Machine Learning. *Journal of Advances in Modeling Earth Systems* **17** e2024MS004542. e2024MS004542 2024MS004542. <https://doi.org/10.1029/2024MS004542>
- KENNEDY, M. C. and O’HAGAN, A. (2001). Bayesian calibration of computer models. *Journal of the Royal Statistical Society: Series B (Statistical Methodology)* **63** 425-464. <https://doi.org/10.1111/1467-9868.00294>
- KIM, H. and SANZ-ALONSO, D. (2024). Enhancing Gaussian Process Surrogates for Optimization and Posterior Approximation via Random Exploration.
- KOCHENDERFER, M. J., AMATO, C., CHOWDHARY, G., HOW, J. P., REYNOLDS, H. J. D., THORNTON, J. R., TORRES-CARRASQUILLO, P. A., ÜRE, N. K. and VIAN, J. (2015). *Decision Making Under Uncertainty: Theory and Application*. The MIT Press, Cambridge, MA. <https://doi.org/10.7551/mitpress/10187.001.0001>
- KOERMER, S., LODA, J., NOBLE, A. and AND, R. B. G. (2024). Augmenting a Simulation Campaign for Hybrid Computer Model and Field Data Experiments. *Technometrics* **66** 638–650. <https://doi.org/10.1080/00401706.2024.2345139>
- KROUGLOVA, A. N., JOHNSON, H. R., CONFAVREUX, B., DEISTLER, M. and GONÇALVES, P. J. (2025). Multifidelity Simulation-based Inference for Computationally Expensive Simulators.
- LAKSHMINARAYANAN, B., PRITZEL, A. and BLUNDELL, C. (2017). Simple and Scalable Predictive Uncertainty Estimation using Deep Ensembles. In *Advances in Neural Information Processing Systems* (I. GUYON, U. V. LUXBURG, S. BENGIO, H. WALLACH, R. FERGUS, S. VISHWANATHAN and R. GARNETT, eds.) **30**. Curran Associates, Inc. <https://doi.org/10.48550/arXiv.1612.01474>
- LARTAUD, P., HUMBERT, P. and GARNIER, J. (2024). Sequential design for surrogate modeling in Bayesian inverse problems. <https://doi.org/10.48550/arXiv.2402.16520>
- LEBEL, D., SOIZE, C., FÜNFSCHILLING, C. and PERRIN, G. (2019). Statistical inverse identification for nonlinear train dynamics using a surrogate model in a Bayesian framework. *Journal of Sound and Vibration* **458** 158-176. <https://doi.org/10.1016/j.jsv.2019.06.024>
- LI, J. and MARZOUK, Y. M. (2014). Adaptive Construction of Surrogates for the Bayesian Solution of Inverse Problems. *SIAM Journal on Scientific Computing* **36** A1163–A1186. <https://doi.org/10.1137/130938189>
- LI, Y., RUDNER, T. G. J. and WILSON, A. G. (2024). A Study of Bayesian Neural Network Surrogates for Bayesian Optimization. In *International Conference on Learning Representations* (B. KIM, Y. YUE, S. CHAUDHURI, K. FRAGKIADAKI, M. KHAN and Y. SUN, eds.) **2024** 47003–47041. <https://doi.org/10.26434/chemrxiv-2024-11>

- [//doi.org/10.48550/arXiv.2305.20028](https://doi.org/10.48550/arXiv.2305.20028)
- LI, C., VEHTARI, A., BÜRKNER, P.-C., RADEV, S. T., ACERBI, L. and SCHMITT, M. (2025). Amortized Bayesian Workflow. <https://doi.org/10.48550/arXiv.2409.04332>
- LIE, H. C., SULLIVAN, T. J. and TECKENTRUP, A. L. (2018). Random Forward Models and Log-Likelihoods in Bayesian Inverse Problems. *SIAM/ASA Journal on Uncertainty Quantification* **6** 1600–1629. <https://doi.org/10.1137/18m1166523>
- LIU, F., BAYARRI, M. and BERGER, J. (2009). Modularization in Bayesian analysis, with emphasis on analysis of computer models. *Bayesian Analysis* **4**. <https://doi.org/10.1214/09-BA404>
- LIU, F. and WEST, M. (2009). A dynamic modelling strategy for Bayesian computer model emulation. *Bayesian Analysis* **4** 393 – 411. <https://doi.org/10.1214/09-BA415>
- LLORENTE, F., MARTINO, L., READ, J. and DELGADO-GÓMEZ, D. (2025). A Survey of Monte Carlo Methods for Noisy and Costly Densities With Application to Reinforcement Learning and ABC. *International Statistical Review* **93** 18-61. <https://doi.org/10.1111/insr.12573>
- LOEPPKY, J. L., MOORE, L. M. and WILLIAMS, B. J. (2010). Batch sequential designs for computer experiments. *Journal of Statistical Planning and Inference* **140** 1452-1464. <https://doi.org/10.1016/j.jspi.2009.12.004>
- LU, F., MORZFELD, M., TU, X. and CHORIN, A. J. (2015). Limitations of polynomial chaos expansions in the Bayesian solution of inverse problems. *Journal of Computational Physics* **282** 138-147. <https://doi.org/10.1016/j.jcp.2014.11.010>
- LUECKMANN, J.-M., BASSETTO, G., KARALETOS, T. and MACKE, J. H. (2019). Likelihood-free inference with emulator networks. In *Proceedings of The 1st Symposium on Advances in Approximate Bayesian Inference* (F. RUIZ, C. ZHANG, D. LIANG and T. BUI, eds.). *Proceedings of Machine Learning Research* **96** 32–53. PMLR. <https://doi.org/10.48550/arXiv.1805.09294>
- MACKAY, D. J. C. (1992). A Practical Bayesian Framework for Backpropagation Networks. *Neural Computation* **4** 448-472. <https://doi.org/10.1162/neco.1992.4.3.448>
- MADDOX, W. J., BALANDAT, M., WILSON, A. G. and BAKSHY, E. (2021). Bayesian Optimization with High-Dimensional Outputs. In *Advances in Neural Information Processing Systems* (M. RANZATO, A. BEYGELZIMER, Y. DAUPHIN, P. S. LIANG and J. W. VAUGHAN, eds.) **34** 19274–19287. Curran Associates, Inc.
- MARINESCU, M., OLIVARES, A., STAFFETTI, E. and SUN, J. (2023). Polynomial Chaos Expansion-Based Enhanced Gaussian Process Regression for Wind Velocity Field Estimation from Aircraft-Derived Data. *Mathematics* **11**. <https://doi.org/10.3390/math11041018>
- MARZOUK, Y. M. and NAJM, H. N. (2009). Dimensionality reduction and polynomial chaos acceleration of Bayesian inference in inverse problems. *Journal of Computational Physics* **228** 1862-1902. <https://doi.org/10.1016/j.jcp>

- 2008.11.024
- MCCLARREN, R. G. (2018). *Uncertainty Quantification and Predictive Computational Science: A Foundation for Physical Scientists and Engineers*. Springer Cham <https://doi.org/10.1007/978-3-319-99525-0>.
- MEDINA-AGUAYO, F. J., LEE, A. and ROBERTS, G. O. (2016). Stability of noisy Metropolis–Hastings. *Statistics and Computing* **26** 1187–1211. <https://doi.org/10.1007/s11222-015-9604-3>
- MEEDS, E. and WELLING, M. (2014). GPS-ABC: Gaussian process surrogate approximate Bayesian computation. In *Proceedings of the Thirtieth Conference on Uncertainty in Artificial Intelligence. UAI'14* 593–602. AUAI Press, Arlington, Virginia, USA.
- MENA, J., PUJOL, O. and VITRIÀ, J. (2021). A Survey on Uncertainty Estimation in Deep Learning Classification Systems from a Bayesian Perspective. *ACM Comput. Surv.* **54**. <https://doi.org/10.1145/3477140>
- MILLER, J. J. and MAK, S. (2025). Targeted Variance Reduction: Effective Bayesian Optimization of Black-Box Simulators with Noise Parameters. *Technometrics* **67** 617–631. <https://doi.org/10.1080/00401706.2025.2495298>
- MOHAMMADI, H., CHALLENGOR, P. and GOODFELLOW, M. (2019). Emulating dynamic non-linear simulators using Gaussian processes. *Computational Statistics & Data Analysis* **139** 178-196. <https://doi.org/10.1016/j.csda.2019.05.006>
- NAESSETH, C. A., LINDSTEN, F. and SCHÖN, T. B. (2019). Elements of Sequential Monte Carlo. *Found. Trends Mach. Learn.* **12** 307–392. <https://doi.org/10.1561/22000000074>
- OAKLEY, J. E. and YOUNGMAN, B. D. (2017). Calibration of Stochastic Computer Simulators Using Likelihood Emulation. *Technometrics* **59** 80–92. <https://doi.org/10.1080/00401706.2015.1125391>
- OSBAND, I., WEN, Z., ASGHARI, S. M., DWARACHERLA, V., IBRAHIMI, M., LU, X. and VAN ROY, B. (2023a). Epistemic Neural Networks. In *Advances in Neural Information Processing Systems (A. OH, T. NAUMANN, A. GLOBERSON, K. SAENKO, M. HARDT and S. LEVINE, eds.)* **36** 2795–2823. Curran Associates, Inc. <https://doi.org/10.48550/arXiv.2107.08924>
- OSBAND, I., WEN, Z., ASGHARI, S. M., DWARACHERLA, V., IBRAHIMI, M., LU, X. and VAN ROY, B. (2023b). Approximate Thompson Sampling via Epistemic Neural Networks. In *Proceedings of the Thirty-Ninth Conference on Uncertainty in Artificial Intelligence (R. J. EVANS and I. SHPITSER, eds.)*. *Proceedings of Machine Learning Research* **216** 1586–1595. PMLR. <https://doi.org/10.48550/arXiv.2302.09205>
- OWEN, A. B. (2013). *Monte Carlo theory, methods and examples*. <https://artowen.su.domains/mc/>.
- PAN, X., CHEN, D., PAN, B., HUANG, X., YANG, K., PIAO, S., ZHOU, T., DAI, Y., CHEN, F. and LI, X. (2025). Evolution and prospects of Earth system models: Challenges and opportunities. *Earth-Science Reviews* **260** 104986. <https://doi.org/10.1016/j.earscirev.2024.104986>
- PAPAMAKARIOS, G. and MURRAY, I. (2016). Fast epsilon-free Inference of

- Simulation Models with Bayesian Conditional Density Estimation. In *Advances in Neural Information Processing Systems* (D. LEE, M. SUGIYAMA, U. LUXBURG, I. GUYON and R. GARNETT, eds.) **29**. Curran Associates, Inc. <https://doi.org/10.48550/arXiv.1605.06376>
- PAPAMAKARIOS, G., STERRATT, D. and MURRAY, I. (2019). Sequential Neural Likelihood: Fast Likelihood-free Inference with Autoregressive Flows. In *Proceedings of the Twenty-Second International Conference on Artificial Intelligence and Statistics* (K. CHAUDHURI and M. SUGIYAMA, eds.). *Proceedings of Machine Learning Research* **89** 837–848. PMLR.
- PAUN, L. M. and HUSMEIER, D. (2021). Markov chain Monte Carlo with Gaussian processes for fast parameter estimation and uncertainty quantification in a 1D fluid-dynamics model of the pulmonary circulation. *International Journal for Numerical Methods in Biomedical Engineering* **37** e3421. <https://doi.org/10.1002/cnm.3421>
- PICCHINI, U., SIMOLA, U. and CORANDER, J. (2023). Sequentially Guided MCMC Proposals for Synthetic Likelihoods and Correlated Synthetic Likelihoods. *Bayesian Analysis* **18** 1099 – 1129. <https://doi.org/10.1214/22-BA1305>
- PLUMMER, M. (2015). Cuts in Bayesian graphical models. **25** 37–43. <https://doi.org/10.1007/s11222-014-9503-z>
- PRICE, L. F., DROVANDI, C. C., LEE, A. and NOTT, D. J. (2018). Bayesian Synthetic Likelihood. *Journal of Computational and Graphical Statistics* **27** 1–11. <https://doi.org/10.1080/10618600.2017.1302882>
- PRITAM RANJAN, D. B. and MICHAELIDIS, G. (2008). Sequential Experiment Design for Contour Estimation From Complex Computer Codes. *Technometrics* **50** 527–541. <https://doi.org/10.1198/004017008000000541>
- RADEV, S. T., MERTENS, U. K., VOSS, A., ARDIZZONE, L. and KÖTHE, U. (2020). BayesFlow: Learning complex stochastic models with invertible neural networks. *IEEE transactions on neural networks and learning systems* **33** 1452–1466.
- RANJAN, P., THOMAS, M., TEISMANN, H. and MUKHOTI, S. (2016). Inverse problem for time-series valued computer model via scalarization. <https://doi.org/10.48550/arXiv.1605.09503>
- RAOULT, N., DOUGLAS, N., MACBEAN, N., KOLASSA, J., QUAIFE, T., ROBERTS, A. G., FISHER, R., FER, I., BACOUR, C., DAGON, K., HAWKINS, L., CARVALHAIS, N., COOPER, E., DIETZE, M. C., GENTINE, P., KAMINSKI, T., KENNEDY, D., LIDDY, H. M., MOORE, D. J. P., PEYLIN, P., PINNINGTON, E., SANDERSON, B., SCHOLZE, M., SEILER, C., SMALLMAN, T. L., VERGOPOLAN, N., VISKARI, T., WILLIAMS, M. and ZOBITZ, J. (2025). Parameter Estimation in Land Surface Models: Challenges and Opportunities With Data Assimilation and Machine Learning. *Journal of Advances in Modeling Earth Systems* **17** e2024MS004733. e2024MS004733. <https://doi.org/10.1029/2024MS004733>
- RASMUSSEN, C. E. (2003). Gaussian Processes to Speed up Hybrid Monte Carlo for Expensive Bayesian Integrals. In *Bayesian Statistics 7: Proceedings of the Seventh Valencia International Meeting* (J. M. Bernardo, M. J. Bayarri,

- J. O. Berger, A. P. Dawid, D. Heckerman, A. F. M. Smith and M. West, eds.) 651–659. Oxford University Press, Oxford, UK. <https://doi.org/10.1093/oso/9780198526155.003.0045>
- RASMUSSEN, C. E. (2004). *Gaussian Processes in Machine Learning* In *Advanced Lectures on Machine Learning: ML Summer Schools 2003, Canberra, Australia, February 2 - 14, 2003, Tübingen, Germany, August 4 - 16, 2003, Revised Lectures* 63–71. Springer Berlin Heidelberg, Berlin, Heidelberg. https://doi.org/10.1007/978-3-540-28650-9_4
- RAY, J., HOU, Z., HUANG, M., SARGSYAN, K. and SWILER, L. (2015). Bayesian Calibration of the Community Land Model Using Surrogates. *SIAM/ASA Journal on Uncertainty Quantification* **3** 199–233. <https://doi.org/10.1137/140957998>
- REISER, P., AGUILAR, J. E., GUTHKE, A. and BÜRKNER, P.-C. (2025). Uncertainty quantification and propagation in surrogate-based Bayesian inference. *Statistics and Computing* **35**. <https://doi.org/10.1007/s11222-025-10597-8>
- RICCIUS, L., ROCHA, I. B. C. M., BIERKENS, J., KEKKONEN, H. and VAN DER MEER, F. P. (2026). Integration of active learning and MCMC sampling for efficient Bayesian calibration of mechanical properties. *European Journal of Mechanics - A/Solids* **117** 106015. <https://doi.org/10.1016/j.euromechsol.2026.106015>
- RIIS, C., ANTUNES, F., HÜTTEL, F. B., AZEVEDO, C. L. and PEREIRA, F. C. (2022). Bayesian active learning with fully Bayesian Gaussian processes. In *Advances in Neural Information Processing Systems. NeurIPS '22* **35**. Curran Associates Inc., Red Hook, NY, USA.
- ROBERTS, A. G., DIETZE, M. and HUGGINS, J. H. (2026). Propagating Surrogate Uncertainty in Bayesian Inverse Problems. <https://doi.org/10.48550/arXiv.2601.03532>
- SACKS, J., WELCH, W. J., MITCHELL, T. J. and WYNN, H. P. (1989). Design and Analysis of Computer Experiments. *Statistical Science* **4** 409 – 423. <https://doi.org/10.1214/ss/1177012413>
- SATNER, T. J., WILLIAMS, B. J. and NOTZ, W. I. (2018). The Design and Analysis of Computer Experiments. <https://doi.org/10.1007/978-1-4939-8847-1>.
- SAUER, A., COOPER, A. and GRAMACY, R. B. (2023). Vecchia-Approximated Deep Gaussian Processes for Computer Experiments. *Journal of Computational and Graphical Statistics* **32** 824–837. <https://doi.org/10.1080/10618600.2022.2129662>
- SAUER, A., GRAMACY, R. B. and HIGDON, D. (2023). Active Learning for Deep Gaussian Process Surrogates. *Technometrics* **65** 4–18. <https://doi.org/10.1080/00401706.2021.2008505>
- SCHUEURER, S., REISER, P., BRÜNNETTE, T., NOWAK, W., GUTHKE, A. and BÜRKNER, P.-C. (2026). Uncertainty-Aware Surrogate-based Amortized Bayesian Inference for Computationally Expensive Models. *Transactions on Machine Learning Research*. <https://doi.org/10.48550/arXiv.2505.0868>

- SCHNEIDER, T., LAN, S., STUART, A. and TEIXEIRA, J. (2017). Earth System Modeling 2.0: A Blueprint for Models That Learn From Observations and Targeted High-Resolution Simulations. *Geophysical Research Letters* **44** 12,396-12,417. <https://doi.org/10.1002/2017GL076101>
- SHAHRIARI, B., SWERSKY, K., WANG, Z., ADAMS, R. P. and DE FREITAS, N. (2016). Taking the Human Out of the Loop: A Review of Bayesian Optimization. *Proceedings of the IEEE* **104** 148-175. <https://doi.org/10.1109/JPROC.2015.2494218>
- SHARMA, M., FARQUHAR, S., NALISNICK, E. and RAINFORTH, T. (2023). Do Bayesian Neural Networks Need To Be Fully Stochastic? In *Proceedings of The 26th International Conference on Artificial Intelligence and Statistics* (F. RUIZ, J. DY and J.-W. VAN DE MEENT, eds.). *Proceedings of Machine Learning Research* **206** 7694-7722. PMLR.
- SINSBECK, M. and NOWAK, W. (2017). Sequential Design of Computer Experiments for the Solution of Bayesian Inverse Problems. *SIAM/ASA Journal on Uncertainty Quantification* **5** 640-664. <https://doi.org/10.1137/15M1047659>
- STUART, A. M. (2010). Inverse problems: A Bayesian perspective. *Acta Numerica* **19** 451-559. <https://doi.org/10.1017/S0962492910000061>
- STUART, A. M. and TECKENTRUP, A. L. (2018). Posterior consistency for Gaussian process approximations of Bayesian posterior distributions. *Mathematics of Computation* **87** 721-753. <https://doi.org/10.1090/mcom/3244>
- SUNG, C.-L. and TUO, R. (2024). A review on computer model calibration. *WIREs Computational Statistics* **16** e1645. <https://doi.org/10.1002/wics.1645>
- SUNNÅKER, M., Busetto, A. G., NUMMINEN, E., CORANDER, J., FOLL, M. and DESSIMOZ, C. (2013). Approximate Bayesian computation. *PLOS Computational Biology* **9** e1002803. <https://doi.org/10.1371/journal.pcbi.1002803>
- TAKHTAGANOV, T. and MÜLLER, J. (2018). Adaptive Gaussian process surrogates for Bayesian inference. *ArXiv abs/1809.10784*. <https://doi.org/10.48550/arXiv.1809.10784>
- TECKENTRUP, A. L. (2020). Convergence of Gaussian Process Regression with Estimated Hyper-Parameters and Applications in Bayesian Inverse Problems. *SIAM/ASA Journal on Uncertainty Quantification* **8** 1310-1337. <https://doi.org/10.1137/19M1284816>
- TRAN, D., DUSENBERRY, M., VAN DER WILK, M. and HAFNER, D. (2019). Bayesian Layers: A Module for Neural Network Uncertainty. In *Advances in Neural Information Processing Systems* (H. WALLACH, H. LAROCHELLE, A. BEYGEZIMMER, F. D'ALCHÉ-BUC, E. FOX and R. GARNETT, eds.) **32**. Curran Associates, Inc. <https://doi.org/10.48550/arXiv.1812.03973>
- VARMA, V., FIELD, S. E., SCHEEL, M. A., BLACKMAN, J., GEROSA, D., STEIN, L. C., KIDDER, L. E. and PFEIFFER, H. P. (2019). Surrogate models for processing binary black hole simulations with unequal masses. *Physical Review Research* **1**. <https://doi.org/10.1103/physrevresearch.1.033015>
- VILLANI, P., UNGER, J. and WEISER, M. (2024). Adaptive Gaussian Pro-

- cess Regression for Bayesian inverse problems. <https://doi.org/10.48550/arXiv.2404.19459>
- WANG, K., BUI-THANH, T. and GHATTAS, O. (2018). A Randomized Maximum A Posteriori Method for Posterior Sampling of High Dimensional Non-linear Bayesian Inverse Problems. *SIAM Journal on Scientific Computing* **40** A142–A171. <https://doi.org/10.1137/16M1060625>
- WANG, H. and LI, J. (2018). Adaptive gaussian process approximation for bayesian inference with expensive likelihood functions. *Neural Comput.* **30** 3072–3094. https://doi.org/10.1162/neco_a_01127
- WILKINSON, R. (2014). Accelerating ABC methods using Gaussian processes. In *Proceedings of the Seventeenth International Conference on Artificial Intelligence and Statistics* (S. KASKI and J. CORANDER, eds.). *Proceedings of Machine Learning Research* **33** 1015–1023. PMLR, Reykjavik, Iceland.
- WILSON, J., HUTTER, F. and DEISENROTH, M. (2018). Maximizing acquisition functions for Bayesian optimization. In *Advances in Neural Information Processing Systems* (S. BENGIO, H. WALLACH, H. LAROCHELLE, K. GRAUMAN, N. CESA-BIANCHI and R. GARNETT, eds.) **31**. Curran Associates, Inc.
- WILSON, J. T., BOROVITSKIY, V., TERENIN, A., MOSTOWSKY, P. and DEISENROTH, M. P. (2020). Efficiently sampling functions from Gaussian process posteriors. In *Proceedings of the 37th International Conference on Machine Learning. ICML'20*. JMLR.org.
- WILSON, J. T., BOROVITSKIY, V., TERENIN, A., MOSTOWSKY, P. and DEISENROTH, M. P. (2021). Pathwise Conditioning of Gaussian Processes. *Journal of Machine Learning Research* **22** 1–47.
- WOOD, S. N. (2010). Statistical inference for noisy nonlinear ecological dynamic systems. *Nature* **466** 1102–1104. <https://doi.org/10.1038/nature09319>
- WYNN, H. P. (1970). The Sequential Generation of D-Optimum Experimental Designs. *The Annals of Mathematical Statistics* **41** 1655–1664.
- XU, Z., ZHU, X., LI, D. and LIAO, Q. (2024). An adaptive Gaussian process method for multi-modal Bayesian inverse problems.
- YEH, S.-T., WANG, X., SUNG, C.-L., MAK, S., CHANG, Y.-H., ZHANG, L., WU, C. F. J. and YANG, V. (2017). Data-Driven Analysis and Common Proper Orthogonal Decomposition (CPOD)-Based Spatio-Temporal Emulator for Design Exploration. <https://doi.org/10.48550/arXiv.1709.07841>
- ZAMMIT-MANGION, A., SAINSBURY-DALE, M. and HUSER, R. (2025). Neural Methods for Amortized Inference. *Annual Review of Statistics and Its Application* **12** 311–335. <https://doi.org/10.1146/annurev-statistics-112723-034123>
- ZENG, F., ZHANG, W., LI, J., ZHANG, T. and YAN, C. (2022). Adaptive Model Refinement Approach for Bayesian Uncertainty Quantification in Turbulence Model. *AIAA Journal* **60** 3502–3516. <https://doi.org/10.2514/1.J060889>
- ZHANG, J., LI, W., ZENG, L. and WU, L. (2016). An adaptive Gaussian process-based method for efficient Bayesian experimental design in ground-water contaminant source identification problems. *Water Resources Research* **52** 5971–5984. <https://doi.org/10.1002/2016WR018598>
- ZHANG, J., ZHENG, Q., CHEN, D., WU, L. and ZENG, L. (2020). Surrogate-

- Based Bayesian Inverse Modeling of the Hydrological System: An Adaptive Approach Considering Surrogate Approximation Error. *Water Resources Research* **56** e2019WR025721. e2019WR025721 2019WR025721. <https://doi.org/10.1029/2019WR025721>
- ÖZGE SÜRER (2026). Batch Sequential Experimental Design for Calibration of Stochastic Simulation Models. *Technometrics* **68** 1–13. <https://doi.org/10.1080/00401706.2025.2520860>
- ÖZGE SÜRER, PLUMLEE, M. and WILD, S. M. (2024). Sequential Bayesian Experimental Design for Calibration of Expensive Simulation Models. *Technometrics* **66** 157–171. <https://doi.org/10.1080/00401706.2023.2246157>